Title
The Chemical Features of Polyanions Modulate Tau Aggregation and Conformational States

Author
Montgomery, Kelly M

Publication Date
2023

Peer reviewed|Thesis/dissertation

The Chemical Features of Polyanions Modulate Tau Aggregation and Conformational States

by
Kelly Montgomery

DISSERTATION
Submitted in partial satisfaction of the requirements for degree of
DOCTOR OF PHILOSOPHY

in

Chemistry and Chemical Biology

in the

GRADUATE DIVISION
of the
UNIVERSITY OF CALIFORNIA, SAN FRANCISCO

Approved:

DocuSigned by:
Jason Gestwicki
4909848DBB404E5...

Jason Gestwicki
Chair

DocuSigned by:
Michelle Arkin

Michelle Arkin

DocuSigned by:
Geeta Narlikar
EE2E6D32EE3043B...

Geeta Narlikar

Committee Members

Acknowledgements

Above all, I am most enthusiastic about the connections I have established during my graduate tenure. Rooted in kindness, blossoming with creativity, and enduring with gentleness, my chosen community has been a personal reservoir of love. My friendships are indeed a great source of joy — to those who indulged in my curiosities, nurtured my creativity, and challenged me to think critically; you have certainly made my days brighter and ensured that my time in the Bay Area was nothing short of an adventure. For that, I am exceedingly thankful.

To my partner, Yaovi — thank you for your endless support, guidance, and judiciousness. Your enthusiasm and certainty in me and my work have bolstered my confidence and resiliency as a scientist.

To my family, especially my mother, Jo-Ann, who has supported my scientific endeavors without restriction, trusted my instincts, and indulged in my decision-making, thank you for allowing me to dive into new spaces and opportunities without question or hesitation. The freedoms you've allotted me to navigate this world have undeniably been pivotal to my success.

Lastly, the work herein is collaborative and would not have been possible without the specific contributions of my wonderful colleagues and collaborators Paige Hodges, Emma Carroll, Aye Thwin, and Athena Quddus. Thank you for your contributions to polyanion optimization (P.H.) and shaping the structural and conformational elements of this work (A.T., E.C., A.Q.).

Contributions

Chapter 1 is reproduced in part from a forthcoming publication.

Chapter 2 is a reprint of the material as it appears in:

Kelly M. Montgomery, Emma C. Carroll, Aye C. Thwin, Athena Y. Quddus, Paige Hodges, Daniel R. Southworth, and Jason E. Gestwicki. “Chemical Features of Polyanions Modulate Tau Aggregation and Conformational States” J. Am. Chem Soc. 2023, 145, 7, 3926–3936.

https://doi.org/10.1021/jacs.2c08004

When the ink dries and the pages turn to dust, so will we.

-Frank Ocean

The Chemical Features of Polyanions Modulate Tau Aggregation Kinetics and Conformational Fate

By

Kelly Monét Montgomery

Abstract

The aggregation of tau into insoluble fibrils is a defining feature of neurodegenerative tauopathies. However, tau has a positive overall charge and is highly soluble; so polyanions, such as heparin, are typically required to promote its aggregation *in vitro*. There are dozens of polyanions in living systems and it is not clear which ones might promote this process. Here, we systematically measure the ability of 37 diverse, anionic biomolecules to initiate tau aggregation, using either wild type (WT) tau or the disease associated P301S mutant. We find that polyanions from many different structural classes can promote fibril formation and that P301S tau is sensitive to a greater number of polyanions (28/37) than WT tau (21/37). We also find that some polyanions preferentially reduce the lag time of the aggregation reactions, while others enhance the elongation rate, suggesting that they act on partially distinct steps. From the resulting structure-activity relationships, the valency of the polyanion seems to be an important chemical feature, such that anions with low valency tend to be weaker aggregation inducers, even at the same overall charge. Finally, the identity of the polyanion influences fibril morphology, based on electron microscopy and limited proteolysis. These results provide insight into the crucial role of polyanion—tau interactions in modulating tau conformational dynamics with implications for understanding the tau aggregation landscape in a complex cellular environment.

Table of Contents

List of Figures

Chapter I

Chapter II

List of Tables

List of Abbreviations

AD	Alzheimer's Disease
BME	2-Mercaptoethanol
CSF	Cerebrospinal fluid
CBD	Corticobasal Degeneration
DTT	Dithiothreitol
CNS	Central Nervous System
FTD	Frontotemporal Dementia
FTDP-17	Frontotemporal Dementia with Parkinsonism
FTLD-Tau	Frontotemporal Lobar Degeneration with Tau Inclusions
FTIR	Fourier Transform Infrared Spectroscopy
GAGs	Glycosaminoglycans
HA	Hyaluronic Acid
IDPs	Intrinsically Disordered Proteins
LLPS	Liquid–Liquid Phase Separation
MAPT	Microtubule Associated Protein Tau
MLOs	Membraneless Organelles
mRNA	Messenger Ribonucleic Acid (mRNA)

MAPT	Microtubule Associated Protein Tau (Tau)
MTs	Microtubules
MTBR	Microtubule Binding Repeats
ND	Neurodegeneration / Neurodegenerative
NMR	Nuclear Magnetic Resonance
NFTs	Neurofibrillary tangles
OS	Oxidative Stress / Oxidative Species
PHF	Paired Helical Filament
PiD	Picks Disease
PLE	Poly-L-Glutamic Acid
polyA	Polyadenine (mRNA)
polyPs	Polyphosphates
Proteostasis	Protein Homeostasis
PSP	Progressive Supranuclear Palsy
PTMs	Post Translational Modifications
RNA	Ribonucleic Acid
ROS	Reactive Oxygen Species
snRNAs	Small Nuclear RNAs

snoRNAs	Small Nucleolar RNAs
TB	Terrific Broth
TEM	Transmission Electron Microscopy
ThT	ThioflavinT
tRNA	Transfer RNA

List of Symbols

ºC	Degrees Celsius
µg	Microgram
µL	Microliter
µM	Micromolar
x g	Times gravity (centrifugal force)

Chapter I

Synchronous Cellular Interactions Govern Tau Aggregation Propensity

1.1 Abstract

In tauopathies, soluble tau proteins form aberrant filamentous lesions in response to dynamic chemical modifications. Soluble tau can sample a number of physical configurations from misfolded monomers to neurofibrillary tangles. A lesser explored contributor of tau conformational fate is the impact of cellular components, including metabolites, metals, and macromolecules on altering tau's charge and electrostatics — and its ultimate ability to form functional or pathological conformers. Tau fibers accumulate in a variety of brain regions, therefore, it's likely that tau proteins interact with diverse cellular components. This perspective seeks to contextualize the scope of possible intracellular interactions driving tau aggregation and the effect of cellular macromolecules and metabolites on directing the conformational fate of tau proteins. Broadly highlighting otherwise obscure small molecule or polyelectrolyte contenders in the aggregation cascade can reveal potential therapeutic targets poised to modulate disease onset and progression. Here, we seek to contribute to the tau aggregation narrative by offering general insights into several metabolites and macromolecules implicated in aggregation induction *in vitro* and describe these molecules with regard to cerebral localization, and chemical composition; when appropriate we convey experimental physiochemical protein outcomes.

1.2 Introduction

The microtubule associated protein tau (MAPT; tau) is an intrinsically disordered protein whose aberrant self-association is linked to a heterogeneous group of age-related neurodegenerative dementias called tauopathies. The tau-microtubule binding interface is an essential and dynamic protein-protein interaction crucial to maintaining neuronal integrity, and axonal outgrowth. Although tau is generally innocuous, perturbations to its physical or chemical composition can disrupt the tau-MT binding interface and enable the proliferation of non-functional proteoforms including neurofibrillary tangles (NFTs) and amorphous aggregates. Tau aggregation is a fascinating biophysical transition, in part because tau's observed self-association contradicts its physiochemical and electrostatic properties. Tau contains a relatively high number of polar residues, and is incredibly hydrophilic — supporting its inherent solubility, extended solution conformation, and intrinsic disorder. Structurally, tau belongs to the class of intrinsically disordered proteins (IDPs), which are void of stable secondary and tertiary folds — instead tau exists as an ensemble of rapidly interconverting conformers. Therefore, self-assembly requires overcoming a number of unfavorable long-range interactions to enable fiber formation.

Tau is composed of four distinct units, negatively charged N- and C-termini which flanks a proline rich region, and positively charged microtubule binding repeats (MTBR) (Figure 1A). The positively charged nature of the MTBR contributes to its association with negatively charged cytoskeletal elements, and also contributes to tau's net positive charge. Each domain has distinct physiochemical properties that corresponds to relative degrees of disorder.[1,2] Spectroscopy experiments revealed transient secondary structures in full-length and truncated isoforms. Further, MTBR repeats contain two hexapeptide motifs, VQIINK and VQIVYK, located in R2 and R3, respectively, which facilitate tau assembly into β-sheet-rich assemblies[3,4] — but on their own, these signatures are not sufficient to stimulate fiber formation. Thus, changes to tau's

physiochemical nature (i.e., post translational modifications or truncations) contribute to tau's susceptibly to become more or less aggregation prone.

Tau expression is precisely regulated at all stages of human development — having six distinct splice isoforms present at any stage of developmental maturity. Tau isoforms are defined by their inclusion or exclusion of 2 N-terminal repeats (0N or 2N) and the inclusion or exclusion of the second microtubule binding repeat (3R or 4R) (Figure 1B). Each isoform presents distinct physiochemical and electrostatic properties — contributing to isoform mediated aggregation propensity. For instance, 3R constructs are generally less aggregation prone compared to 4R, likely due to the exclusion of the VQIINK amyloid motif. Moreover, truncations are often more aggregation prone compared to their full-length counterparts — likely due to lessened electrostatic interference and reduction of long-range interactions which enables compaction of the MTBR.[5,6]

What unifies tauopathies is the accumulation of fibrillar plaques which accumulate in and destroy neurons, although, diseases diverge in their physiological accumulation and physical presentation. Strikingly, tau can form a diverse range of macromolecular ensembles[7–9] whose morphology is thought to direct disease states.[10] Tauopathies are broadly grouped into two categories, primary and secondary tauopathies. Primary tauopathies are inclusive of frontotemporal lobar degeneration with tau inclusions (FTLD-Tau) and include Pick's disease (PiD), progressive supranuclear palsy (PSP), corticobasal degeneration (CBD), and frontotemporal dementia with Parkinsonism (FTDP-17). Alzheimer's disease (AD) is a secondary tauopathy colocalized with extracellular inclusions of Amyloid-β (Aβ). Tauopathies are further classified by isoform composition, i.e., the inclusion or exclusion of 3R or 4R repeat regions; 4R tauopathies include PSP and CBD, 3R:4R tauopathies are inclusive of FTDP-17 and AD, and 3R-tauopathy (PiD).

Linking cellular and chemical interactions to conformational heterogeneity is an important and warranted characterization that remains elusive in neurobiology. Even for a single sequence, tau's amyloid core is polymorphic[11] — suggesting amyloid fibers are sensitive to local environmental factors. It's speculated that cellular factors of the diverse cellular milieu including local concentrations of polyanions, metals and cellular metabolites likely contribute to stabilizing tau conformers, and thus contributing to fibril diversity. Many intrinsically disordered proteins rely on interactions with biding partners before they can perform intrinsic functions. Functional tau relies on binding to its innate bunding partner, tubulin, but cytosolic tau's broad interactions with cellular constituents likely direct non-functional and pathogenic mechanisms of action.

1.3 Tau's Conformational Landscape is Diverse

Protein folding is a rapid and complex process — many folding intermediates happen within millisecond time intervals and are difficult to capture with great resolution. Tau aggregation progresses via an ensemble of rapid interconversions from soluble and misfolded conformers, but intermediates don't converge on a simple progressive pathway that leads to a singular conformation.[12,13] Energetic landscapes of intrinsically disordered proteins (IDPs) are distinctly divergent from ordered protein regimes where a single folding funnel corresponds to a single conformation. The energetic landscapes corresponding to IDPs en route to aggregated conformers feature several energetic minima of competing low energy structures;[12] suggesting a complex interplay of competing interactions and energetics governing local and global tau folding dynamics and mechanisms of action.

Tau's predominant conformers and physical configurations are inclusive of microtubule (MT) bound species which stabilize structural elements. On the MT, tau can undergo liquid-liquid phase transitions[14] and eventually converge on fibrillar aggregates. Upon MT dissociation, soluble tau

can interconvert between phase separated, oligomeric, and misfolded tau before converging on highly ordered fibers (figure 2).

1.3.1 Microtubule Bound

Tau is an essential regulator of neuronal microtubule (MT) assembly, stabilization, and organization. Tau stabilizes MTs by binding at the interface between tubulin heterodimers; the residues involved this interaction are three or four imperfect repeats, termed the microtubule binding region (MTBR), which populates β-structure and forms the core of tau filaments. When bound, residues outside of the MTBR remain flexible and are thought to behave like a polyelectrolyte brush.[15] The tau-MT binding interface is a dynamic, cyclical interaction precisely regulated by a number of factors, including post translational modifications (PTMs) which modifies tau's affinity for tubulin heterodimers and directs protein cycling on the structure.[16,17] The interaction between tau binding and dissociation demonstrates a complex interplay between MT association and pathogenic misfolding in solution.

1.3.2 Soluble Tau

Loss of MT stabilizing capacity can arise in response to aberrant physiological modification or physical perturbation rendering tau restricted to the cytosol as a free monomer and increase its susceptibility to self-association. In solution, tau transiently samples a number of conformational ensembles,[18,19] including a restricted capacity to adopt alpha helices;[20] but principally, tau lacks the ability to form stable secondary or tertiary structure as determined by a number of spectroscopic techniques including CD, Fourier Transform Infrared Spectroscopy (FTIR), and NMR.[4]

Long-range structural studies using full-length hTau40 revealed an electrostatically driven hairpin-like fold in solution.[21] Förster resonance energy transfer (FRET) experimentation demonstrates

intrinsic compaction of the MTBR, as observed by the proximity of residue 291 near 310 and residue 310 nearing 322. Additionally, the negatively charged N- and C-termini fold onto the positively charged MTBR — suggesting that tau has preferred solution orientation governed by its electrostatics. Tau's distinct charge presentation (Figure 1A) is thought to influence its intramolecular interactions, therefore, modulation of tau's charge density along its domains or solution properties can influence tau's conformational orientation, even driving protein de-mixing[22] and the formation of immiscible liquid phases (electrostatic coacervates) in solution.

1.3.3 Membrane-less Organelles & Biomolecular Condensation

Eukaryotic cells contain several membraneless structures formed via condensation of cellular material in a process termed liquid–liquid phase separation (LLPS). Membraneless organelles (MLOs) arise in response to cellular demand for specialized compartments in the absence of lipid membranes, aiding in spatiotemporal organization, cellular regulation, and improving cellular fitness during stress.[23,24] Often, membraneless organelles are formed from proteins containing low complexity domains and RNAs coalesced into a condensed state to perform physiological functions.

Tau is one of several proteins containing low-complexity domains that undergoes LLPS. Tau's propensity to de-mix in solution is driven primarily by electrostatic intermolecular interactions (simple coacervation),[25] but is also prompted by crowding agents[26] and interactions with negatively charged polymers, specifically RNAs (complex coacervation).[27] In aged tau-rich droplets, aberrant liquid to solid phase transitions promote protein fibrilization in the condensed state,[24] highlighting a delicate interconversion from functional biomolecular condensates to pathogenic conformers. Explicit mechanisms directing tau's interconversion in condensates is still unclear, however, it's clear that tau's dynamicity is significantly reduced in coacervates and ultimately results in progressive protein accumulation and the formation of higher order static

structures. Dynamic modeling of tau free-energy landscapes proposes divergent channels of tau aggregation: one which converges toward static, fibrillar aggregates and another which converges toward amorphous phases.[28] Both aggregation landscapes encompass amorphous and prefibrillar oligomers which are considered the most toxic and pathologically significant tau aggregate.[29]

1.3.4 Oligomers & Protofibrils

Amongst tau's conformational regime are prefibrillar intermediates (oligomers) which can behave as templates for misfolding soluble tau and triggering synaptic and mitochondrial dysfunction. Tau oligomers are higher-order assemblies which are considered the neurotoxic species directing clinical pathogenicity.[29–31] To achieve pathogenicity, tau oligomers traverse cellular barriers, propagating infective conditions to healthy cells, thus facilitating the spread of the neurotoxic aggregates. Because these species are transient and relatively short lived, characterizing pathogenic oligomers in high resolution is proven challenging. Nevertheless, mounting evidence suggests tau oligomers are structurally and functionally diverse,[14,31,32] continuing to reveal the role of tau oligomers in the natural progression of NFT formation.

Substantial structural reordering of native tau is required for integration of stable β-strand registers, which ultimately converge toward static fibrils. Energetic landscape analysis of pathogenic tau conformers suggests a nucleation mechanism where oligomeric β-strand registry and organization directs aggregation pathways and conformational specificity. Oligomeric species containing parallel β-strand registry converge on amyloid fibrils, whereas species containing less-ordered and random β-strand registry converges on amorphous oligomers; suggesting early compositional reorganization is crucial to directing mature fiber configurations.[28]

1.3.5 Neurofibrillary Tangles and Paired Helical Filaments

Tau protein fibrilization is a multistep process initiated by a preliminary misfolding event followed by iterative annealing, oligomerization, and fragmentation events until it is enriched with compact β-assemblies. Investigation of tau molecular structure has established tau's fibrillar heterogeneity in pathological states. Tau can adopt a variety of mature fibrillar conformations — advances in cryo-electron microscopy (cryo-EM) techniques have enabled high-resolution elucidation of atomic structures of fibrils associated with a number of neurodegenerative tauopathies, including AD, PiD, CTE, and CBD. Fibers are generally composed of a rigid core encompassing the MTBR and several amino acids (AAs) flanking the imperfect repeats. Although excluded from the core fold, N- and C-terminal projections termed the "fuzzy coat", are also believed to adopt local structure.[33,34]

An increasing body of literature suggests a direct correlation between fibrillar heterogeneity and discrete neuropathological outcomes. How does tau's fibrillar diversity emerge? The conversion from healthy to pathological forms certainly demands further investigation. It's speculated that a dimension of fibrillar heterogeneity is likely linked to tau's interaction with cellular components including polyanions and salts.[35] Great progress is underway to reveal how tau ultra-structures associate and how cellular macromolecules direct conformational states.[33] By contextualizing how cellular macromolecular interactions drive tau conformational diversity, we can begin to zoom in on the specific electrostatic interactions that contribute to directing functional and pathological conformers. In support of this idea, detection of unresolved densities in cryo-EM structures are observed.[7,11,36] It remains unclear what is occupied by these densities, but it is apparent that these cofactors are not proteins, rather its postulated they are cellular components including metabolites, salts, or polyanions which could have been incorporated during the fibril formation to modulate tau's conformational fate.

1.4 Chemical, Physical and Genetic Perturbations Direct Tau Aggregation Outcomes.

Tau aggregation can progress via multiple pathways[37] directed by specific physiochemical modifications and converge on distinct conformational states.[38] A number of chemical and physical perturbations, including cleavage, post translational modification (PTMs), and polyelectrolytes initiate the misfolding and propagation of aggregates to disrupt tau homeostasis. Chiefly, these perturbations modulate the strength of inter- and intramolecular electrostatic interactions, to stabilize or (destabilize) aggregation prone conformers and modulate kinetic equilibriums.[39] Constituents of the diverse cellular milieu, including cellular metabolites, metals, and polyanions, likely contribute to stabilizing tau conformers, and thus contributing to aggregate multiplicity and fibril diversity.[35,40] Early conformational changes in the MTBR and PRR are crucial for directing aggregation induction.[5] *In vitro*, several polyanions demonstrate preferential activity for early aggregation events.[33]

1.4.1 Splicing Isoforms & Proteolytic Cleavage.

In the human brain, six different isoforms of tau (comprising 352–441 residues) is expressed (Figure 1B). Tau isoforms are generated via alternative splicing of the MAPT gene and contain either 0, 1, or 2 N-terminal inserts (0N, 1N or 2N, respectively) and 3 to 4 repeat sequences at the C-terminus (3R or 4R). β-structure in the repeat domains governs tau aggregation propensity,[38] therefore, isoform specificity (e.g., 3R vs 4R) and proteolytic truncations modulate tau's inherently susceptibility to self-association.

Moreover, disruption of tau's primary structure via truncations is generally permissive of aggregation. A substantial proportion of endogenous tau exists in fragments in the human brain;[41] pro-aggregation neurotoxic tau fragments are generally produced via proteolytic cleavage or physiological damage. Proteolytic processing of tau regulates the abundance of full-length proteins and produces truncated forms that are important for normal neuronal function and

pathological mechanisms in neurodegeneration. Upon removal of the N- and C-termini, tau exhibits faster aggregation than full-length tau[42] and tau truncation selectively enables pathogenicity.[43,44] Several tau fragments generated by endogenous proteases have been reported in human disease and in murine models.[42,45,46] ΔK280, a toxic gain of function truncation is associated with some forms of FTD,[47] elicits tau aggregation in mice[48] and promotes spontaneous aggregation of recombinant tau. Further, several caspase-mediated[49–51] and calpain-mediated truncations[45] are detected in NFTs of AD brains. Terminal regions of tau sustain tau solubility and counteract aggregation via unfavorable long-range interactions, therefore, are essential to sustaining soluble, functional tau. In rarer instances, tau truncations are protective. A truncated form of tau generated by intron 12 retention termed TIR-MAPT (Truncated by Intron Retention MAPT) is protective, and less prone to aggregation, as it stabilizes a local aggregation resistant conformation.[52]

1.4.2 Post Transitional Modifications

In addition to truncation, tau homeostasis is intricately regulated by post translational modifications which modulate its physiological and pathophysiological functions. Tau is prone to modification by a number of functional moieties including, phosphorylation,[53] acetylation,[54] ubiquitination, glycation, glycosylation, SUMOylation, methylation, oxidation, and nitration which have all been explored in great detail. In disease, chemical modulation to tau's local charge presentation via PTMs is thought to induce dissociation of tau from the MT rendering tau localized to the cytoplasm, increasing its probability of self-association instigated by cellular metabolites and cellular machineries. In AD brain, Tau is abnormally hyperphosphorylated at many sites, to date, more than 40 phosphorylation sites have been identified[53,55] — although many are permissive of aggregation, some site-specific modifications inhibit aggregation.[56] Many have beautifully described how posttranslational modifications can influence its physiological

outcomes, we don't seek to rehash this work, rather, contribute to the growing narrative contextualizing the expansive tau interactome.

1.4.3 Genetic Modifications (De)stabilize Local Structure. Point mutations in the tau gene amend the aggregation propensity of Tau. A number of disease-associated point mutations produce high-aggregation propensity species.[57] Indeed, charge is a critical feature of protein folding regimes, but not all modifications will significantly alter tau's charge presentation. Disease associated mutations[58] and proline isomerization[1] can renders tau's charge state unmodified, but exacerbate aggregation. Mutation of a critical proline at position 301 demonstrates an instance wherein modification, destabilizes the local structure flanking an aggregation motif ^{306}VQIVYK^{311}, resulting in high aggregation propensity.[59] Therefore, it becomes more apparent that charge alone isn't the sole indicator of aggregation induction, rather one feature of many plausible cellular interactions directing this fascinating protein conversion.

1.5 Macromolecules Regulate Charge Presentation

1.5.1 Polyelectrolytes

In vitro, tau protein folding does not occur autonomously. Polyelectrolytes neutralize tau's charge along its domains to stabilize or destabilize tau conformers. Polyelectrolytes have ionizable groups in their repeat domains which contribute to modulating the ionic strength of the counter ions (tau) in solutions to screen tau's electrostatic repulsion. Many intrinsically disordered proteins require interaction with binding with partners before they can perform Intrinsic functions.[60] Tau's interaction with its native binding partner, tubulin, facilitates neuronal stability, but non-native binding to anionic biopolymers facilitates pathological aggregation and neuronal deterioration.[33,61–63] Several polyanionic biomolecules including heparins, anionic micelles, acidic peptides, and nucleic acids have been implicated in tau aggregation and associated with postmortem brain slices of individuals with tauopathies.[64] Polyanion binding to tau is believed to

partially shield its positive charge and stabilize aggregation domains, facilitating self-association. Other reports suggest that some electrostatic interactions can destabilize the hexapeptide motifs, suggesting a model were a number of synergistic and antagonistic tau-polyelectrolyte interactions function in synchrony to enable or deter protein aggregation.[65] Below we describe a several biomolecules known to interact with tau and enable or inhibit its aggregation capacity.

1.5.1.1 Glycosaminoglycans

Glycosaminoglycans (GAGs) are long (roughly 10–100 kDa), linear, unbranched polysaccharides consisting of repeating disaccharide units which regulate a suite of physiological reactions.[66] GAGs are broadly grouped into two categories: non-sulfated (hyaluronic acids, HA), and sulfated (chondroitin sulfate, dermatan sulfate, keratan sulfate, heparin and heparan sulfate).[67] Indeed, tau and GAGs differ in cellular localization, GAGs localize near the cell surface or in the extracellular matrix whereas tau is an intracellular protein. However, tau's ability to traverse synapses, in its prion-like spreading mechanism increases the probability tau-GAG interactions.

Hyaluronic Acid

Hyaluronic acid (HA), a non-sulfated homo-polymer consisting of alternating residues of β-D-(1,3) glucuronic acid (GlcA) and β-D-(1,4)-N-acetylglucosamine (GlcNAc).[66] HAs are reported as a non-functional tau co-factor unable to produce aggregation prone species *in vitro,* even with increasing polymer valency and charge screening.[33] Mechanistically, it is unclear why these molecules are functionally inert, but sulfate groups on sugar backbones are considered an essential regulator of aggregation induction for sugar scaffolds, [68,69] which HA lacks.

Heparin and Heparan Sulfate

Heparin (HS), a member of the glycosaminoglycan (GAG) family of sulfated polysaccharides are highly sulfated linear polysaccharides of various chain lengths ranging from 2 - 40 kDa decorated

with variable sulfates on repeating units of (1,4) α-l-iduronic or β-d-glucuronic acid (d-GlcA), and α-d-glucosamine (d-GlcN) disaccharide units.[66] Sulfate variability in the disaccharide contributes to complex microheterogeneity of heparins.[70] Structurally, heparin is similar to a lesser sulfated isoform, heparan sulfate. Heparan has a defined domain structure with fewer l-iduronate residues,[66,71] but both polymers are capable of binding tau and initiating aggregation.[69,72]

HS is the most well studied polysaccharide used for tau aggregation induction *in vitro*. It's postulated that heparin-induced electrostatic interactions stabilize aggregation prone tau conformers by increasing ionic strength of the system and decreasing unfavorable long-range electrostatic interactions between heparins and tau. Early research has demonstrated recombinant 3R tau isoforms form PHFs under physiological conditions *in vitro* when incubated with heparin or heparan sulphate.[73] NMR chemical-shift perturbations of full-length tau binding to heparin confirmed its biding to repeat domains but also reveal conversions to alpha-helical structures in regions outside of the core, [72,74,75] demonstrating early conformational reorganization of tau upon heparin binding. Additional studies assessing the glycan determinants of the heparin-induced tau aggregation, reveal that sulfation patterning and oligosaccharide chain lengths directs nucleation speeds, aggregation kinetics, and fibril morphology.[76] Using immobilized heparin and tau K18/K19 truncations demonstrated K18/K19 preferentially binds to longer-chain heparin oligosaccharides,[70] suggesting a specific role for valency in tau-polyanion aggregation regimes. Further, heparan is associated with NFTs in AD brains and other tauopathies,[77,78] suggesting GAGs might play a pivotal role in fiber formation *in vivo*.

Chondroitin Sulfates. Chondroitin Sulfate (CS) is a major component of brain extracellular matrix that interacts with other matrix proteins and cell surface receptors. Chondroitin sulfate A (CS-A) consists of an alternating copolymer β-glucuronic acid-(1-3)-N-acetyl-β-galactosamine-4-sulfate.[66] Dermatan sulfate (DS), otherwise known as chondroitin sulfate B (CS-B) consists of

the same scaffold. CS is known to associate with lesions of AD and possibly potentiate the regression of neurites around senile plaques and NFTs.[79] In murine models, CS with reduced molecular sizes and altered disaccharide composition is associated with AD pathology, suggesting molecular scaffold and size are important features directing ND tauopathies.

Protein-glycan interactions are functionally diversified by a unique sulfation code. Naturally occurring sugars can be modified to produce a number of unique patterning on glycans to modulate their function such that they vary in side chain presentation, and conjugation (i.e. α or β conjugations) to increase structural diversity.[80] Therefore, tau's potential for conformational diversity could possibly be as vast as its glycan interactome and diversity of binding partners in physiological environments.

1.5.1.2 Polypeptides

Polyamino acids (polypeptides) are biopolymers consisting of repeating amino acid units (-[NH-CHR-CO]x-) formed by condensation polymerization of amino acid monomers. In solution, polyaminoacids can adopt higher-ordered structures through cooperative hydrogen bonding which directs specific physiological outcomes. Of the charged amino acids, glutamic acid and aspartic acid are anionic at physiological pH and could be important biopolymers directing tau aggregation. Poly-L-Glutamic Acids (PLEs) are observed to bind to K18 and K19 repeat domains[74,81] and preferentially decrease the lag time of 0N4R tau constructs in concentration-dependent manner *in vitro*[33] — suggesting PLE likely contributes to early remodeling events of tau self-association.

Considerably less mechanistic information is known about these polyaminoacids in directing tau aggregation compared to GAGs. While polyamino acids likely modulate aggregation induction via similar charge screening mechanisms as previously discussed; it's plausible that polyaminos

specifically behave like a polyelectrolyte brush when in close proximity to a charged solid interface (tau), forcing them to stretch orthogonally to the protein interface, instead of adopting random-coil arrangement. Consistent with this model, glutamic acid oligomers (PLEs) have been observed to form polyelectrolyte brushes with functionally divergent behaviors directly correlated with their chain length, grafting density, and chemical structure.[82]

1.5.1.3 Polyphosphates

Polyphosphates (PolyPs) are linear polymers consisting of up to 3-1000s of orthophosphate units linked by energy-rich phosphoanhydride bonds.[83] PolyP exists in mammalian brain at micromolar concentrations,[84] and functions as a regulator of neuronal excitability.[85] In the human brain, inorganic PolyP functions as a calcium-dependent glio- and neurotransmitter to mitigate communication between astrocytes.[86,87] The link between polyP and ND disease still requires investigation, but recent investigation proposes a model that suggests excessive release of neuronal polyP is correlated to neuronal cell death in ALS and FTD.[88] Thus, polyP could possibly serve as a novel clinical biomarker for detecting disease.

In vitro polyphosphate is believed to initiate tau aggregation by increasing the local concentration of tau seeds via inter- and intramolecular scaffolding.[62,89] Consistent with this hypothesis, increasing evaluation of multivalent phosphates reveals a mechanism that associates polymer activity to its valency — where low valency phosphates tend to behave as weak inducers of tau aggregation *in vitro.* Low valency triphosphates, cyclic phosphates, and phospo-nucleic acid conjugates poorly stimulate aggregation induction, and longer, multivalent chains are generally more permissive of aggregation. [33]

1.5.1.4 Nucleic acids

Ribonucleic Acids

Ribonucleic acid (RNA) is an essential polymeric molecule that regulates genetic coding, regulation, and expression. Growing evidence suggest tau regulates RNA metabolism in dysregulated states,[90,91] NFTs are enriched for RNAs,[92,93] and tau-RNA binding initiates aggregation *in vitro*.[94] In ND pathologies, positive RNA biomarkers are observed in aggregates of patients samples derived from Pick's and AD brains,[92] suggesting a direct correlation between tau-RNA binding and pathology. Mechanistically, RNA prompts tau's conversion to insoluble material via charge neutralization through the phosphate backbone which binds near the MTBR allowing tighter packing of tau molecules and cross-β fibril formation.[90] The interaction of RNA (polyA and polyG) and tau side chains reveals essential contacts with R406, H407 that supports the formation of C-terminal core fibers (residues 391 – 426),[95] which are distinct from cores observed in patient samples and heparin-derived samples, revealing how polyanion identity can shift fiber conformation, and possibly potentiate distinct pathology.

In vivo, cytosolic and nuclear tau aggregates are enriched with diverse RNAs, including small nuclear RNAs (snRNAs), small nucleolar RNAs (snoRNAs), mRNA, tRNA.[93] Recombinant 2N4R tau can non-specifically bind adenine (A), cytidine (C), and uracil (U) heteropolymers and induce tau aggregation and induces unique tau strains.[96] Interestingly, RNA-induced fibrils exclude the R2 as revealed by cryo-EM[95] and modulate R2 protease sensitivity.[33] RNA-induction enables a dramatic downstream c-terminal shift in the fibrillar core that significantly diverges from established core structures.[8,11] The significance of the R2 repeat is unclear, but some pathologically derived fibrils also exclude R2[95] suggesting that RNA modulates protein stability in pathogenic states, and shifts its early self-association events converging on fibrillar species exclusive of the MTBR region — but it's unclear if a similar core would form in the presence of a higher ordered RNA species, like tRNA or rRNA, which would likely differentially interact with tau.

Deoxyribonucleic Acid

Deoxyribonucleic acid (DNA) is a nuclear polymer composed of two polynucleotide chains responsible for transmitting genetic information and regulating the growth and development for all organisms. Although tau is primarily considered a cytosolic protein, early reports demonstrate tau's association with DNA and chromatin.[97] Isoform specificity, phosphorylation, and aging has been shown to alter tau's cellular localization and is permissive of localization in the nucleus of neuronal and non-neuronal cells.[98–100]

In addition to endogenous nucleic acids, several reports suggest microorganisms and viruses potentiate AD and other neurodegenerative diseases. Bacterial pathogens have the potential to cross the blood brain barrier (BBB) and invade the brain parenchyma. Invasive extracellular pathogens have including *Porphyromonas gingivalis* (the main pathogen that causes periodontitis), have been detected in the CSF and in post mortem brain of individuals with AD.[101–104] The interplay of pathogenic infections and ND disorders has received increasing attention suggesting a direct link between infectious disease burden and neurodegenerative progression *in vivo and in vitro*.[105,106]

1.5.1.5 Anionic Micelles and Vesicles

Anionic lipids are a broad group of naturally occurring molecules composed of a hydrophilic head and a non-polar tail group with diverse physiological functions. Lipids are an essential structural component of the cell membrane and have several critical functions regulating energy storage, and cell signaling. In ND pathology, the lipid surface may facilitate protein-protein associations by increasing their local concentration and promoting the stabilization of aggregation-competent protein conformers, similar to the proposed mechanism of action of polyanionic biopolymers.

Increasing evidence demonstrates a correlation between aberrant lipid metabolism and neurodegenerative disease. Lipidomics assessments of Alzheimer's disease (AD) patients revealed augmented quantities of glycerophospholipids, sphingolipids, and diacylglycerols (DAG) in plasma and brain[107] and associated with lipid rafts in murine models AD.[108] Above critical concentrations free fatty acids form micelles through a self-assembly process governed by a complex interplay of solvent-mediated interactions, where hydrophobic moieties are sequestered in aqueous solution and hydrophilic groups are exposed. Fatty acids such as arachidonic acid, linoleic acid, and phosphatidyl-L-serine, and oleic acid promote aggregation induction *in vitro* above their reported CMCs,[109] consistent with acting in micellar form.[110] Further, small quantities of lipids, including phosphatidylcholine (PC), cholesterol, and sphingolipid, are associated (PHFs) purified from the brains of AD patients,[111] further supporting the idea that tau can bind to membranes and higher-order lipid aggregates.

1.5.2 Protein Quality Control and Redox Imbalance

Importantly, its crucial to contextualize the significance of cellular aging and its contribution to proteostasis decline in the neurodegenerative process, as declining proteostasis machinery is a hallmark of neurodegenerative tauopathies. Because of the postmitotic nature of neurons and their limited regenerative capacity, ensuring balanced handling of protein synthesis, folding, unfolding and degradation is indispensable to preserve functions of the CNS.

Indeed, a degree of disruption to protein homeostasis, including neuroinflammation is present in normal aging regimes and in response to harmful stimuli. Neuroinflammation is an advantageous physiological response that supports the clearance of cellular debris and assists in tissue repair.[112] However, sustained inflammatory signaling can alter cellular redox status, by disrupting the balance of oxidative species (OS) and antioxidant enzymes, ultimately contributing to ND pathology.[113,114] Neuronal redox potential is critical for tau PHF assembly — imbalances between

ROS and the anti-oxidation pathway promote to enhanced tau polymerization by oxidation of SH groups in critical cysteine residues.[114] Tau contains two cysteines, Cys^{322} and Cys^{291}, located in the MTBR capable of forming disulfide cross-links.[115,116] Cysteine oxidation of tau is crucial for attenuating tau aggregation, however, Cys^{322} and Cys^{291} are functionally distinct and are differentially incorporated into patient-derived tau fibers. Tau cysteine to alanine substitutions revealed disruptions to Cys^{322} destabilizes oligomer formation, and mediates toxicity and dysfunction *in vitro*[115] and in *Drosophila* tauopathy models.[117]

1.5 Discussion

As more research emerges, tau's vast interactome is becoming ever evident and highlights a semi-selective interaction regime with diverse cellular constituents that vary in molecular scaffold, backbone flexibility, and chemical substitutions. To thoroughly assess how tau might confer its conformational diversity, understanding the neuronal chemical landscape in healthy and perturbed states is necessary to achieve this purpose. A combination of native cellular factors including PTMs, inducers, metabolites, and cellular proteostasis networks likely act synergistically or antagonistically to regulate tau homeostasis and conformational fate. Understanding these unique tau interactions are warranted to further rationalize anion mediated protein folding regimes and what this might mean in the context of disease. Uncovering the molecular details of tau inter- and intramolecular interactions upon ligand binding is of fundamental importance in molecular biology and is of practical significance in deconvoluting the molecular features of macromolecules in directing tauopathies. Can we one day resolve enough molecular resolution to correlate anion binding to folding pathways?

Establishing a comprehensive look at the complexity of the cellular environment as it pertains to tau protein aggregation could benefit drug discovery regimes. Developing a detailed understanding of the effects and significance of individual and combinatorial changes in the tau

assembly pathway is required for selecting the best molecular species to target for detection and therapeutic strategies. Employing comprehensive metabolomics studies to reveal metabolites associated with ND patients could indeed be a plausible start to guide investigative and targeted therapeutic tactics. Defining the chemical landscape that directs protein structure and function, is certainly valuable for informing strategic mechanisms for targeting disease pathways.

1.7 Figures

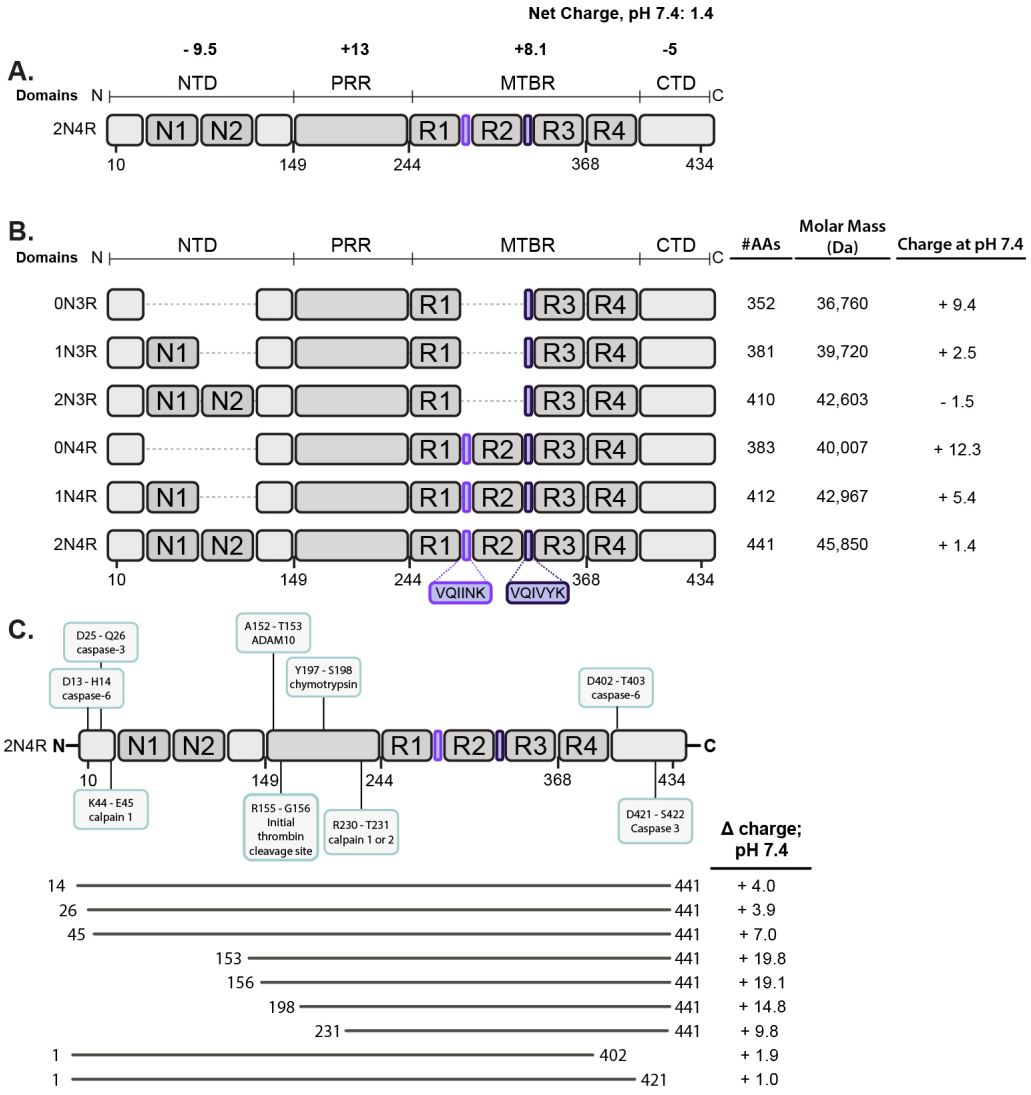

Figure 1.1. Domain architecture of tau isoforms and common caspase modifications. Amino acid numbering corresponds to the 441-residue isoform. (A) Domain architecture of the full-length 2N4R tau isoform. The overall charge and charge of each domain is indicated. N-terminal domain (NTD); proline-rich region (PRR); microtubule-binding repeats (MTBR); C-terminal domain (CTD). (B) Domain architecture of tau's six splice isoforms, construct size, and charge at neutral pH are indicated. (C) Common tau truncations. The charge (delta) for each truncation compared to 2N4R tau is indicated.

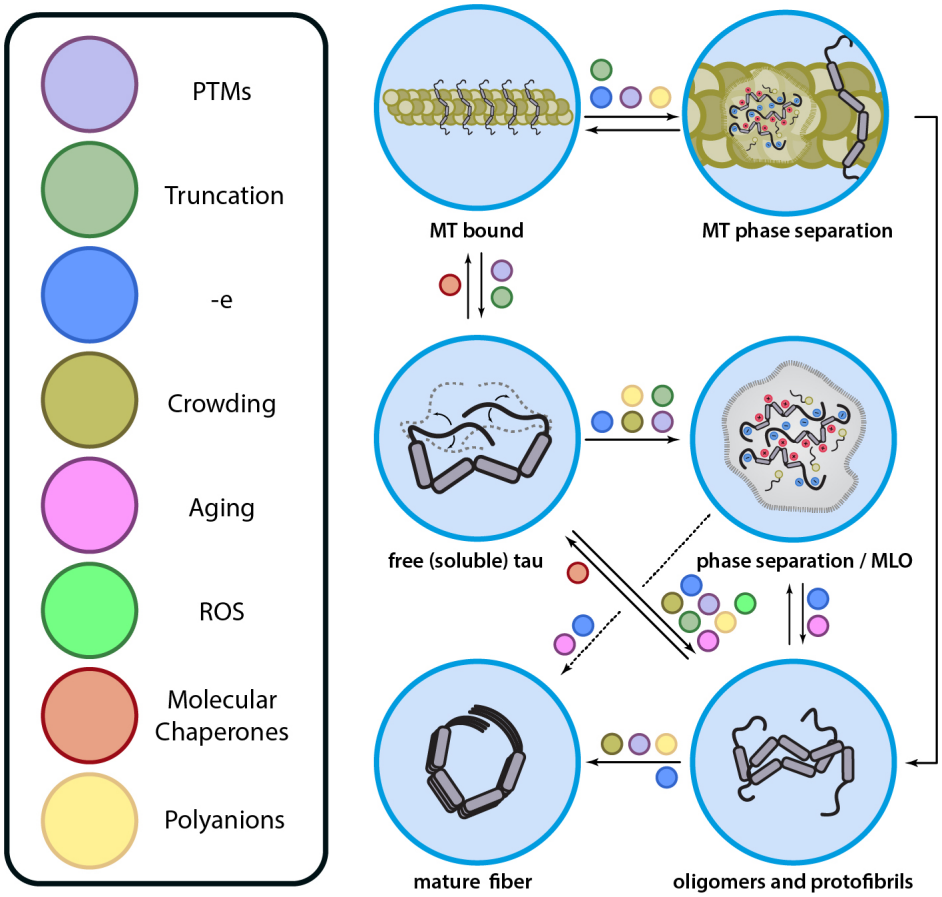

Figure 1.2. Tau's cellular interactome is vast. In a cell, tau interacts with diverse cellular components, is exposed to cellular stressors, and is modified by enzymes, proteostasis networks, and PTMs (left) — which directs conformational ensembles and eventual NFT assembly (right).

1.8 References

(1) Chen, D.; Drombosky, K. W.; Hou, Z.; Sari, L.; Kashmer, O. M.; Ryder, B. D.; Perez, V. A.; Woodard, D. N. R.; Lin, M. M.; Diamond, M. I.; Joachimiak, L. A. Tau Local Structure Shields an Amyloid-Forming Motif and Controls Aggregation Propensity. *Nat. Commun.* **2019**, *10* (1). https://doi.org/10.1038/s41467-019-10355-1.

(2) Eschmann, N. A.; Do, T. D.; Lapointe, N. E.; Shea, J.; Feinstein, S. C.; Bowers, M. T.; Han, S. Tau Aggregation Propensity Engrained in Its Solution State. **2015**. https://doi.org/10.1021/acs.jpcb.5b08092.

(3) Von Bergen, M.; Friedhoff, P.; Biernat, J.; Heberle, J.; Mandelkow, E. M.; Mandelkow, E. Assembly of τ Protein into Alzheimer Paired Helical Filaments Depends on a Local Sequence Motif (306VQIVYK311) Forming β Structure. *Proc. Natl. Acad. Sci. U. S. A.* **2000**, *97* (10), 5129–5134. https://doi.org/10.1073/pnas.97.10.5129.

(4) Schweers, O.; Schönbrunn-Hanebeck, E.; Marx, A.; Mandelkow, E. Structural Studies of Tau Protein and Alzheimer Paired Helical Filaments Show No Evidence for β-Structure. *J. Biol. Chem.* **1994**, *269* (39), 24290–24297. https://doi.org/10.1016/s0021-9258(19)51080-8.

(5) Elbaum-Garfinkle, S.; Rhoades, E. Identification of an Aggregation-Prone Structure of Tau. *J. Am. Chem. Soc.* **2012**, *134* (40), 16607–16613. https://doi.org/10.1021/ja305206m.

(6) Gustke, N.; Trinczek, B.; Biernat, J.; Mandelkow, E. M.; Mandelkow, E. Domains of Tau Protein and Interactions with Microtubules. *Biochemistry* **1994**, *33* (32), 9511–9522. https://doi.org/10.1021/bi00198a017.

(7) Falcon, B.; Zhang, W.; Murzin, A. G.; Murshudov, G.; Garringer, H. J.; Vidal, R.; Crowther, R. A.; Ghetti, B.; Scheres, S. H. W.; Goedert, M. Structures of Filaments from Pick's Disease Reveal a Novel Tau Protein Fold. *Nature* **2018**, *561* (7721), 137–140. https://doi.org/10.1038/s41586-018-0454-y.

(8) Lövestam, S.; Koh, F. A.; van Knippenberg, B.; Kotecha, A.; Murzin, A. G.; Goedert, M.; Scheres, S. H. W. Assembly of Recombinant Tau into Filaments Identical to Those of Alzheimer's Disease and Chronic Traumatic Encephalopathy. *Elife* **2022**, *11*, 1–27. https://doi.org/10.7554/eLife.76494.

(9) Radamaker, L.; Baur, J.; Huhn, S.; Haupt, C.; Hegenbart, U.; Schönland, S.; Bansal, A.; Schmidt, M.; Fändrich, M. Cryo-EM Reveals Structural Breaks in a Patient-Derived Amyloid Fibril from Systemic AL Amyloidosis. *Nat. Commun.* **2021**, *12* (1), 1–10. https://doi.org/10.1038/s41467-021-21126-2.

(10) Alicea, J. V.; Diamond, M. I.; Joachimiak, L. A. Tau Strains Shape Disease. *Acta Neuropathol.* **2021**, *142* (1), 57–71. https://doi.org/10.1007/s00401-021-02301-7.

(11) Fitzpatrick, A. W. P.; Falcon, B.; He, S.; Murzin, A. G.; Murshudov, G.; Garringer, H. J.; Crowther, R. A.; Ghetti, B.; Goedert, M.; Scheres, S. H. W. Cryo-EM Structures of Tau Filaments from Alzheimer's Disease. *Nature* **2017**, *547*, 185.

(12) Raskatov, J. A.; Teplow, D. B. Using Chirality to Probe the Conformational Dynamics and Assembly of Intrinsically Disordered Amyloid Proteins. *Sci. Rep.* **2017**, No. August, 1–7. https://doi.org/10.1038/s41598-017-10525-5.

(13) Adamcik, J.; Mezzenga, R. Amyloid Polymorphism in the Protein Folding and Aggregation Energy Landscape. *Angew. Chemie Int. Ed.* **2018**, *57* (28), 8370–8382. https://doi.org/https://doi.org/10.1002/anie.201713416.

(14) Gyparaki, M. T.; Arab, A.; Sorokina, E. M.; Santiago-Ruiz, A. N.; Bohrer, C. H.; Xiao, J.; Lakadamyali, M. Tau Forms Oligomeric Complexes on Microtubules That Are Distinct from Tau Aggregates. *Proc. Natl. Acad. Sci. U. S. A.* **2021**, *118* (19), 1–12. https://doi.org/10.1073/pnas.2021461118.

(15) Wegmann, S.; Medalsy, I. D.; Mandelkow, E.; Müller, D. J. The Fuzzy Coat of Pathological Human Tau Fibrils Is a Two-Layered Polyelectrolyte Brush. *Proc. Natl. Acad. Sci. U. S. A.* **2012**, *110* (4), E313–E321. https://doi.org/10.1073/pnas.1212100110.

(16) Weingarten, M. D.; Lockwood, A. H.; Hwo, S. Y.; Kirschner, M. W. A Protein Factor Essential for Microtubule Assembly. *Proc. Natl. Acad. Sci. U. S. A.* **1975**, *72* (5), 1858–1862. https://doi.org/10.1073/pnas.72.5.1858.

(17) Kadavath, H.; Hofele, R. V.; Biernat, J.; Kumar, S.; Tepper, K.; Urlaub, H.; Mandelkow, E.; Zweckstetter, M. Tau Stabilizes Microtubules by Binding at the Interface between Tubulin Heterodimers. *Proc. Natl. Acad. Sci. U. S. A.* **2015**, *112* (24), 7501–7506. https://doi.org/10.1073/pnas.1504081112.

(18) Mukrasch, M. D.; Markwick, P.; Biernat, J.; Von Bergen, M.; Bernadó, P.; Griesinger, C.; Mandelkow, E.; Zweckstetter, M.; Blackledge, M. Highly Populated Turn Conformations in Natively Unfolded Tau Protein Identified from Residual Dipolar Couplings and Molecular Simulation. *J. Am. Chem. Soc.* **2007**, *129* (16), 5235–5243. https://doi.org/10.1021/ja0690159.

(19) Castro, T. G.; Munteanu, F. D.; Cavaco-Paulo, A. Electrostatics of Tau Protein by Molecular Dynamics. *Biomolecules* **2019**, *9* (3). https://doi.org/10.3390/biom9030116.

(20) Kunjithapatham, R.; Oliva, F. Y.; Doshi, U.; Pérez, M.; Ávila, J.; Muñoz, V. Role for the α-Helix in Aberrant Protein Aggregation. *Biochemistry* **2005**, *44* (1), 149–156. https://doi.org/10.1021/bi048564t.

(21) Jeganathan, S.; Von Bergen, M.; Brutlach, H.; Steinhoff, H. J.; Mandelkow, E. Global Hairpin Folding of Tau in Solution. *Biochemistry* **2006**, *45* (7), 2283–2293. https://doi.org/10.1021/bi0521543.

(22) Kanaan, N. M.; Hamel, C.; Grabinski, T.; Combs, B. Liquid-Liquid Phase Separation Induces Pathogenic Tau Conformations in Vitro. *Nat. Commun.* **2020**, *11* (1). https://doi.org/10.1038/s41467-020-16580-3.

(23) Hirose, T.; Ninomiya, K.; Nakagawa, S.; Yamazaki, T. A Guide to Membraneless Organelles and Their Various Roles in Gene Regulation. *Nat. Rev. Mol. Cell Biol.* **2022**. https://doi.org/10.1038/s41580-022-00558-8.

(24) Gomes, E.; Shorter, J. The Molecular Language of Membraneless Organelles. *J. Biol. Chem.* **2019**, *294* (18), 7115–7127. https://doi.org/10.1074/jbc.TM118.001192.

(25) Boyko, S.; Qi1, X.; Chen, T. H.; Surewicz, K.; Surewicz, W. K. Liquid-Liquid Phase Separation of Tau Protein: The Crucial Role of Electrostatic Interactions. *J. Biol. Chem.* **2019**, *294* (29), 11054–11059. https://doi.org/10.1074/jbc.AC119.009198.

(26) Wegmann, S.; Eftekharzadeh, B.; Tepper, K.; Zoltowska, K. M.; Bennett, R. E.; Dujardin, S.; Laskowski, P. R.; MacKenzie, D.; Kamath, T.; Commins, C.; Vanderburg, C.; Roe, A. D.; Fan, Z.; Molliex, A. M.; Hernandez-Vega, A.; Muller, D.; Hyman, A. A.; Mandelkow, E.; Taylor, J. P.; Hyman, B. T. Tau Protein Liquid–Liquid Phase Separation Can Initiate Tau Aggregation. *EMBO J.* **2018**, *37* (7), 1–21. https://doi.org/10.15252/embj.201798049.

(27) Najafi, S.; Lin, Y.; Longhini, A. P.; Zhang, X.; Delaney, K. T.; Kosik, K. S.; Fredrickson, G. H.; Shea, J. Liquid – Liquid Phase Separation of Tau by Self and Complex Coacervation. **2021**, No. March, 1393–1407. https://doi.org/10.1002/pro.4101.

(28) Chen, X.; Chen, M.; Schafer, N. P.; Wolynes, P. G. Exploring the Interplay between Fibrillization and Amorphous Aggregation Channels on the Energy Landscapes of Tau Repeat Isoforms. *Proc. Natl. Acad. Sci. U. S. A.* **2020**, *117* (8), 4125–4130. https://doi.org/10.1073/pnas.1921702117.

(29) Lasagna-Reeves, C. A.; Castillo-Carranza, D. L.; Sengupta, U.; Clos, A. L.; Jackson, G. R.; Kayed, R. Tau Oligomers Impair Memory and Induce Synaptic and Mitochondrial Dysfunction in Wild-Type Mice. *Mol. Neurodegener.* **2011**, *6* (1), 1–14. https://doi.org/10.1186/1750-1326-6-39.

(30) Hill, E.; Wall, M. J.; Moffat, K. G.; Karikari, T. K. Understanding the Pathophysiological Actions of Tau Oligomers: A Critical Review of Current Electrophysiological Approaches. *Front. Mol. Neurosci.* **2020**, *13* (August), 1–9. https://doi.org/10.3389/fnmol.2020.00155.

(31) Kjaergaard, M.; Dear, A. J.; Kundel, F.; Qamar, S.; Meisl, G.; Knowles, T. P. J.; Klenerman, D. Oligomer Diversity during the Aggregation of the Repeat Region of Tau.

2018. https://doi.org/10.1021/acschemneuro.8b00250.

(32) Lo, C. H. Heterogeneous Tau Oligomers as Molecular Targets for Alzheimer ' s Disease and Related Tauopathies. **2022**, 440–451.

(33) Montgomery, K. M.; Carroll, E. C.; Thwin, A.; Hodges, P.; Southworth, D. R.; Gestwicki, J. E. The Chemical Features of Polyanions Modulate Tau Aggregation and Conformational States. *J. Am. Chem. Soc.* **2023**. https://doi.org/10.1101/2022.07.28.501920.

(34) Dregni, A. J.; Mandala, V. S.; Wu, H.; Elkins, M. R.; Wang, H. K.; Hung, I.; DeGrado, W. F.; Hong, M. In Vitro 0N4R Tau Fibrils Contain a Monomorphic β-Sheet Core Enclosed by Dynamically Heterogeneous Fuzzy Coat Segments. *Proc. Natl. Acad. Sci. U. S. A.* **2019**, *116* (33), 16357–16366. https://doi.org/10.1073/pnas.1906839116.

(35) Li, D.; Liu, C. Hierarchical Chemical Determination of Amyloid Polymorphs in Neurodegenerative Disease. *Nat. Chem. Biol.* **2021**, *17* (3), 237–245. https://doi.org/10.1038/s41589-020-00708-z.

(36) Kotecha, A.; Beers, M. Van; Tarutani, A.; Kametani, F.; Garringer, H. J.; Yoshida, M.; Tanaka, H.; Kakita, A.; Ikeuchi, T.; Robinson, A. C. Structure-Based Classification of Tauopathies. *Nature* **2021**, *598* (June). https://doi.org/10.1038/s41586-021-03911-7.

(37) Huseby, C. J.; Bundschuh, R.; Kuret, J. The Role of Annealing and Fragmentation in Human Tau Aggregation Dynamics. *J. Biol. Chem.* **2019**, *294* (13), 4728–4737. https://doi.org/10.1074/jbc.RA118.006943.

(38) Smit, F. X.; Luiken, J. A.; Bolhuis, P. G. Primary Fibril Nucleation of Aggregation Prone Tau Fragments PHF6 and PHF6 *. **2017**. https://doi.org/10.1021/acs.jpcb.6b07045.

(39) Rajan, R.; Ahmed, S.; Sharma, N.; Kumar, N.; Debas, A.; Matsumura, K. Review of the Current State of Protein Aggregation Inhibition from a Materials Chemistry Perspective: Special Focus on Polymeric Materials. *Mater. Adv.* **2021**, *2* (4), 1139–1176. https://doi.org/10.1039/d0ma00760a.

(40) Kim, A. C.; Lim, S.; Kim, Y. K. Metal Ion Effects on Aβ and Tau Aggregation. *Int. J. Mol.*

Sci. **2018**, *19* (1), 1–15. https://doi.org/10.3390/ijms19010128.

(41) Friedrich, M. G.; Skora, A.; Hancock, S. E.; Mitchell, T. W.; Else, P. L.; Truscott, R. J. W. Tau Is Truncated in Five Regions of the Normal Adult Human Brain. **2021**.

(42) Yin, H.; Kuret, J. C-Terminal Truncation Modulates Both Nucleation and Extension Phases of τ Fibrillization. *FEBS Lett.* **2006**, *580* (1), 211–215. https://doi.org/10.1016/j.febslet.2005.11.077.

(43) Gu, J.; Xu, W.; Jin, N.; Li, L.; Zhou, Y.; Chu, D.; Gong, C. X.; Iqbal, K.; Liu, F. Truncation of Tau Selectively Facilitates Its Pathological Activities. *J. Biol. Chem.* **2020**, *295* (40), 13812–13828. https://doi.org/10.1074/jbc.RA120.012587.

(44) Quinn, J. P.; Corbett, N. J.; Kellett, K. A. B.; Hooper, N. M. Tau Proteolysis in the Pathogenesis of Tauopathies: Neurotoxic Fragments and Novel Biomarkers. *J. Alzheimers. Dis.* **2018**, *63* (1), 13–33. https://doi.org/10.3233/JAD-170959.

(45) Chen, H.; Liu, P.; Auger, P.; Lee, S.; Adolfsson, O.; Rey-, L.; Lafrance-vanasse, J.; Friedman, B. A.; Pihlgren, M.; Muhs, A.; Pfeifer, A.; Ernst, J.; Ayalon, G.; Wildsmith, K. R.; Beach, T. G.; Brug, M. P. Van Der. Calpain-Mediated Tau Fragmentation Is Altered in Alzheimer ' s Disease Progression. **2018**, No. July, 1–15. https://doi.org/10.1038/s41598-018-35130-y.

(46) Amadoro, G.; Latina, V.; Corsetti, V.; Calissano, P. N-Terminal Tau Truncation in the Pathogenesis of Alzheimer's Disease (AD): Developing a Novel Diagnostic and Therapeutic Approac. *BBA - Mol. Basis Dis.* **2020**, *1866* (3), 165584. https://doi.org/10.1016/j.bbadis.2019.165584.

(47) Rizzu, P.; Swieten, J. C. Van; Joosse, M.; Hasegawa, M.; Stevens, M.; Tibben, A.; Niermeijer, M. F.; Hillebrand, M.; Ravid, R.; Oostra, B. A.; Goedert, M.; Duijn, C. M. Van; Heutink, P. High Prevalence of Mutations in the Microtubule-Associated Protein Tau in a Population Study of Frontotemporal Dementia in the Netherlands. **1999**, 414–421.

(48) Eckermann, K.; Mocanu, M.; Khlistunova, I.; Biernat, J.; Nissen, A.; Hofmann, A.; Scho,

K.; Bujard, H.; Haemisch, A.; Mandelkow, E.; Zhou, L.; Rune, G.; Mandelkow, E. The ᴺʟ - Propensity of Tau Determines Aggregation and Synaptic Loss in Inducible Mouse Models of Tauopathy *. **2007**, *282* (43), 31755–31765. https://doi.org/10.1074/jbc.M705282200.

(49) Means, J. C.; Gerdes, B. C.; Kaja, S.; Sumien, N.; Payne, A. J.; Stark, D. A.; Borden, P. K.; Price, J. L.; Koulen, P. Caspase 3 - Dependent Proteolytic Cleavage of Tau Causes Neurofibrillary Tangles and Results in Cognitive Impairment During Normal Aging. *Neurochem Res* **2016**, *41* (9), 2278–2288. https://doi.org/10.1007/s11064-016-1942-9.Caspase.

(50) Zhang, Q.; Zhang, X.; Sun, A. Truncated Tau at D421 Is Associated with Neurodegeneration and Tangle Formation in the Brain of Alzheimer Transgenic Models. *Acta Neuropathol.* **2009**, *117* (6), 687–697. https://doi.org/10.1007/s00401-009-0491-6.

(51) Meduri, G.; Guillemeau, K.; Dounane, O.; Sazdovitch, V.; Duyckaerts, C.; Chambraud, B.; Baulieu, E. E.; Giustiniani, J. Caspase-Cleaved Tau-D421 Is Colocalized with the Immunophilin FKBP52 in the Autophagy-Endolysosomal System of Alzheimer's Disease Neurons. *Neurobiol. Aging* **2016**, *46*, 124–137. https://doi.org/https://doi.org/10.1016/j.neurobiolaging.2016.06.017.

(52) Escudero, V. G.; Gabarre, D. R.; Gargini, R.; Pérez, M.; García, E.; Hernández, F.; Ávila, J. A New Non - Aggregative Splicing Isoform of Human Tau Is Decreased in Alzheimer ' s Disease. *Acta Neuropathol.* **2021**, *142* (1), 159–177. https://doi.org/10.1007/s00401-021-02317-z.

(53) Alquezar, C.; Arya, S.; Kao, A. W. Tau Post-Translational Modifications: Dynamic Transformers of Tau Function, Degradation, and Aggregation. *Front. Neurol.* **2021**, *11* (January), 1–24. https://doi.org/10.3389/fneur.2020.595532.

(54) Cohen, T. J.; Guo, J. L.; Hurtado, D. E.; Kwong, L. K.; Mills, I. P.; Trojanowski, J. Q.; Lee, V. M. Y. The Acetylation of Tau Inhibits Its Function and Promotes Pathological Tau

Aggregation. *Nat. Commun.* **2011**, *2* (252). https://doi.org/10.1038/ncomms1255.The.

(55) Xia, Y.; Prokop, S.; Giasson, B. I. “ Don ’ t Phos Over Tau ” : Recent Developments in Clinical Biomarkers and Therapies Targeting Tau Phosphorylation in Alzheimer ’ s Disease and Other Tauopathies. **2021**, 1–19.

(56) Haj-yahya, M.; Gopinath, P.; Rajasekhar, K.; Mirbaha, H.; Diamond, M. I.; Lashuel, H. A. Proteins Site-Specific Hyperphosphorylation Inhibits , Rather than Promotes , Tau Fibrillization , Seeding Capacity , and Its Microtubule Binding ** Research Articles Angewandte. **2020**, 4059–4067. https://doi.org/10.1002/anie.201913001.

(57) Strang, K. H.; Croft, C. L.; Sorrentino, Z. A.; Chakrabarty, P.; Golde, T. E.; Giasson, B. I. Distinct Differences in Prion-like Seeding and Aggregation between Tau Protein Variants Provide Mechanistic Insights into Tauopathies. *J. Biol. Chem.* **2018**, *293* (7), 2408–2421. https://doi.org/10.1074/jbc.M117.815357.

(58) Wolfe, M. S. Tau Mutations in Neurodegenerative Diseases. *J. Biol. Chem.* **2009**, *284* (10), 6021–6025. https://doi.org/10.1074/jbc.R800013200.

(59) Bergen, M. Von; Barghorn, S.; Li, L.; Marx, A.; Biernat, J.; Mandelkow, E.; Mandelkow, E. Mutations of Tau Protein in Frontotemporal Dementia Promote ␣ -Structure *. **2001**, *276* (51), 48165–48174. https://doi.org/10.1074/jbc.M105196200.

(60) Wright, P. E.; Dyson, H. J. Intrinsically Disordered Proteins in Cellular Signaling and Regulation. **2015**, *16* (1), 18–29. https://doi.org/10.1038/nrm3920.Intrinsically.

(61) Dinkel, P. D.; Holden, M. R.; Matin, N.; Margittai, M. RNA Binds to Tau Fibrils and Sustains Template-Assisted Growth. *Biochemistry* **2015**, *54* (30), 4731–4740. https://doi.org/10.1021/acs.biochem.5b00453.

(62) Wickramasinghe, S. P.; Lempart, J.; Merens, H. E.; Murphy, J.; Huettemann, P.; Jakob, U.; Rhoades, E. Polyphosphate Initiates Tau Aggregation through Intra- and Intermolecular Scaffolding. *Biophys. J.* **2019**, *117* (4), 717–728.

https://doi.org/10.1016/j.bpj.2019.07.028.

(63) Fichou, Y.; Lin, Y.; Rauch, J. N.; Vigers, M.; Zeng, Z.; Srivastava, M.; Keller, T. J.; Freed, J. H.; Kosik, K. S.; Han, S. Cofactors Are Essential Constituents of Stable and Seeding-Active Tau Fibrils. *Proc. Natl. Acad. Sci. U. S. A.* **2018**, *115* (52), 13234–13239. https://doi.org/10.1073/pnas.1810058115.

(64) Paudel, H. K.; Li, W. Heparin-Induced Conformational Change in Microtubule-Associated Protein Tau as Detected by Chemical Cross-Linking and Phosphopeptide Mapping. *J. Biol. Chem.* **1999**, *274* (12), 8029–8038. https://doi.org/10.1074/jbc.274.12.8029.

(65) Wegmann, S.; Schöler, J.; Bippes, C. A.; Mandelkow, E.; Muller, D. J. Competing Interactions Stabilize Pro- and Anti-Aggregant Conformations of Human Tau. *J. Biol. Chem.* **2011**, *286* (23), 20512–20524. https://doi.org/10.1074/jbc.M111.237875.

(66) Lima, M.; Rudd, T.; Yates, E. New Applications of Heparin and Other Glycosaminoglycans. **2017**, 1–11. https://doi.org/10.3390/molecules22050749.

(67) Iannuzzi, C.; Irace, G.; Sirangelo, I. The Effect of Glycosaminoglycans (GAGs) on Amyloid Aggregation and Toxicity. **2015**, 2510–2528. https://doi.org/10.3390/molecules20022510.

(68) Hurst, R. E.; Poon, M. C.; Griffith, M. J. Structure-Activity Relationships of Heparin. Independence of Heparin Charge Density and Antithrombin-Binding Domains in Thrombin Inhibition by Antithrombin and Heparin Cofactor II. *J. Clin. Invest.* **1983**, *72* (3), 1042–1045.

(69) Mah, D.; Zhao, J.; Liu, X.; Zhang, F.; Liu, J.; Wang, L. The Sulfation Code of Tauopathies : Heparan Sulfate Proteoglycans in the Prion Like Spread of Tau Pathology. **2021**, *8* (May), 1–12. https://doi.org/10.3389/fmolb.2021.671458.

(70) Zhao, J.; Huvent, I.; Lippens, G.; Eliezer, D.; Zhang, A.; Li, Q.; Tessier, P.; Linhardt, R. J.; Zhang, F.; Wang, C. Glycan Determinants of Heparin-Tau Interaction. *Biophysj* **2017**, *112* (5), 921–932. https://doi.org/10.1016/j.bpj.2017.01.024.

(71) Shriver, Z.; Street, W. K. Heparin and Heparan Sulfate: Analyzing Structure and Microheterogeneity. *Handb Exp Pharmacol.* **2012**, No. 207, 159–176. https://doi.org/10.1007/978-3-642-23056-1.

(72) Sibille, N.; Sillen, A.; Leroy, A.; Wieruszeski, J. M.; Mulloy, B.; Landrieu, I.; Lippens, G. Structural Impact of Heparin Binding to Full-Length Tau as Studied by NMR Spectroscopy. *Biochemistry* **2006**, *45* (41), 12560–12572. https://doi.org/10.1021/bi060964o.

(73) Goedert, M.; Jakes, R.; Spillantini, M. G.; Hasegawa, M.; Smith, M. J.; Crowther, R. A. Assembly of Microtubule-Associated Protein Tau into Alzheimer-like Filaments Induced by Sulphated Glycosaminoglycans. *Nature* **1996**, *383*, 550–553.

(74) Mukrasch, M. D.; Biernat, J.; Von Bergen, M.; Griesinger, C.; Mandelkow, E.; Zweckstetter, M. Sites of Tau Important for Aggregation Populate β-Structure and Bind to Microtubules and Polyanions. *J. Biol. Chem.* **2005**, *280* (26), 24978–24986. https://doi.org/10.1074/jbc.M501565200.

(75) Perez, M.; Valpuesta, J. M.; Avila, J. Role of Glycosaminoglycans in Determining the Helicity of Paired Helical Filaments. **1997**, *151* (4), 1115–1122.

(76) Townsend, D.; Fullwood, N. J.; Yates, E. A.; Middleton, D. A. Aggregation Kinetics and Filament Structure of a Tau Fragment Are Influenced by the Sulfation Pattern of the Cofactor Heparin. *Biochemistry* **2020**, *59* (41), 4003–4014. https://doi.org/10.1021/acs.biochem.0c00443.

(77) Snow, A. D.; Mar, H.; Nochlin, D.; Kimata, K.; Kato, M.; Suzuki, S.; Hassell, J.; Wight, T. N. The Presence of Heparan Sulfate Proteoglycans in the Neuritic Plaques and Congophilic Angiopathy in Alzheimer's Disease. *Am. J. Pathol.* **1988**, *133* (3), 456–463.

(78) Snow, A. D.; Wight, T. N.; Nochlin, D.; Koike, Y.; Kimata, K.; DeArmond, S. J.; Prusiner, S. B. Immunolocalization of Heparan Sulfate Proteoglycans to the Prion Protein Amyloid Plaques of Gerstmann-Straussler Syndrome, Creutzfeldt-Jakob Disease and Scrapie.

Lab. Invest. **1990**, *63* (5), 601–611.

(79) DeWitt, D. A.; Silver, J.; Canning, D. R.; Perry, G. Chondroitin Sulfate Proteoglycans Are Associated with the Lesions of Alzheimer's Disease. *Exp. Neurol.* **1993**, *121* (2), 149–152. https://doi.org/https://doi.org/10.1006/exnr.1993.1081.

(80) Reily, C.; Stewart, T. J.; Renfrow, M. B.; Novak, J. Glycosylation in Health and Disease. *Nat. Rev. Nephrol.* **2019**, *15*. https://doi.org/10.1038/s41581-019-0129-4.

(81) Akoury, E.; Mukrasch, M. D.; Biernat, J.; Tepper, K.; Ozenne, V.; Mandelkow, E.; Blackledge, M.; Zweckstetter, M. Remodeling of the Conformational Ensemble of the Repeat Domain of Tau by an Aggregation Enhancer. *Protein Sci.* **2016**, *25* (5), 1010–1020. https://doi.org/10.1002/pro.2911.

(82) Tolmachev, D.; Mamistvalov, G.; Lukasheva, N.; Larin, S.; Karttunen, M. Effects of Amino Acid Side-Chain Length and Chemical Structure on Anionic Polyglutamic and Polyaspartic Acid. **2021**, *13* (11).

(83) Xie, L.; Jakob, U. Inorganic Polyphosphate, a Multifunctional Polyanionic Protein Scaffold. *J. Biol. Chem.* **2019**, *294* (6), 2180–2190. https://doi.org/10.1074/jbc.REV118.002808.

(84) Holmström, K. M.; Marina, N.; Baev, A. Y.; Wood, N. W.; Gourine, A. V.; Abramov, A. Y. Signalling Properties of Inorganic Polyphosphate in the Mammalian Brain. *Nat. Commun.* **2013**, *4*, 1–8. https://doi.org/10.1038/ncomms2364.

(85) Stotz, S. C.; Scott, L. O.; Drummond-Main, C.; Avchalumov, Y.; Girotto, F.; Davidsen, J.; Gómez-Gárcia, M. R.; Rho, J. M.; Pavlov, E. V.; Colicos, M. A. Inorganic Polyphosphate Regulates Neuronal Excitability through Modulation of Voltage-Gated Channels. *Mol. Brain* **2014**, *7* (1), 1–9. https://doi.org/10.1186/1756-6606-7-42.

(86) Maiolino, M.; Neill, N. O.; Lariccia, V.; Amoroso, S.; Sylantyev, S.; Angelova, P. R.; Abramov, X. A. Y. Inorganic Polyphosphate Regulates AMPA and NMDA Receptors and Protects Against Glutamate Excitotoxicity via Activation of P2Y Receptors. **2019**, *39* (31),

6038–6048.

(87) Lempart, J.; Jakob, U. Role of Polyphosphate in Amyloidogenic Processes. *Cold Spring Harb. Perspect. Biol.* **2019**, 1–12. https://doi.org/10.1101/cshperspect.a034041.

(88) Arredondo, C.; Cefaliello, C.; Dyrda, A.; Jury, N.; Martinez, P.; Díaz, I.; Amaro, A.; Tran, H.; Morales, D.; Pertusa, M.; Stoica, L.; Fritz, E.; Corvalán, D.; Abarzúa, S.; Méndez-Ruette, M.; Fernández, P.; Rojas, F.; Kumar, M. S.; Aguilar, R.; Almeida, S.; Weiss, A.; Bustos, F. J.; González-Nilo, F.; Otero, C.; Tevy, M. F.; Bosco, D. A.; Sáez, J. C.; Kähne, T.; Gao, F.-B.; Berry, J. D.; Nicholson, K.; Sena-Esteves, M.; Madrid, R.; Varela, D.; Montecino, M.; Brown, R. H.; van Zundert, B. Excessive Release of Inorganic Polyphosphate by ALS/FTD Astrocytes Causes Non-Cell-Autonomous Toxicity to Motoneurons. *Neuron* **2022**, *110* (10), 1656-1670.e12. https://doi.org/https://doi.org/10.1016/j.neuron.2022.02.010.

(89) Cremers, C. M.; Knoefler, D.; Gates, S.; Martin, N.; Dahl, J. U.; Lempart, J.; Xie, L.; Chapman, M. R.; Galvan, V.; Southworth, D. R.; Jakob, U. Polyphosphate: A Conserved Modifier of Amyloidogenic Processes. *Mol. Cell* **2016**, *63* (5), 768–780. https://doi.org/10.1016/j.molcel.2016.07.016.

(90) Koren, S.; Galvis-escobar, S.; Abisambra, J. F. Tau-Mediated Dysregulation of RNA: Evidence for a Common Molecular Mechanism of Toxicity in Frontotemporal Dementia and Other Tauopathies. *Neurobiol Dis* **2021**, 1–16. https://doi.org/10.1016/j.nbd.2020.104939.

(91) Maziuk, B. F.; Apicco, D. J.; Cruz, A. L.; Jiang, L.; Ash, P. E. A.; Lummertz, E.; Zhang, C.; Yu, W. H.; Leszyk, J.; Abisambra, J. F.; Li, H.; Wolozin, B. RNA Binding Proteins Co-Localize with Small Tau Inclusions in Tauopathy. **2018**, 1–14.

(92) Ginsberg, S. D.; Crino, P. B.; Lee, V. M.-Y.; Eberwine, J. H.; Trojanowski, J. Q. Sequestration of RNA in Alzheimer's Disease Neurofibrillary Tangles and Senile Plaques. *Ann. Neurol.* **1997**, *41* (2), 200–209.

https://doi.org/https://doi.org/10.1002/ana.410410211.

(93) Lester, E.; Ooi, F. K.; Bakkar, N.; Ayers, J.; Woerman, A. L.; Wheeler, J.; Bowser, R.; Carlson, G. A.; Prusiner, S. B.; Parker, R. Tau Aggregates Are RNA-Protein Assemblies That Mislocalize Multiple Nuclear Speckle Components. *Neuron* **2021**, *109* (10), 1675-1691.e9. https://doi.org/10.1016/j.neuron.2021.03.026.

(94) Dinkel, P. D.; Holden, M. R.; Matin, N.; Margittai, M. RNA Binds to Tau Fibrils and Sustains Template-Assisted Growth. *Biochemistry* **2015**, *54* (30), 4731–4740. https://doi.org/10.1021/acs.biochem.5b00453.

(95) Abskharon, R.; Sawaya, M. R.; Cao, Q.; Nguyen, B. A.; Boyer, D. R.; Cascio, D.; Eisenberg, D. S. Cryo-EM Structure of RNA-Induced Tau Fibrils Reveals a Small C-Terminal Core That May Nucleate Fibril Formation. *Proc. Natl. Acad. Sci. U. S. A.* **2022**, *119* (15), 1–26. https://doi.org/10.1073/pnas.2119952119.

(96) Zwierzchowski-Zarate, A. N.; Mendoza-Oliva, A.; Kashmer, O. M.; Collazo-Lopez, J. E.; White, C. L.; Diamond, M. I. RNA Induces Unique Tau Strains and Stabilizes Alzheimer's Disease Seeds. *J. Biol. Chem.* **2022**, *298* (8), 102132. https://doi.org/10.1016/j.jbc.2022.102132.

(97) Villasante, A.; Corces, V. G.; Manso-Martínez, R.; Avila, J. Binding of Microtubule Protein to DNA and Chromatin: Possibility of Simultaneous Linkage of Microtubule to Nucleic Acid and Assembly of the Microtubule Structure. *Nucleic Acids Res.* **1981**, *9* (4), 895–908. https://doi.org/10.1093/nar/9.4.895.

(98) Rady, R. M.; Zinkowski, R. P.; Binder, L. I. Presence of Tau in Isolated Nuclei from Human Brain. *Neurobiol. Aging* **1995**, *16* (3), 479–486. https://doi.org/https://doi.org/10.1016/0197-4580(95)00023-8.

(99) Lu, J.; Li, T.; He, R. Q.; Bartlett, P. F.; Götz, J. Visualizing the Microtubule-Associated Protein Tau in the Nucleus. *Sci. China Life Sci.* **2014**, *57* (4), 422–431. https://doi.org/10.1007/s11427-014-4635-0.

(100) Maina, M. B.; Al-Hilaly, Y. K.; Serpell, L. C. Nuclear Tau and Its Potential Role in Alzheimer's Disease. *Biomolecules* **2016**, *6* (1), 2–20. https://doi.org/10.3390/biom6010009.

(101) Dehhaghi, M.; Kazemi Shariat Panahi, H.; Guillemin, G. J. Microorganisms' Footprint in Neurodegenerative Diseases. *Front. Cell. Neurosci.* **2018**, *12* (December). https://doi.org/10.3389/fncel.2018.00466.

(102) Coureuil, M.; Lécuyer, H.; Bourdoulous, S.; Nassif, X. A Journey into the Brain: Insight into How Bacterial Pathogens Cross Blood-Brain Barriers. *Nat. Rev. Microbiol.* **2017**, *15* (3), 149–159. https://doi.org/10.1038/nrmicro.2016.178.

(103) Dominy, S. S.; Lynch, C.; Ermini, F.; Benedyk, M.; Marczyk, A.; Konradi, A.; Nguyen, M.; Haditsch, U.; Raha, D.; Griffin, C.; Holsinger, L. J.; Arastu-kapur, S.; Kaba, S.; Lee, A.; Ryder, M. I.; Potempa, B.; Mydel, P.; Hellvard, A.; Adamowicz, K.; Hasturk, H.; Walker, G. D.; Reynolds, E. C.; Faull, R. L. M.; Curtis, M. A. Porphyromonas Gingivalis in Alzheimer's Disease Brains: Evidence for Disease Causation and Treatment with Small-Molecule Inhibitors. **2019**, 1–21.

(104) Tkáčová, Z.; Pulzová, L. B.; Mochnáčová, E.; Jiménez-Munguía, I.; Bhide, K.; Mertinková, P.; Majerová, P.; Kulkarni, A.; Kováč, A.; Bhide, M. Identification of the Proteins of Borrelia Garinii Interacting with Human Brain Microvascular Endothelial Cells. *Ticks Tick. Borne. Dis.* **2020**, *11* (4), 101451. https://doi.org/https://doi.org/10.1016/j.ttbdis.2020.101451.

(105) Colnaghi, L.; Rondelli, D.; Muzi-falconi, M.; Sertic, S. Brain Sciences Tau and DNA Damage in Neurodegeneration. **2020**, 1–15.

(106) Farmen, K.; Tofiño-Vian, M.; Iovino, F. Neuronal Damage and Neuroinflammation, a Bridge Between Bacterial Meningitis and Neurodegenerative Diseases . *Frontiers in Cellular Neuroscience* . 2021.

(107) Wood, P. L.; Tippireddy, S.; Feriante, J.; Woltjer, R. L. Augmented Frontal Cortex

Diacylglycerol Levels in Parkinson ' s Disease and Lewy Body Disease. **2018**, 1–15.

(108) Kawarabayashi, T.; Shoji, M.; Younkin, L. H.; Wen-lang, L.; Dickson, D. W.; Murakami, T.; Matsubara, E.; Abe, K.; Ashe, K. H.; Younkin, S. G. Dimeric Amyloid ᵑʟ Protein Rapidly Accumulates in Lipid Rafts Followed by Apolipoprotein E and Phosphorylated Tau Accumulation in the Tg2576 Mouse Model of Alzheimer ' s Disease. **2004**, *24* (15), 3801–3809. https://doi.org/10.1523/JNEUROSCI.5543-03.2004.

(109) Wilson, D. M.; Binder, L. I. Free Fatty Acids Stimulate the Polymerization of Tau and Amyloid Beta Peptides. In Vitro Evidence for a Common Effector of Pathogenesis in Alzheimer's Disease. *Am. J. Pathol.* **1997**, *150* (6), 2181–2195.

(110) Chirita, C. N.; Necula, M.; Kuret, J. Anionic Micelles and Vesicles Induce Tau Fibrillization in Vitro. *J. Biol. Chem.* **2003**, *278* (28), 25644–25650. https://doi.org/10.1074/jbc.M301663200.

(111) Gellermann, G. P.; Appel, T. R.; Davies, P.; Diekmann, S. Paired Helical Filaments Contain Small Amounts of Cholesterol, Phosphatidylcholine and Sphingolipids. **2006**, *387* (9), 1267–1274. https://doi.org/doi:10.1515/BC.2006.157.

(112) Shao, F.; Wang, X.; Wu, H.; Wu, Q.; Zhang, J. Microglia and Neuroinflammation : Crucial Pathological Mechanisms in Traumatic Brain Injury-Induced Neurodegeneration. **2022**, *14* (March), 1–16. https://doi.org/10.3389/fnagi.2022.825086.

(113) Bartolome, F.; Carro, E. Oxidative Stress in Tauopathies : From Cause to Therapy. **2022**, 1–23.

(114) Elise, L.; Banna, N. El; Heneman-masurel, A. Causative Links between Protein Aggregation and Oxidative Stress : A Review. *Int. J. Mol. Sci.* **2019**, *20* (3896).

(115) Chen, H.; Liu, S.; Li, S.; Chen, J.; Ni, J.; Liu, Q. Blocking the Thiol at Cysteine-322 Destabilizes Tau Protein and Prevents Its Oligomer Formation. **2018**. https://doi.org/10.1021/acschemneuro.8b00003.

(116) Hatters, D. M. Flipping the Switch : How Cysteine Oxidation Directs Tau Amyloid Conformations. *J. Biol. Chem.* **2021**, *297* (5), 101309. https://doi.org/10.1016/j.jbc.2021.101309.

(117) Prifti, E.; Tsakiri, E. N.; Vourkou, E.; Stamatakis, G.; Samiotaki, M.; Papanikolopoulou, K. The Two Cysteines of Tau Protein Are Functionally Distinct and Contribute Differentially to Its Pathogenicity in Vivo. *Neurobiol Dis* **2021**, *41* (4), 797–810.

Chapter II

Chemical Features of Polyanions Modulate Tau Aggregation and Conformational States

2.1 Abstract

The aggregation of tau into insoluble fibrils is a defining feature of neurodegenerative tauopathies. However, tau has a positive overall charge and is highly soluble; so polyanions, such as heparin, are typically required to promote its aggregation *in vitro*. There are dozens of polyanions in living systems and it is not clear which ones might promote this process. Here, we systematically measure the ability of 37 diverse, anionic biomolecules to initiate tau aggregation, using either wild type (WT) tau or the disease associated P301S mutant. We find that polyanions from many different structural classes can promote fibril formation and that P301S tau is sensitive to a greater number of polyanions (28/37) than WT tau (21/37). We also find that some polyanions preferentially reduce the lag time of the aggregation reactions, while others enhance the elongation rate, suggesting that they act on partially distinct steps. From the resulting structure-activity relationships, the valency of the polyanion seems to be an important chemical feature, such that anions with low valency tend to be weaker aggregation inducers, even at the same overall charge. Finally, the identity of the polyanion influences fibril morphology, based on electron microscopy and limited proteolysis. These results provide insight into the crucial role of polyanion—tau interactions in modulating tau conformational dynamics with implications for understanding the tau aggregation landscape in a complex cellular environment.

2.2 Introduction

The class of neurodegenerative disorders known as tauopathies, including Alzheimer's disease (AD), cortical basal degeneration (CBD) and progressive supranuclear palsy (PSP), are characterized by the accumulation of insoluble protein aggregates in the brain[1,2]. These aggregates are primarily composed of microtubule-associated protein tau (MAPT/tau), an intrinsically disordered protein that is expressed as a series of six distinct splice isoforms[3,4]. Tau's isoforms are composed of a variable number of N-terminal domains (0N, 1N or 2N), a proline-rich domain and either three or four microtubule-binding repeats (3R or 4R; Fig 1A). The common adult isoform of tau, 0N4R, is strongly cationic at physiological pH, with an isoelectric point of ~9.5. Accordingly, it has been known for decades that purified tau is highly soluble and not prone to spontaneously self-associate *in vitro,* even at extremes of pH and temperature[5]. Rather, tau aggregation is typically initiated by the addition of polyanionic biomolecules, such as heparin sodium (HS), which leads to relatively rapid self-assembly[6]. It is thought that the polyanions reduce charge repulsion between cationic tau monomers, allowing the juxtaposition of aggregation motifs within the R repeats[7,8]. These observations suggest that polyanions could also be involved in the initiation of tau aggregation *in vivo*. In support of this idea, HS is associated with tau pathology in patient brains[9] and unresolved densities are observed in some purified, patient-derived tau fibril samples, which are hypothesized to be anions or salts[10,11]. At present, we do not know the identity of the critical natural anion(s) or how their chemical properties might contribute to tau aggregation or fibril structure.

Structural studies have revealed that the core of tau can adopt a variety of conformations within fibrils; for instance, postmortem brain slices derived from patients with PSP and CBD contain tau fibrils with distinct folds[12–15]. Could the identity of the anion help dictate these specific conformations? To reach the fibril state, tau is known to transition through intermediate structures,

including oligomers[16,17]. While many factors likely contribute to the eventual structural differences between fibrils[18–20], we hypothesize that the polyanion could help guide early stages of the self-assembly process and contribute to determining the final structure. Indeed, an increasing body of evidence suggests that polyanions have an effect on early stages of fibril nucleation *in vitro*[21–23]. Yet, only a limited number of anions, including those in the broad categories of sugars[8], fatty acids[24], nucleic acids[25], and phosphates[26,27] have been studied for their ability to promote tau self-assembly and a systematic study, involving direct comparisons between these varied molecules under the same experimental conditions, is lacking.

Here, we collected 37 chemically and structurally diverse anions and tested them side-by-side in a thioflavin T (ThT) assay to identify those that mediate tau's aggregation. We find that a surprisingly large number of anionic biomolecules, including sugars, polypeptides, nucleic acids, amino acids and lipids, promote this process. Valency appears to be an important feature of these molecules, because only polyanions of sufficient repeat length were able to promote fibril formation. We also find that a disease-associated mutant, P301S tau, is sensitive to a larger number of anions (28/37) than wild type (21/37), which could be one reason why it is linked to severe disease. A subset of the inert anions were found to inhibit tau aggregation in the presence of heparin. To explore the potential impact of polyanions on the conformation of tau fibrils, we selected some of the most potent inducers and explored the resulting fibrils by limited proteolysis, sedimentation and transmission electron microscopy (TEM). Remarkably, we find that the identity of the polyanion has a dramatic effect on tau fibril conformation. Together, these results expand our knowledge of the role of polyanions in tau aggregation *in vitro.* Based on these findings, we speculate that the chemical composition of specific anions is one important factor in shaping induction potential and fibril conformation.

2.3 Experimental Section

2.3.1 Recombinant protein expression and purification

The gene encoding human 0N4R tau was cloned into a pET-28a vector and transfected into *E. coli* BL21(DE3) competent cells. Starter cultures were grown in Luria broth (LB) containing 50 µg/mL kanamycin overnight at 37 °C with constant shaking at 200 rpm. Then, 20 mL of the starter culture was used to inoculate 1L of Terrific broth (TB), containing 50 µg/mL of kanamycin. Cells were grown at 37 °C, with constant shaking, until OD_{600} between 0.6 and 0.8 was reached. At this point, the incubation temperature was set to 30 °C, and NaCl (500 mM) and betaine (10 mM), were included in the growth medium. After 30 minutes, expression was induced with 200 µM IPTG for 3.5 h at 30 °C.

To purify tau, cells were pelleted and resuspended in a lysis buffer containing 20 mM MES (pH 6.8), 1 mM EGTA, 0.2 mM $MgCl_2$, 5 mM DTT, and 1x cOmplete™ protease inhibitor cocktail (Roche). Cells were lysed by sonication and then boiled for 20 minutes. The lysate was clarified by centrifugation for 30 minutes at 30,000 x g. The clarified supernatant was dialyzed overnight into His binding buffer (1x PBS, 20 mM imidazole, 200 mM NaCl, and 5 mM b-mercaptoethanol (BME)) and purified by affinity purification.

His-tagged tau was bound to Ni-NTA resin for 1 h at 4 °C with constant mixing. The resin was washed using 500 mL of His binding buffer (1x PBS, 20 mM imidazole, 200 mM NaCl, and 5 mM BME), wash buffer 1 (1x PBS, 10 mM imidazole, 300 mM NaCl, and 5 mM BME) and, wash buffer 2 (1x dPBS, 15 mM imidazole, 100 mM NaCl, and 5 mM BME), and then eluted using 30 mL of elution buffer (1x PBS, 300 mM imidazole, 200 mM NaCl, and 5 mM BME). Tau was further purified using reverse-phase HPLC, as described previously[14]. The His tag was not removed, as it was found to not interfere with the aggregation reactions[28,29]. The protein was then lyophilized and resuspended in tau buffer (1x dPBS, 2 mM $MgCl_2$, and 1 mM DTT). Protein concentration

was determined using the bichinchronic acid (BCA) method. Purity was >95%, as judged by Coomassie gels (Supplementary Fig. S11).

2.3.2 Compound Preparation

All compounds including anions and polyanions were sourced from commercial vendors and used without further purification. See Tables 1 and 2 for details of the catalog numbers. Each polyanion was freshly prepared in assay buffer (1x Dulbecco's PBS pH 7.4, 2 mM $MgCl_2$, 1 mM DTT) and sterilized with a 0.2-micron filter before each experiment. Lipid inducers (arachidonic acid, linoleic acid, phosphatidyl-L-serine) were handled similarly, except that they contained a final concentration of 5% ethanol to maintain solubility.

2.3.3 Tau aggregation and kinetic screening

The ThT-based aggregation screen was performed in a miniaturized, 384-well plate format[24]. The microplates (Corning 4511) were pre-rinsed with 20 µL 0.01% Triton-X to minimize interactions with the sides of the plate. In each well, tau (10 µM), thioflavin T (10 µM), polyanion (see Tables 1 and 2) for concentrations) and assay buffer (Dulbecco's PBS pH 7.4, 2 mM $MgCl_2$, 1 mM DTT) were added to each well, to a total volume of 20 µL. The aggregation reaction was carried out at 37 °C with continuous shaking and monitored via fluorescence (excitation=444 nm, emission=485 nm, cutoff=480 nm) in a Spectramax M5 microplate reader (Molecular Devices). Readings were taken every 5 min for at least 24 h. Each experiment was performed in triplicate wells. All components of the aggregation reaction were freshly prepared each day.

2.3.4 Data processing

For data processing, the ThT signal produced by three replicates of the tau-only controls (no inducer) were averaged and this background was subtracted from corresponding samples. These values were typically less than 5 to 10% of the overall signal. For inducers with ThT background

greater than 10%, mainly chondroitin sulfate A, inducer + ThT background was further subtracted. To identify the dose of inducer for subsequent kinetic analyses, we first determined the inducer concentration required to produce half-maximal ThT fluorescence signal by fitting the fluorescence curves to a sigmoid in GraphPad PRISM. Using the half maximal concentration, we analyzed the kinetic parameters of tau aggregation using the Grace plotting program (http://plasma-gate.weizmann.ac.il/Grace/) and fitting the aggregation curves to the Gompertz function: $y=Ae^{(-e^{((t-ti\_i)/b))}}$, as previously described[24]. In that equation, the lag-time is defined by the inflection point; the inverse of apparent elongation rate constant (ti-b). In addition, A represents the maximum ThT signal, and the apparent elongation rate constant is 1/b. For error analysis, we considered the kinetic measurements from individual experiments and used them to calculate standard error of the mean (SEM), without considering additional error introduced by goodness of fit.

2.3.5 Fibril preparation for proteolysis

The aggregation reaction was performed in 1.5 mL Eppendorf tubes for 48 hours with constant agitation at 1200 rpm. The reactions included tau (10 µM) and inducer (see Tables 1 and 2 for concentrations) in assay buffer (Dulbecco's PBS pH 7.4, 2 mM $MgCl_2$, 1 mM DTT) with a total volume of 300 µL. After 48 hours, the reactions were subjected to ultracentrifugation (Beckman Optima™ Max-XP Tabletop Ultracentrifuge) using a TLA-55 Fixed-Angle Rotor at 103,000 rcf to remove monomeric tau and excess inducer. Pelleted tau fibrils were then resuspended in 1/3-1/4 of the reaction volume and the concentration was determined by Coomassie band intensity measured against a standard and quantified in ImageLab (BioRad).

2.3.6 Limited proteolysis

Soluble tau and freshly prepared fibrils were digested with Promega sequencing grade trypsin at a protein:protease ratio 500:1 for 60 minutes at 37 °C. The reaction was performed in 40 mM

HEPES 40 mM NaCl pH 8.0. Reactions were quenched with 3X SDS loading buffer + 1 mM PMSF and immediately heat denatured at 95 °C for 5 minutes. The proteolysis reactions were separated using a 4-20% polyacrylamide Tris-glycine SDS-PAGE denaturing gel (Invitrogen). Gels were transferred to nitrocellulose using a TurboBlot (BioRad) and analyzed using antibodies corresponding to several tau epitopes (anti-tau 1, 5, 13 and anti-tau 4R). Mouse anti-tau 1, 5 (Thermo) and rabbit anti-4R tau (Abcam) were prepared 1:1000 in Intercept T20 (TBS) Antibody Diluent (LiCor) and anti-tau 13 (Abcam) was prepared 1:5000. All secondary antibodies were prepared 1:10000 in 1:1 TBST and T20 (TBS) Antibody Diluent (LiCor).

2.3.7 Transmission electron microscopy

0N4R tau^{WT} fibrils were freshly prepared as described above in the kinetic screening assay, for 36 hours without ThT present. The corresponding samples were pooled and subsequently immobilized on 600-mesh carbon-coated copper grids (SPI). The samples were incubated for 30 seconds on a glow-discharged grid, and then the solution was removed by filter paper. Three washing steps with double distilled H_2O were followed by three staining steps with 0.75% (w/v) uranyl formate (Electron Microscopy Sciences). The samples were imaged using a FEI Tecnai 10 operated at 100 keV. Micrograph images were recorded using a 4kx 4k CCD camera (Gatan). The fibril dimensions were measured using the ImageJ software.

2.3.8 Fibril Sedimentation

Tau fibrils were prepared as described in the kinetic screening assay, excluding ThT. Samples were subsequently pooled and centrifuged at 13,000 rpm for 30 minutes at RT. Supernatants were removed, and the insoluble material was washed with 100 µL of assay buffer (1x dPBS, 2 mM $MgCl_2$, 1 mM DTT) followed by an additional 30-minute centrifugation at 13,000 rpm. Following the wash, the buffer was removed, and fresh assay buffer was added to each sample. Samples were sonicated for 10 minutes, mixed with 3X SDS loading buffer, and boiled for 5

minutes prior to analysis on a 2-20% denaturing gel. Gels were stained using Coomassie brilliant blue and imaged using a ChemiDoc Imaging system.

2.4 Results and Discussion

2.4.1 Creation of an anion library

In choosing anions for a chemical library, we sought to incorporate benchmark compounds, such as heparin sodium (HS), as well as molecules from a variety of structural classes that had never been previously tested for their effects on tau aggregation. Accordingly, we purchased anionic sugars (**1**-**12**), polyphosphates (**13**-**19**), short chain fatty acids (**20**-**24**), polypeptides (**25**-**30**) and oligonucleotides (**31-34**; Fig 1B), as well as anions from more chemically diverse classes, such as antibiotics (**36**), biladienes (**37**) and synthetic polymers (*i.e* polystyrene sulfonate, **35**). Only a subset of these compounds (**1, 6, 13, 15**, and **31**), had, to our knowledge, been previously tested for their effects on tau aggregation. While the major goal of this panel was to sample different scaffolds, some of the library members varied in their chemical properties. For example, fondaparinux (**7**), polyphosphate (**15**), and polyadenylic-polyuridylic acid (poly-AU; **32**) have varying charge density: -10 per monomer for compound **7**, -1 per monomer for **13** and -2 for **25** (Fig 1B). Thus, we also hoped that screening this collection might also begin to reveal chemical features important for tau aggregation.

Previous work had shown that anions employ at least two mechanisms to promote tau self-assembly. For example, HS (**1**) is an example of the polymer class of inducers, and it is decorated with sulfates from a repeating disaccharide unit (Fig 1B). HS and related compounds are thought to mitigate the unfavorable, long-range electrostatic interactions in tau, favoring hydrophobic collapse of the core[5,30–32]. However, another mechanism is linked to monovalent anions, such as arachidonic acid (**20**), which are thought to function by first forming micelles on which tau assembles[33–35]. In our anion library, examples of both categories are included, and we anticipated

that polymers, such as sugars, nucleotides, and phosphates, might function similarly to HS, while the lipids and other non-polymers, might potentially function as micelles**.**

2.4.2 Screens identify the subset of anions that promote tau aggregation

To evaluate the anion library, we measured tau aggregation using a 384-well, plate-based, ThT platform (Fig 1C)[24]. Briefly, our goal was to first screen each anion at a range of concentrations to reveal which ones could support tau aggregation; then, we would focus on the most potent inducers to perform more detailed kinetic and structural studies. In these experiments, we employed two purified, recombinant human proteins; 0N4R tau (WT; Table 1) and a 0N4R P301S mutant (P301S; Table 2). P301S is a genetic mutation associated with FTD-linked Parkinsonism-17 (FTDP-17) that produces severe frontal temporal atrophy[36]. It is known that P301S is more aggregation prone than WT in the presence of HS[37,38] so we reasoned that it might be more sensitive to weaker inducers.

In the initial screens, we tested each member of the anion library at a range of concentrations. These ranges (see Supplemental Tables 1 and 2) were either selected from the literature (for known inducers) or chosen empirically (for those that had not been studied previously). These experiments were performed in triplicate using ThT signal measured every 5 minutes for a minimum of 24 hours with shaking at 37 °C (see Methods). At the same time, we performed experiments in the absence of tau protein to reveal any anions that might produce artifacts. Indeed, this control was important because we found that gangliosides (**23-24**), and several nucleic acids, including tRNA (**33**), polyA (**31**), and polyAU (3**2**), produced ThT signal in the absence of protein (Supplemental Fig S1) and, accordingly they were excluded from further analysis (Supplemental Tables 1 and 2). Chondroitin sulfate A (CS; **2**) produced a relatively modest tau-independent signal which could be subtracted from the experimental samples (Supplemental Fig S1), so this inducer was carried forward into the next experiments. For the

remaining anions, we placed them into three categories based on the maximum ThT signal that they produced. Those considered to be “inactive” failed to reach saturation and yielded 40 or less RFUs (ΔRFU ≤ 40) above baseline at 24 hours (Supplemental Tables 1 and 2; Supplemental Fig S2). Inducers were determined to be “moderately active” if they yielded a ΔRFU > 40, but did not reach a maximum ThT signal at the highest tested concentration of the anion (Supplemental Fig S3). Finally, inducers were “active” if they produced ΔRFU > 40 with a full sigmoidal curve (Supplemental Figures S4 and S5). For these anions, we determined their relative potency by fitting the sigmoid of the dose response and determining the half-maximal value (EC_{50}). Importantly, we noted that a subset of “active” anions produced a hook-like effect in their dose response; they initially promote ThT signal at lower concentrations and then become inhibitory with increased dosing (Supplemental Fig S6). For example, polystyrene sulfonate (**35**) becomes inhibitory at concentrations above 250 µg/mL. For this subset of molecules, we estimated EC_{50} using the upper inflection point as the top concentration.

One of the striking results from this screen is that tau aggregation is achieved with a large number of diverse anions. More specifically, for WT tau, we find that (11/37) molecules are strongly active and (10/37) are modestly active (Supplemental Table 1). Together, these active molecules represent 6 out of the 7 structural categories (Fig 2), suggesting that many classes of anions, with a variety of backbones, can support tau self-assembly. However, these molecules were not all equally potent. Of the molecules tested, the sugars (**1, 2, 8-10**) and generally have the lowest EC_{50} values (*e.g.* active at the lowest concentrations; Tables 1 and 2), while phosphates (**15-18**) tend to be the least potent (*e.g.* require the highest concentrations). It is important to note that these comparisons are imperfect because the natural polymers used here are heterogeneous in length and valency, so it is difficult to compare their molar concentrations. Finally, we were surprised to find that several of the anions are “inert” (unable to produce ThT signal), including

hyaluronic acids (**3-6**), kappa carrageenan (**11**), pectin (**12**), dibasic pyrophosphate (**13**), trimetaphosphate (**19**), fusidic acid (**36**) and bilirubin (**37**) (Tables 1 and 2). This finding suggests that charge alone is not sufficient to drive the amyloid process. We wondered whether a subset of these "inert" molecules might serve as inhibitors of other anions. To test this idea, we co-induced WT tau with heparin and a subset of the "inert" molecules. We found that some compounds, such as hyaluronic acid (**6**) and kappa carrageenan (**11**) did not interfere with HS-mediated tau aggregation (Supplemental Figure S2C. Others, such as fusidic acid (**36**) and pectin (**12**) partially blocked heparin's activity (Supplemental Figure S2C). We reason that these inhibitory anions might partially limit heparin and other active anions from binding to tau.

In addition to having different potency values, we also find that anions produced different levels of maximal ThT signal (Supplemental Table 1 and 2). Maximum ThT fluorescence is likely a product of the number of fibrils, the number of ThT binding sites in those structures and the chemical features of the binding sites (*e.g.* hydrophobicity)[39]. Thus, these results begin to suggest that the conformation(s) of the fibrils formed by the different anions might be distinct.

2.4.3 Kinetic studies reveal the differential effects of anions on lag time and/or elongation rate

In aggregation reactions, the lag time is used to estimate the time required for an inducer to initiate formation of oligomers, while the elongation rate is representative of multiple steps, including monomer addition and fibril fragmentation.[40] Thus, we reasoned that comparing these values for reactions initiated by different anions might provide further insight into the steps that are affected. In these experiments, we used each anion at or near its EC_{50} concentration, using triplicate wells and repeating the studies three times with independent tau protein samples (n=9, three biological replicates). This type of comparison is important because it normalizes anion potency and allows direct comparisons between them. From the resulting data, the lag time and elongation rate were

determined with the Gompertz function using the grace plotting program (see the Experimental Section). To facilitate comparisons between anions, we plotted the reciprocal of the lag time (lag time^{-1}) to calculate an "induction strength"; where higher values are indicative of faster aggregation (Fig 2). Although there is considerable variability within classes, we find that sugars generally initiate fibril formation the fastest, with lag times around 2 to 2.5 hours for WT tau (Fig 2B; Supplemental Table 1). In contrast, the polyphosphates promote aggregation with considerably longer lag times (~6 to 9 hours). Next, we similarly plotted the reciprocal of the elongation rate for each reaction (Fig 2C); where high values are indicative of faster progression of fibril assembly. Again, there are differences between and within chemical classes, but sugars tend to produce the fastest elongation speeds. With both sets of values in-hand, we could then identify anions that might preferentially impact lag time or elongation rate. Indeed, we noted that HS (**1**) tended to produce dramatic effects on lag time, with comparatively little effect on elongation rate, as previously reported[7]. However, other sugars, such as **2** and **8**, had relatively strong effects on both steps. Other compounds, such as **7** and **9**, had a disproportionate impact on elongation rate. Thus, the identity of an anion seems to determine which steps in the aggregation process are most impacted.

2.4.4 Mutant P301S is sensitive to a wider range of anions

Although we have, to this point, focused on the results obtained with WT tau, these experiments were also performed, in parallel, using mutant P301S tau. A comparison between the results obtained with these two proteins suggested that, as expected, most anions that induce weak or moderate ThT signals for WT tau give relatively stronger signals using the P301S construct, with shorter lag times (Supplemental Table 2). Indeed, for a few anions, such as **14 and 27-29**, aggregation was only detected with P301S. We also noted that even the cation, poly-L-lysine (**30**), which was originally selected as a negative control, was able to weakly stimulate ThT signal for P301S. Crowding agents are known to accelerate aggregation[41], so it is possible that poly-L-

lysine might operate by this mechanism. Another unexpected result was that a small number of anions, such as **2, 9, 20**, and **35**, produced relatively faster elongation rates for WT vs. P301S (Fig 2). Regardless, in most cases, we found that P301S was more sensitive than WT for nearly all of the anions. These findings support a model in which the strong link between this mutation and FTD could be, in part, a product of its sensitivity to a wider range of naturally occurring anions.

2.4.5 Anions require a combination of both charge density and valency to support tau aggregation

In these screens, we found that molecules from a surprising number of chemical classes could support tau assembly. Therefore, it seems likely that the individual details of the scaffold backbone (*e.g.* sugar, peptide, *etc*.) might be relatively less important than their shared physical features, such as charge and valency. Indeed, careful studies using purified heparins and polyphosphates have also pointed to a key role for valency in tau aggregation[26]. To test this idea in more detail, we obtained additional anions, including dimeric ones, within the phosphate and amino acid chemical series and tested them in ThT assays. Within these series of chemically defined molecules, we compared their activity on a per monomer, molarity basis. The results supported the idea that anion valency seems to be an essential feature of inducers. For example, synthetic poly-L-glutamic acids (**26 – 29**) decrease lag times with increasing valency (Fig 3A; p value 0.0002), but have do not have a specific effect on elongation rate constants (Supplemental Figure S9; p value 0.1549). Similar relationships were observed with phosphates of varying length (Supplemental Figure S9). We next wondered whether other chemical features, such as charge density, might similarly correlate with effects on lag time or elongation rate. However plots of charge density (-e/kD and -e/Å) showed no correlation (Fig 3B; Supplemental Figure S9), suggesting that this feature is not critical. As previously suggested,[7] we speculate that multivalent anions might bridge multiple tau monomers, increasing their local concentration and, ultimately, enhancing self-assembly. However, valency is clearly not the only important feature because

highly valent compounds with sparse charge, such as hyaluronic acids (**3-6**), are ineffective inducers, suggesting that an optimal balance of charge density and polymer valency may be important.

2.4.6 The identity of the polyanion modulates protease sensitivity and fibril conformation

In addition to their effects on assembly kinetics, we hypothesized that the identity of the polyanion might impact the structure of the fibrils. Here, we define structural conformation based on differences in susceptibility to limited proteolysis and appearance of the fibrils by negative stain transmission electron microscopy (TEM). The advantage of limited proteolysis is that it reveals potential differences in the "fuzzy coat" of tau fibrils (*e.g.* regions outside of the well-folded core), a region that makes up the bulk of tau fibrils and has been shown to adopt heterogeneous conformers[14,42–45]. Accordingly, WT tau fibrils formed from some of the most potent inducers: HS (**1**), polyphosphate (**15**), poly-L-glutamic acid (**25**), polyA (**31**), sodium alginate (**9**), and polystyrene sulfonate (**35**), were incubated for 60 min with the protease trypsin at a protein:protease ratio of 500:1 and then analyzed by SDS-PAGE. To distinguish fibril regions resistant to digestion, we probed these samples using several anti-tau antibodies (Tau 1, Tau 5, 4R, and Tau 13), which have epitopes that span the domains of tau (Fig 4A).

In the limited proteolysis experiments, we observed rapid degradation of soluble tau, which is consistent with its intrinsic disorder and many trypsin cleavage sites (Fig 4b; Supplemental Fig. S7). For the fibrils, we generally observed resistance to proteolysis and, more importantly, we observed differential proteolytic banding between samples. Conformational divergence is perhaps most apparent when probing the proline rich region (PRR). For example, using the anti-tau-5 antibody (residues 210-230) three bands ranging from 25 – 37 kDa are apparent for heparin- (**1**), poly-L-glutamic acid- (**25)** and sodium alginate- (**9**) induced samples, whereas a single faint band persists for polyP (**15**), and no protease resistant banding is observed in this same region using

polyA (**31)**, or polystyrene sulfonate (**35**)**.** Probing further upstream in the PRR, using the anti-tau-1 antibody (residues 192 – 204), the initial similarities observed between **1** and **9**, and **25** diverge. Specifically, heparin (**1**) and sodium alginate (**9**) maintain a similar proteolysis profile with two bands between 30 to 37 kDa, in addition to the emergence of a ~15 kDa band. For poly-L-glutamic acid (**25)**, however, the fibrils remain resistant to degradation in this region, with two intense bands appearing around 25 to 30 kDa. Interestingly, the 15 kDa fragment also appears in samples induced with polystyrene sulfonate (**35**) and this is the only region where this sample displayed protease resistance. Probing the N-terminal domain (NTD; residues 20 – 35) reveals that the fibrils formed using poly-L-glutamic acid (**25**) and heparin (**1**) were most resistant to digestion, whereas polyP (**15**), polyA (**31)**, and sodium alginate (**9**) conferred moderate resistance, and PSS (**35**) is susceptible. This result suggests that the fibrils formed in the presence of compounds **1, 9, 15, 25,** and **31** have NTDs that are oriented in manner that completely or partially shields them from proteolysis (Fig 4C). Other anions, such as polyA (**31**) and PSS (**35**) might create fibrils or protofibrils that are considerably less stable. Together, findings using these three antibodies (Tau 5, Tau 1 and Tau 13) support a conclusion in which inducers impact the conformation(s) of the fuzzy coat.

The R2 repeat region of tau is particularly important because previous work has shown that it is included in a subset of patient-derived core structures but excluded from others[11,12]. Interestingly, we observe that the R2 repeat is included in the protected core of fibrils formed in the presence of heparin (**1**), which is consistent with heparin-induced tau structures[46], sodium alginate (**9**), poly-L-glutamic acid (**25**), and polyphosphate (**15**), but that it is excluded from those formed using polyA (**31**) or polystyrene sulfonate (**35**). Thus, it seems likely that only a subset of the inducers promote the formation of R2-containing fold. Indeed, our results with polyA (**31**) are consistent with cryo-EM evidence, which has shown that the R2 region is excluded from the cores of fibrils formed using RNA[29]. The biological and/or structural significance of R2 positioning is not yet

known, but it is interesting that the identity of the polyanion can cause dramatic changes to R2 protease sensitivity.

To confirm that the partial proteolysis samples were enriched for fibrils, we also performed SDS-PAGE analysis on the soluble (S) and insoluble, pellet (P) components after centrifugation. These sedimentation studies also serve the important objective of confirming the ThT assays and providing an independent measure of fibril formation. For both WT and P301S tau (Supplementary Figure S8), we confirmed that anions that are strongly active in ThT (**1**, **8, 10, 15**) also shift tau into the pellet, with nearly full conversion to insoluble material. Likewise, anions determined to be weakly active (**17**) or inert (**3 - 6**) yielded incomplete conversion (Supplemental Figure S8). Thus, these sedimentation studies both corroborate the ThT assays and provide further evidence of differences in the potency of anions.

Finally, we used negative stain transmission electron microscopy (EM) to examine and compare the supramolecular architecture of tau fibrils. These experiments also served the added goal of independently confirming whether the measured ThT signals were due to the formation of amyloid fibrils. AD-associated tau fibrils tend to have a twisted or straight conformation by TEM, with relatively long fibrils that have an average diameter around 30 nm to 15 nm. Therefore, we wanted to study the fibrils formed by our anions and compare them to this benchmark. A full set of representative TEM images are shown in Suplemental Fig S10. Focusing just on those that were studied by limited proteolysis, we found that samples prepared using heparin (**1**), fondaparinux (**7**), polyphosphate (**15**) sodium hexametaphosphate (**18**), and, nadroparin calcium (**8**) had characteristic amyloid morphologies (Fig 4D). Those formed from **8**, **7** and **20** were particularly interesting, as they yielded twisted and straight fibrils with an average diameter of ~25 to 30 nm. The results with HS (**1**) are consistent with previous findings[46] and included a mixture of twisted and straight fibrils. In contrast, filaments generated using sodium alginate (**9**) and polystyrene

sulfonate (**35**) are relatively monomorphic and distinct. Fibrils formed using sodium alginate (**9**) were particularly striking in their unusual and consistent morphology; moreover, they tended to produce slightly thicker fibers (33 nm, n = 30) compared to the other inducers (Fig 4E). In the broader TEM screen, we also observed oligomeric (*i.e.* spherical) and amorphous structures in samples formed from polyAU (**31**) and hyaluronic acid (**6**). These anions produced poor ThT signals, so their lack of ThT reactivity correlates well with the imaging. Together, these results support our hypothesis that polyanion identity strongly impacts the conformation of tau fibrils, such that the protein can be directed into strikingly different shapes by the chemical properties of the inducer.

2.5 Conclusion

The role(s) of anions in tau self-assembly have remained elusive. Many pioneering manuscripts have shown that individual polyanions promote this process[22,27,35,47,48], with the most attention placed on heparins and polyphosphates. Here, we expand the landscape of tested anions, with a special focus on those naturally occurring ones that tau might encounter in the brain. We also tested them side-by-side to avoid interpretations that could arise due to differences in experimental conditions (*e.g.,* buffer, tau concentration). From these screens, we found that tau aggregation is enhanced by a wide variety of anions. Indeed, the most pervasive theme is that anions with dramatically different scaffolds (*e.g.,* sugar, polyphosphate, *etc*) are capable of supporting tau self-assembly. This finding suggests that degenerate physical features, such as valency and charge, are more important than the specifics of the scaffold from which the anions are displayed (*e.g,* polymer, micelle). For example, the sparsely charged hyaluronic acids (**3**-**6**; 1 charge per repeat) and the low valency compounds (**14**, **29**, **30**) were relatively poor at promoting fibril formation, but highly charged and multivalent molecules (**1**, **2**, **7**, **15**, **20**, **21**, **35**) from many chemical series can induce this process. Together, these results are broadly consistent with a model in which polyanion-assisted aggregation proceeds via minimizing the electrostatic repulsion between positively charged tau monomers, allowing subsequent inter- or intra-

molecular scaffolding of monomers. Yet, the identity of the scaffold must also be important at some level because different anions produce distinct tau fibril morphologies. For scaffolds that have sufficient valency, it seems likely that more subtle features, such as flexibility or charge density, might then favor differential effects on lag time, elongation rate, and, ultimately, the structure of the resulting fibrils. For example, heparin sulfate (**1**) and sodium alginate (**9**) are both repeating di-saccharides, yet they produce dramatically different tau fibrils, as judged by either proteolysis or EM (see Fig 5). We speculate that the molecular details of the tau-anion contacts might be an important step in "folding" and fibril formation.

In the intact brain, soluble tau likely encounters many diverse and abundant biological molecules that bear a negative charge, including many of the proteins, lipids, nucleic acids, and metabolites tested here. Thus, it is interesting to consider the implications of the results in that context. For example, we find that the identity of the anion can have a strong impact on the structure of tau fibrils; thus, differences in the anion composition of specific brain regions could help dictate what types of fibrils are supported. In addition, it is possible that mixtures of anions, as likely encountered in complex cellular environments, could produce new structures or structures of mixed conformation. This is an important consideration because structural studies have shown that filaments formed *in vitro* using HS as an inducer do not have the same structure(s) as those isolated from patient brains.[46] It is possible that different anions or combinations of anions might better replicate the patient-derived structures *in vitro*. Finally, we found that several polyanions, such as hyaluronic acids, are not capable of supporting aggregation at all. Similarly, low valency anions, such as triphosphate, were also remarkably poor at promoting tau aggregation and others, such as fusidic acid **36**, are even inhibitors. This is an important observation because these anions might serve as competitors *in vivo*; binding to cationic sites on tau and buffering the protein's interactions with other, aggregation-promoting polyanions. If this supposition is true, then

the relative concentrations of both active and inert and inhibitory anions might combine to dictate whether tau forms fibrils.

It is important to note that recombinant tau produced from *Escherichia coli* was used in these studies, so the proteins are devoid of post-translational modifications (PTMs). *In vivo*, the overall charge of tau will be tuned by multiple PTMs, including phosphorylation, acetylation, and ubiquitination[49,50]. These modifications can either add a negative charge (phosphate) or neutralize a positive one (acetylation), thus altering the isoelectric point and, in turn, adjusting tau's sensitivity to polyanions[51]. Indeed, recombinant tau fibrils induced using HS (**1**) are significantly different than those formed using phosphorylated tau[52]. Future studies will be needed to deconvolute the impact of the vast number of possible PTM combinations. Likewise, mutations in tau might also impact its interactions with anions by altering the overall structural landscape of the protein. Indeed, we found that P301S tau was sensitive to a wider range of anions than WT, which might partly underlie this mutation's important role in FTD. There are hundreds of additional mutations linked to tauopathy[53], which might also vary in their response to polyanions.

More broadly, electrostatic forces are essential in mediating protein-protein interactions (PPIs)[54,55], not just those found in tau. Here, we screened a library of naturally occurring and synthetic polyanions and found striking differences in how they promote tau self-assembly. It seems likely that a similar, screening-based approach could be adopted to probe the potential roles of polyanions on other PPIs. While crowding agents, such as polyethylene glycol, are sometimes explored[56], systematic studies of polyanion libraries are less common.

2.6 Main Figures

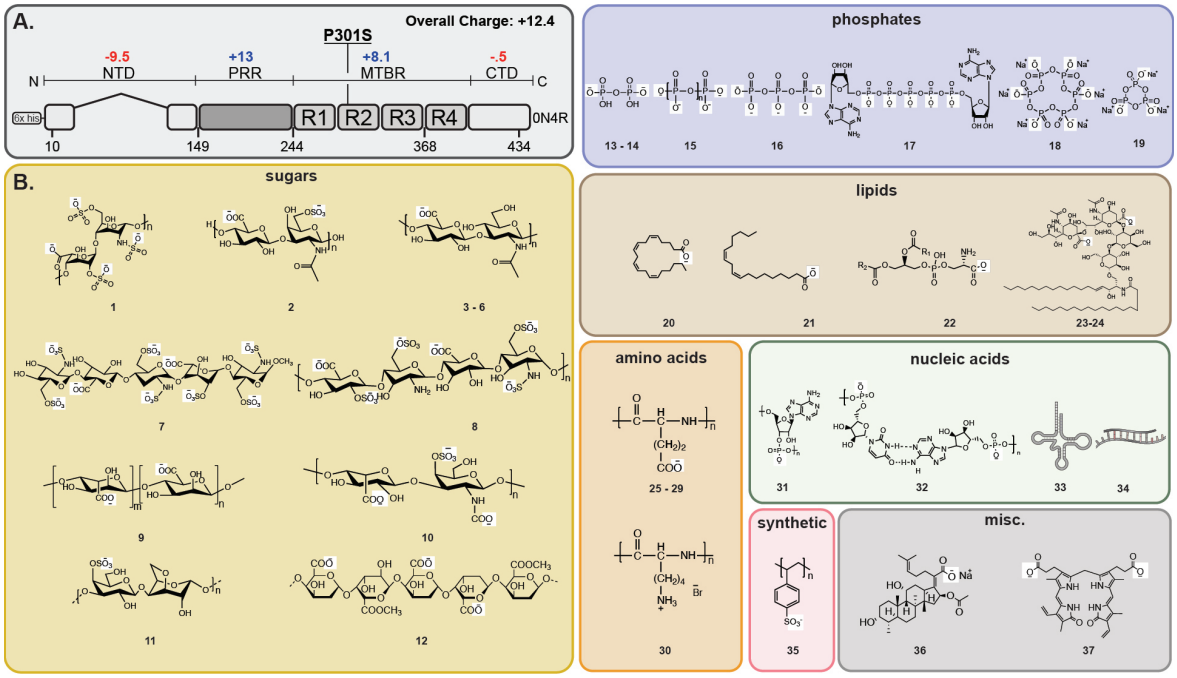

1. heparin sodium **2.** chondroitin sulfate A **3.** hyaluronic acid (8-15 kD) **4.** hyaluronic acid (30 - 50 kD) **5.** hyaluronic acid (120 - 350 kD) **6.** hyaluronic acid (mixed mw) **7.** fondaparinux **8.** nadroparin calcium **9.** sodium alginate **10.** dermatan sulfate and over sulfated chondroitin sulfate (DSOSCS) **11.** kappa carrageenan **12.** pectin **13.** pyrophosphate dibasic **14.** pyrophosphate tetrabasic **15.** polyphosphate **16.** tripolyphosphate **17.** diadenosine pentaphosphate **18.** sodium hexametaphosphate **19.** sodium trimetaphosphate **20.** arachadonic acid (ArA) **21.** linoleic acid **22.** phospatidyl L-serine **23.** ganglioside disodium salt **24.** ganglioside diammonium salt **25-29.** poly-L-glutamic acid **30.** poly-Llysine hydrobromide **31.** polyA (mRNA) **32.** polyadenylic-polyuridylic acid (polyAU) **33.** tRNA **34**. random sequence **35.** polystyrene sulfonate **36**. fusidic acid sodium **37.** bilirubin

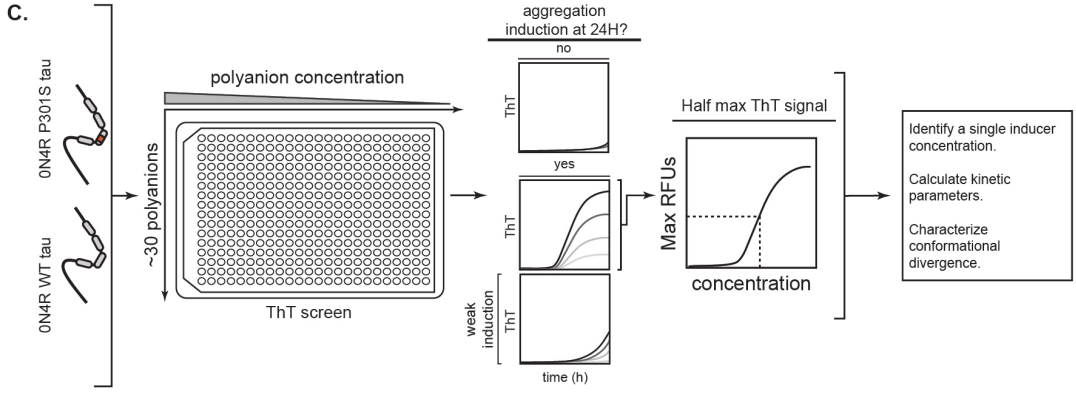

Figure 2.1. Workflow for testing the effects of a polyanion library on tau self-assembly. (A) The domain architecture of the common adult isoform of tau (0N4R). The overall charge of the domains is indicated and the location of the his-tag and the P310S missense mutation are shown. N-terminal domain (NTD); proline-rich region (PRR); microtubule-binding repeats (MTBR); C-terminal domain (CTD). (B) Chemical structures of 37 anionic biomolecules, grouped by series. When appropriate, the minimal repeating unit is shown, and the average polymer length (n) is indicated in the (Supplemental Tables 1 and 2). Compounds 33 and 34 are shown as cartoons because they do have repeating structure (see Methods). (C) The workflow for screening the anion library. Briefly, 0N4R tau (WT) and 0N4R P301S mutant tau (P301S) proteins were first tested against a range of concentrations of each library member in ThT assays. Anions were excluded from further analysis if they produced artifacts (Supplemental Fig. 1) or if they failed to produce a ThT signal 40 RFUs above baseline fluorescence (ΔRFU $\leq$ 40) at 24 hours. For the remaining molecules, the half-maximal effective concentration (EC50) was determined, and subsequent kinetic studies performed at that anion concentration. From those studies, the kinetic parameters, including lag-time and elongation rate were determined.

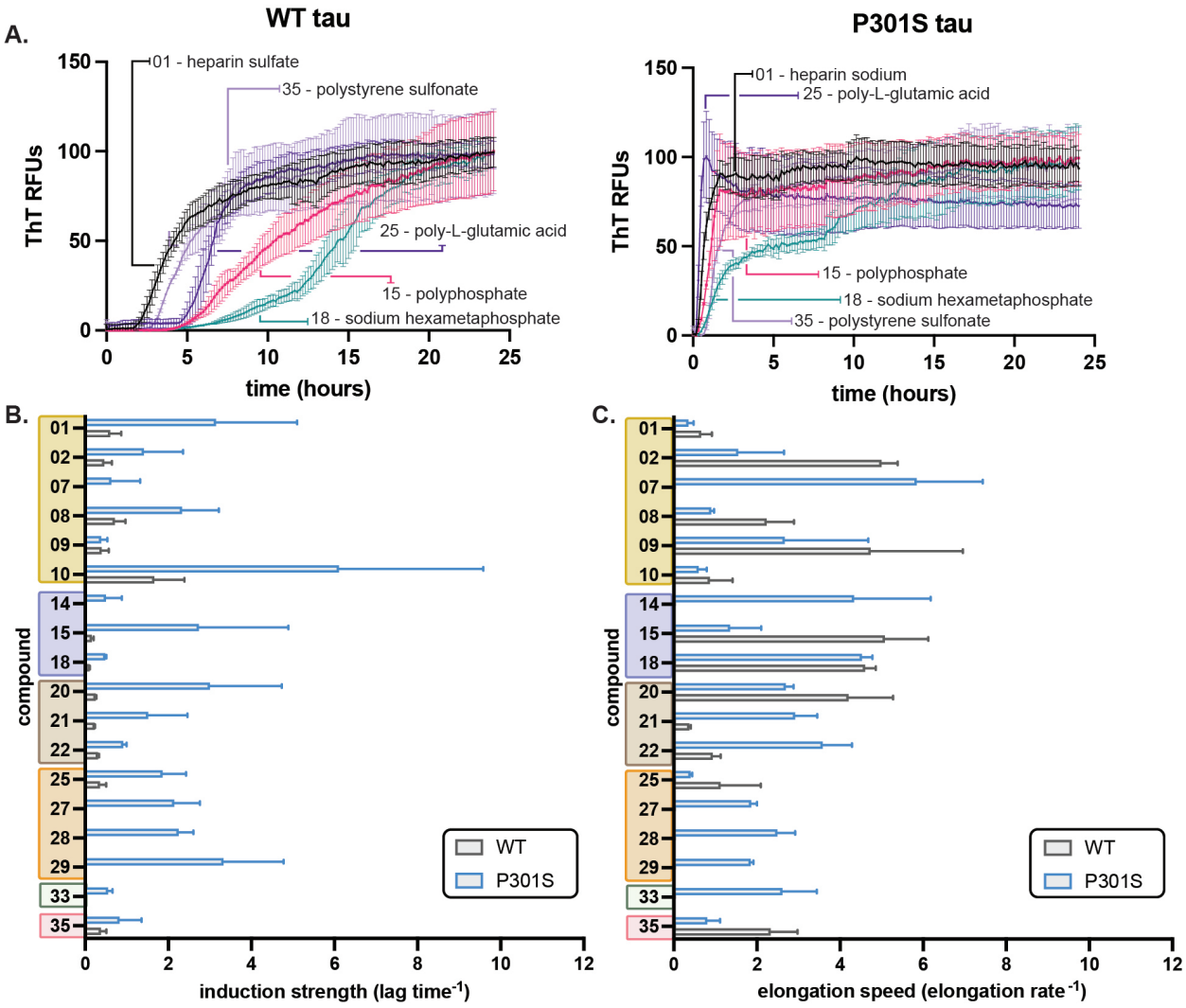

Figure 2.2. Anions have differential effects on lag time and elongation rate. (A) Representative ThT assay results, comparing heparin sodium (1), polyphosphate (15), sodium hexametaphosphate (18), poly-L glutamic acid (25), and polystyrene sulfonate (35) on recombinant 0N4R WT Tau (left) and 0N4R Tau P301S (right) aggregation kinetics. The anions were used at their half-maximum concentration (see Tables 1 and 2) and tau proteins at 10 μM. Results are the average of at least three independent experiments performed in triplicate and the error bars represent SEM. For each result, the signal from control experiments using no tau was subtracted. (B) Anions have differential effects on lag time. Values are plotted as reciprocal (lag-1), termed the induction strength. Inactive inducers and those with weak signal were omitted from the analysis (see text). Results are the average of at least three independent experiments performed in triplicate and the error bars represent SEM. (C) From the same aggregation reactions, the elongation rate was calculated and plotted as the reciprocal (elongation rate-1), termed the elongation speed. Results are the average of at least three independent experiments performed in triplicate and the error bars represent SEM.

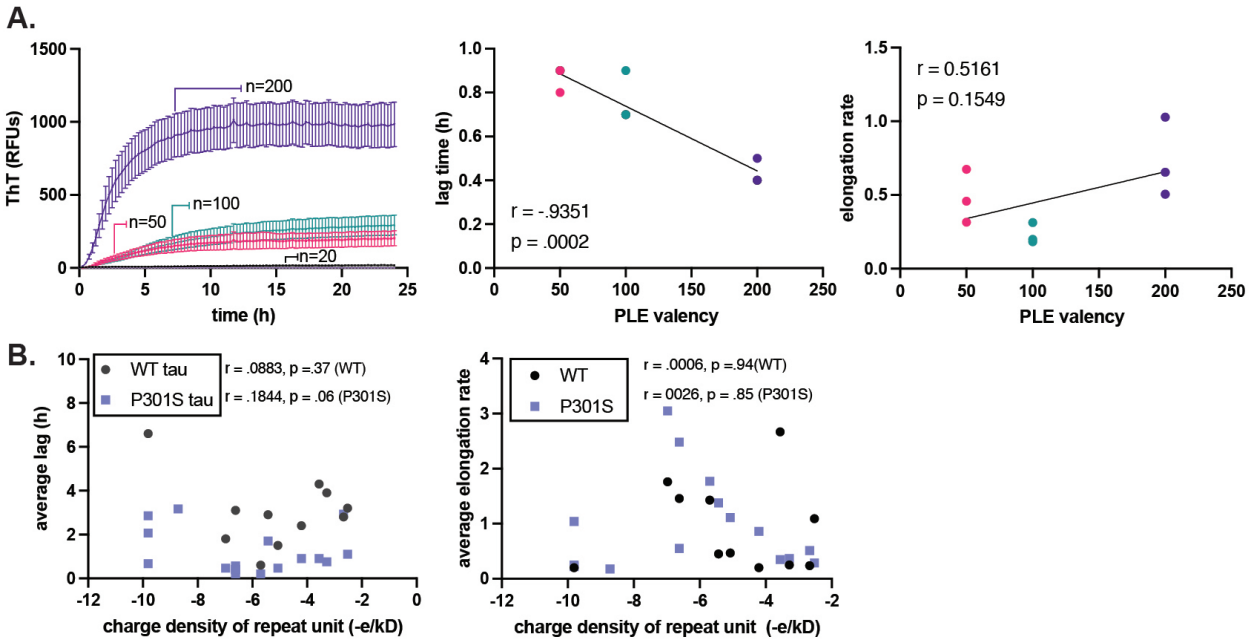

Figure 2.3. Polyanion valency is an important parameter in dictating tau fibril formation. (A) 2N solutions of poly-L-glutamic acid (PLE) of discrete molecular weights (n = 20, 50, 100 or 200) were used to induce WT and P301S tau (10 μM) for 24 hours at 37°C with constant shaking (left). From the resulting curves, lag time and elongation rate were extracted (right). A Pearson t-test was performed to measure the correlation between valency and kinetic parameters. Results are the average of at least three experiments performed in triplicate and the error bars represent s.e.m (n=9). Results are shown for P301S because it gives more robust signal compared to WT tau. (B) A Pearson t-test was performed to determine the correlation between charge density (-e/kD) on the lag time (left) and elongation rate constants (right).

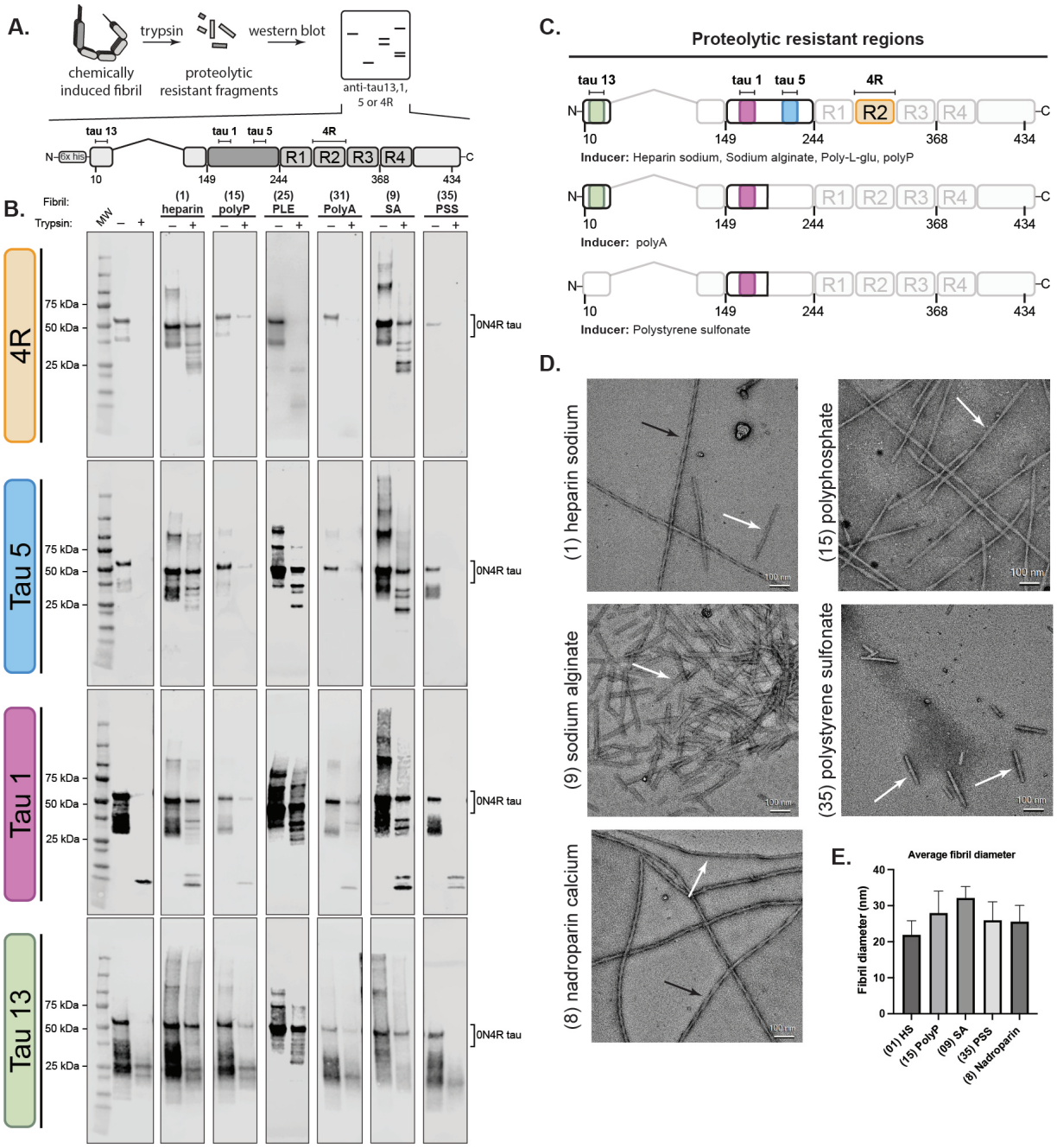

Figure 2.4. The identity of the polyanion impacts tau fibril structure. (A) The general workflow for tau fibril proteolysis. Fibrils were prepared using the corresponding inducer at its analysis concentration (see supplemental table 1), purified by ultracentrifugation, and subsequently proteolyzed using trypsin. Proteolysis products were separated by SDS PAGE and probed using anti-tau antibodies (anti-tau 13, 1, 5, and 4R) (top). The domain architecture of 0N4R tau, showing the location of the epitopes for anti-tau antibodies (bottom). (B) Tau fibrils are generally resistant to proteolysis, but the digestion patterns depend on the identity of the inducer. The protease resistant fragmentation of 0N4R WT tau filaments differentially induced using heparin (1), polyphosphate (15), poly-L-glutamic acid (25), polyA (31), sodium alginate (9), or polystyrene sulfonate (35). (C) Summary of the proteolytic regions of each fibril samples. (E) Representative electron micrographs of negatively stained fibrils from recombinant 0N4R tau assembled in vitro at the end point of each reaction. Scale bar, 100 nm. Black arrows indicate twisted filaments, and white arrows indicate straight fibers. (D) Quantification of the average diameter of recombinant fibrils (n = 30).

2.7 Supplemental Figures

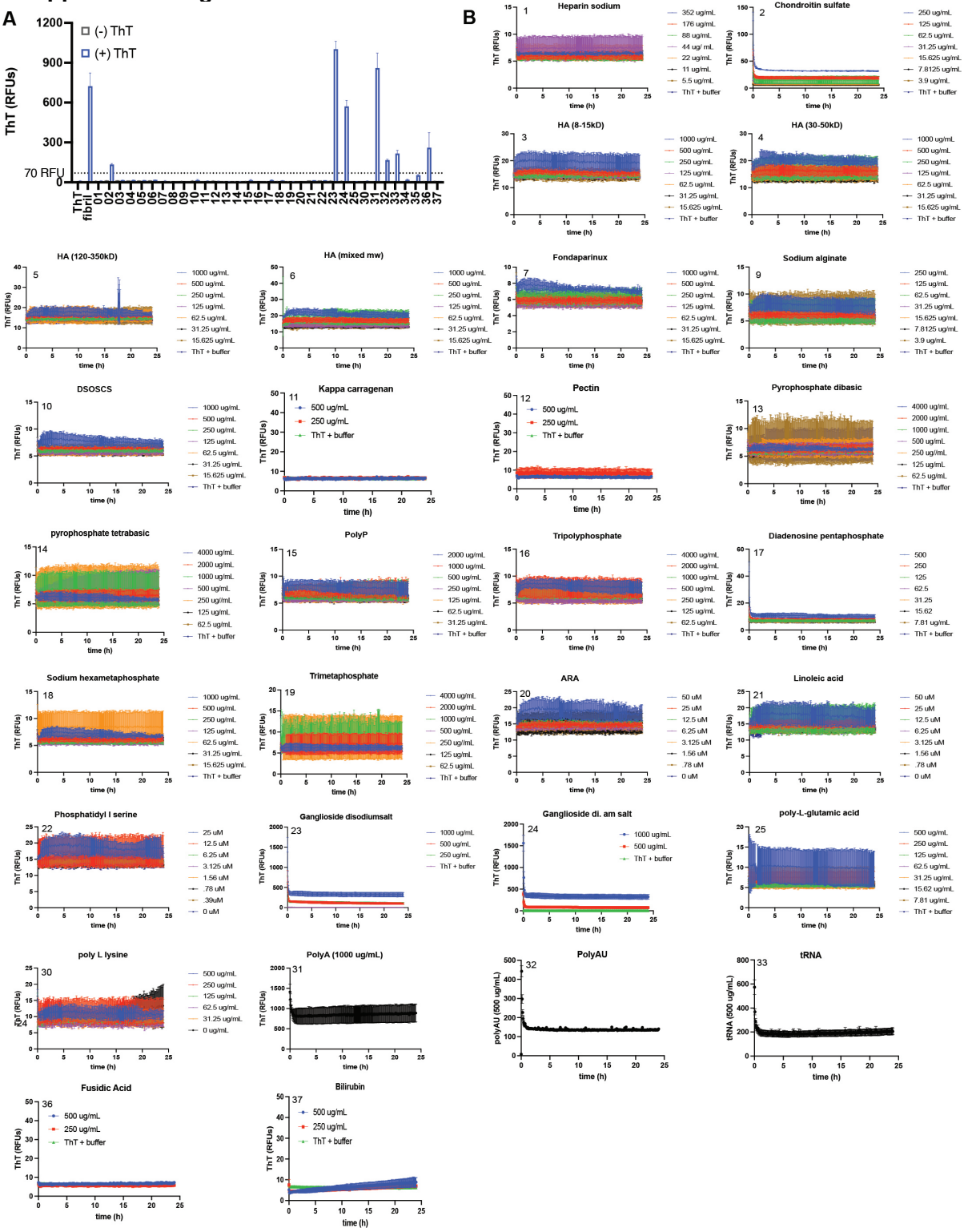

Figure 2.S1. Identification of anions that produce thioflavin T (ThT) artifacts inthe absence of tau fibrils. (A) Summary of the screen, in which anions were incubated with 10 μM ThT in the absence of fibrils. A subset, including chondroitin sulfate A (2), Ganglioside disodium salt (23), Ganglioside diammonium salt (24), polyA (mRNA) (31), Polyadenylic-polyuridylic acid (polyAU) (32), tRNA (33), and fusidic acid (36) produced ThT fluorescence in the absence of protein. (B) Raw data from the “no protein” controls. Results are the average of technical triplicates and error is SEM.

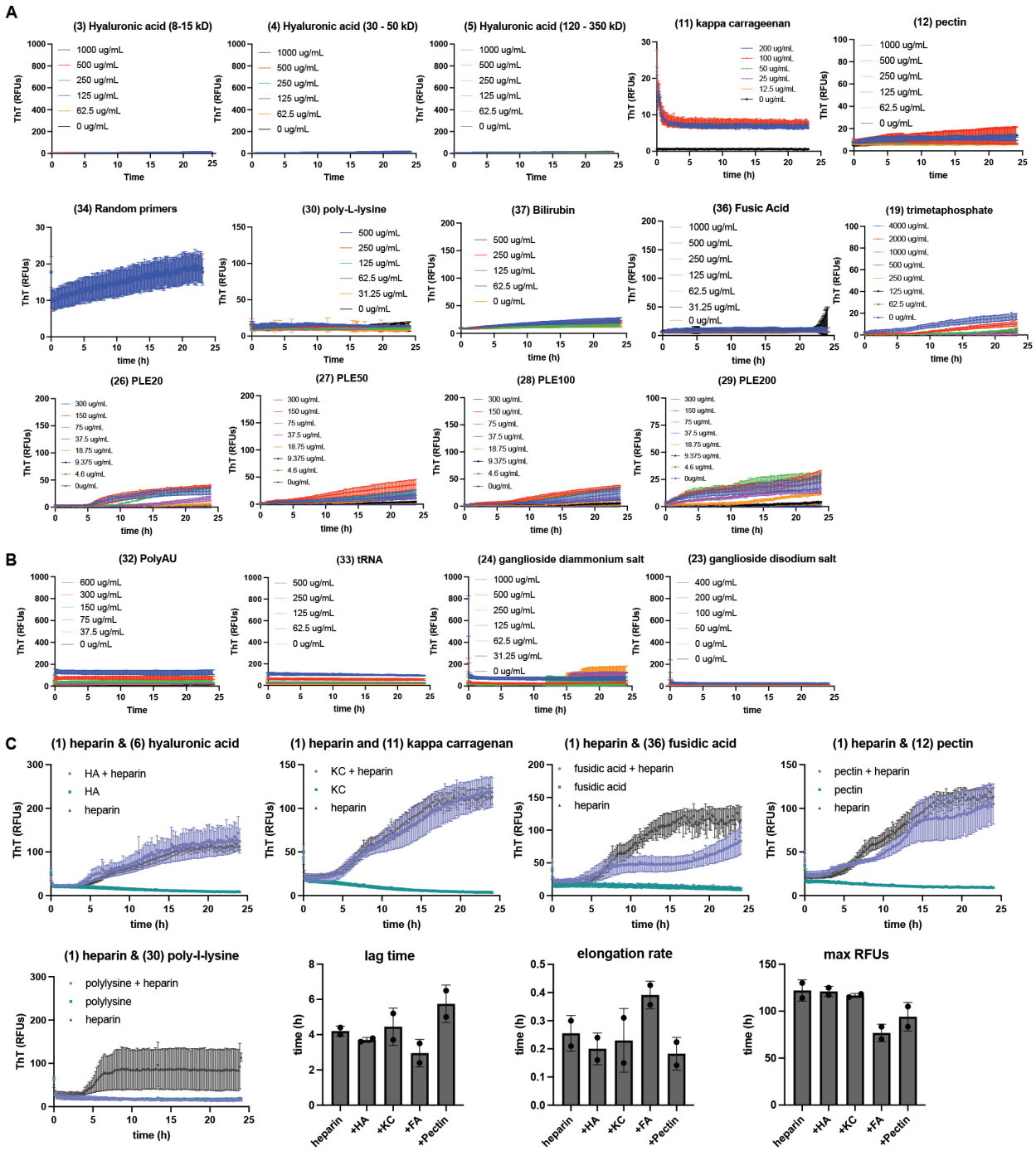

Figure 2.S2. Raw curves supporting the activity of anions in the ThT assays. (A) Results from ThT assays for the subset of anions that are unable to promote tau aggregation (termed "inert"). (B) Results from ThT assays for the anions that have high background. For these anions, we rely more heavily on the sedimentation and TEM experiments. (C) A subset of the "inert" anions (36, fusidic acid; 12, pectin) are able to partially inhibit the activity of heparin when added simultaneously, while others (6, hyaluronic acid; 11 kappa-carragenan) are not. All results are the average of technical triplicates and error is SEM. Results are the average of two independent experiments performed in triplicate and error is SEM.

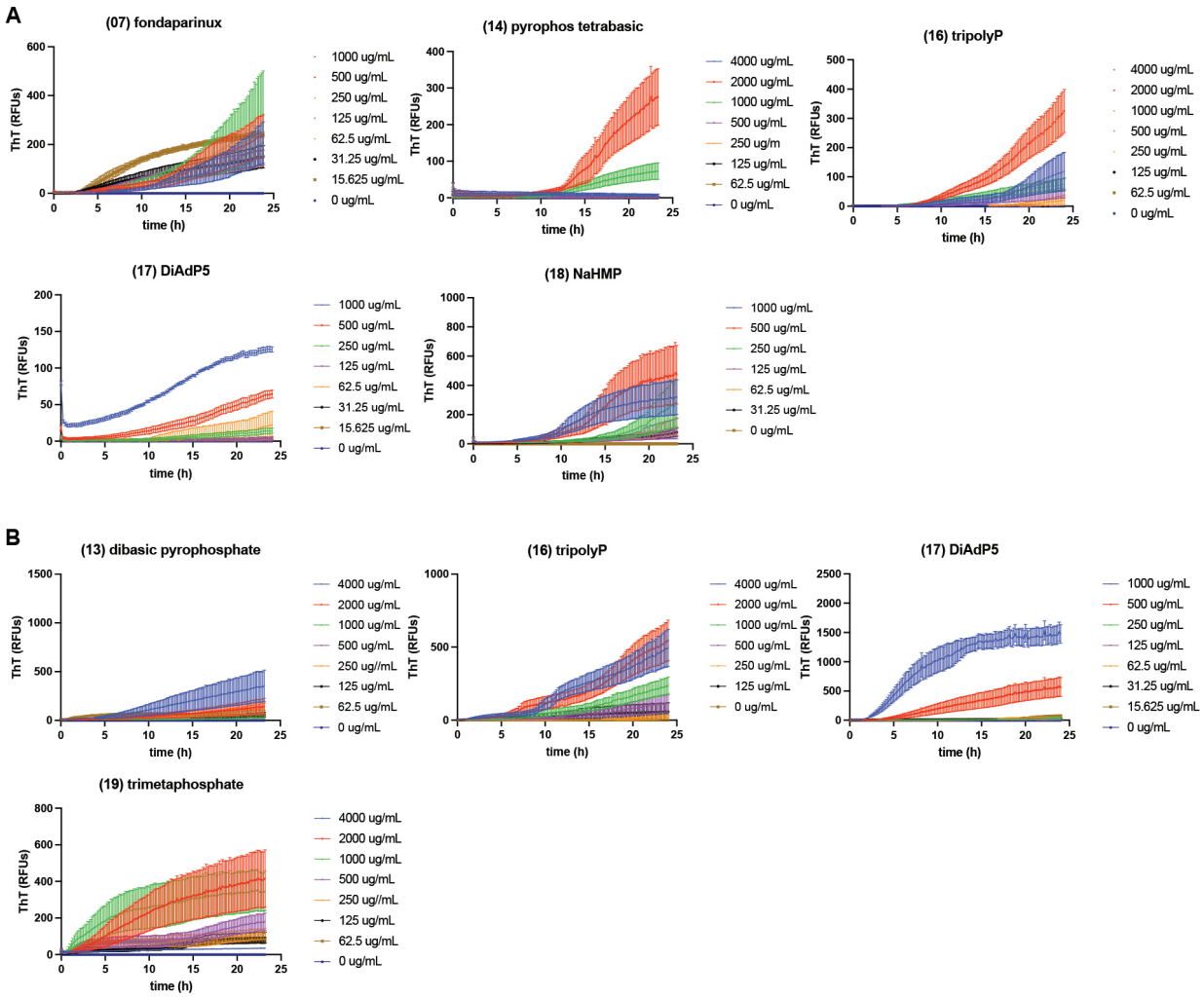

Figure 2.S3. A subset of anions weakly induce tau aggregation. Raw ThT plots for the subset of anions that were designated as "weakly active" for (A) WT tau and (B) P301S tau. Results are the average of at least three independent experiments performed in triplicate and error is SEM.

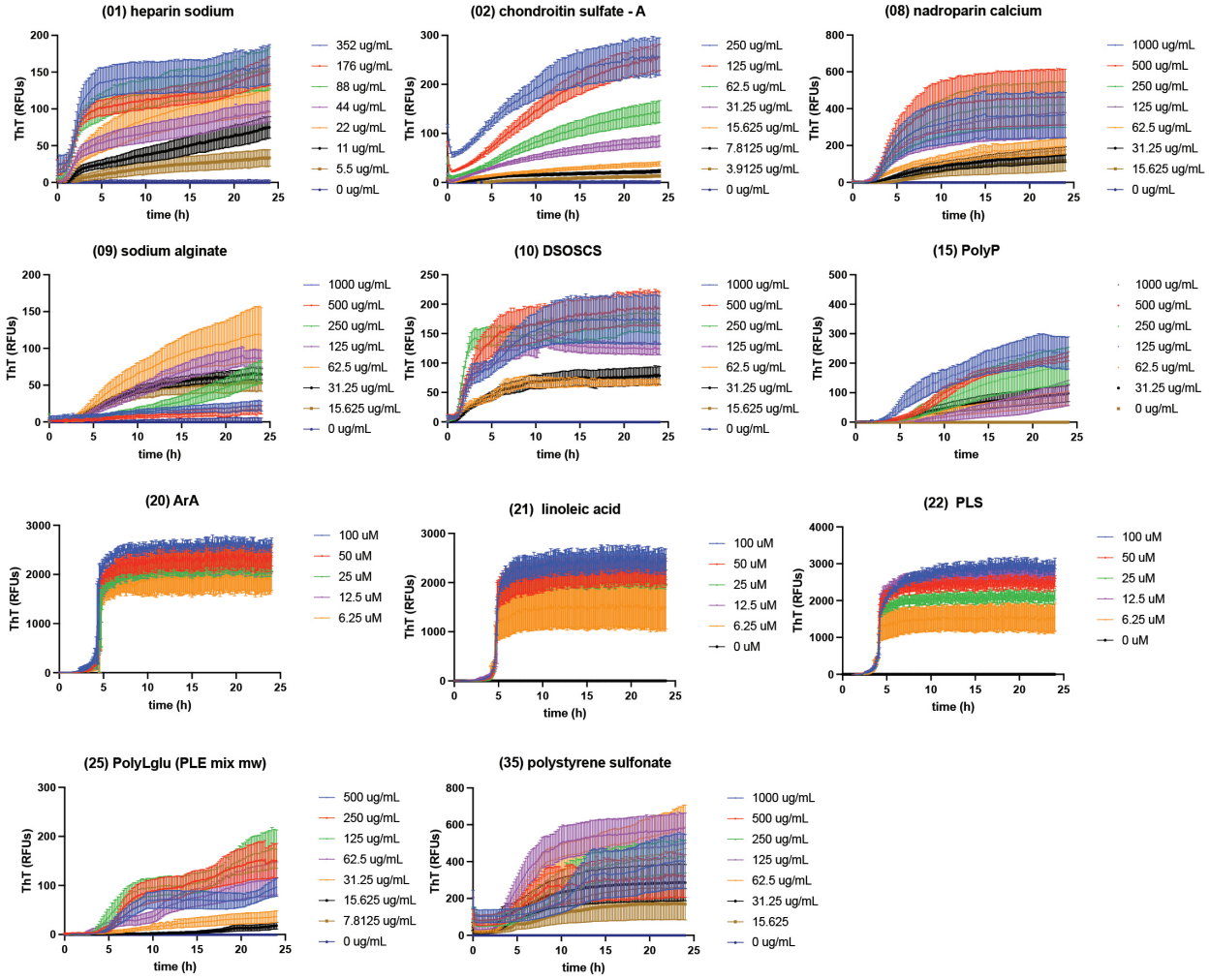

Figure 2.S4. Raw ThT results for the anions determined to be "active" against WT tau. For these anions, we performed full kinetic and dose range screening. Results are the average of at least three independent experiments performed in triplicate and the error bars represent SEM (n=9).

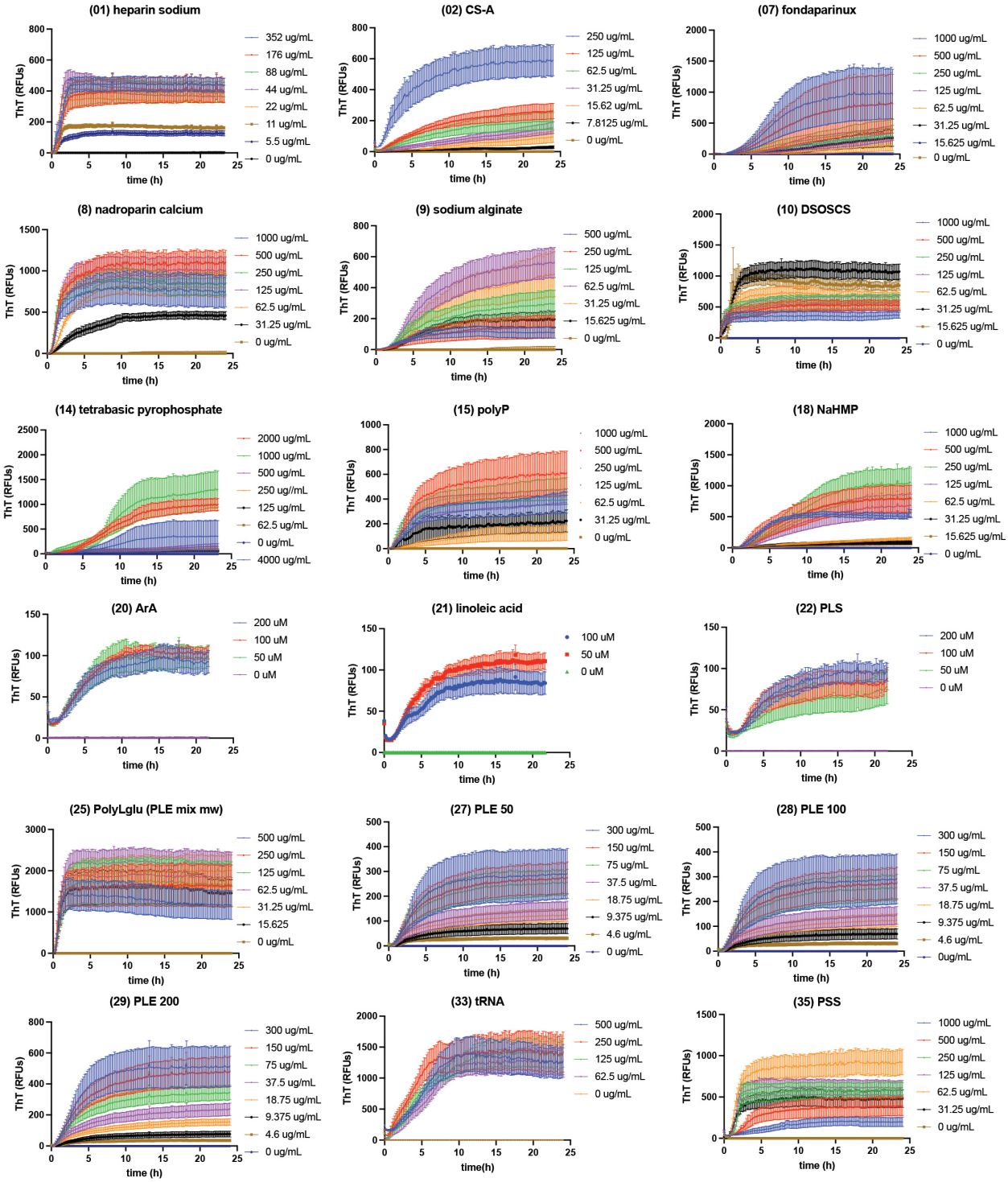

Figure 2.S5. Raw ThT results for the anions determined to be "active" against P301S tau. For these anions, we performed full kinetic and dose range screening. Results are the average of at least three independent experiments performed in triplicate and the error bars represent SEM (n=9).

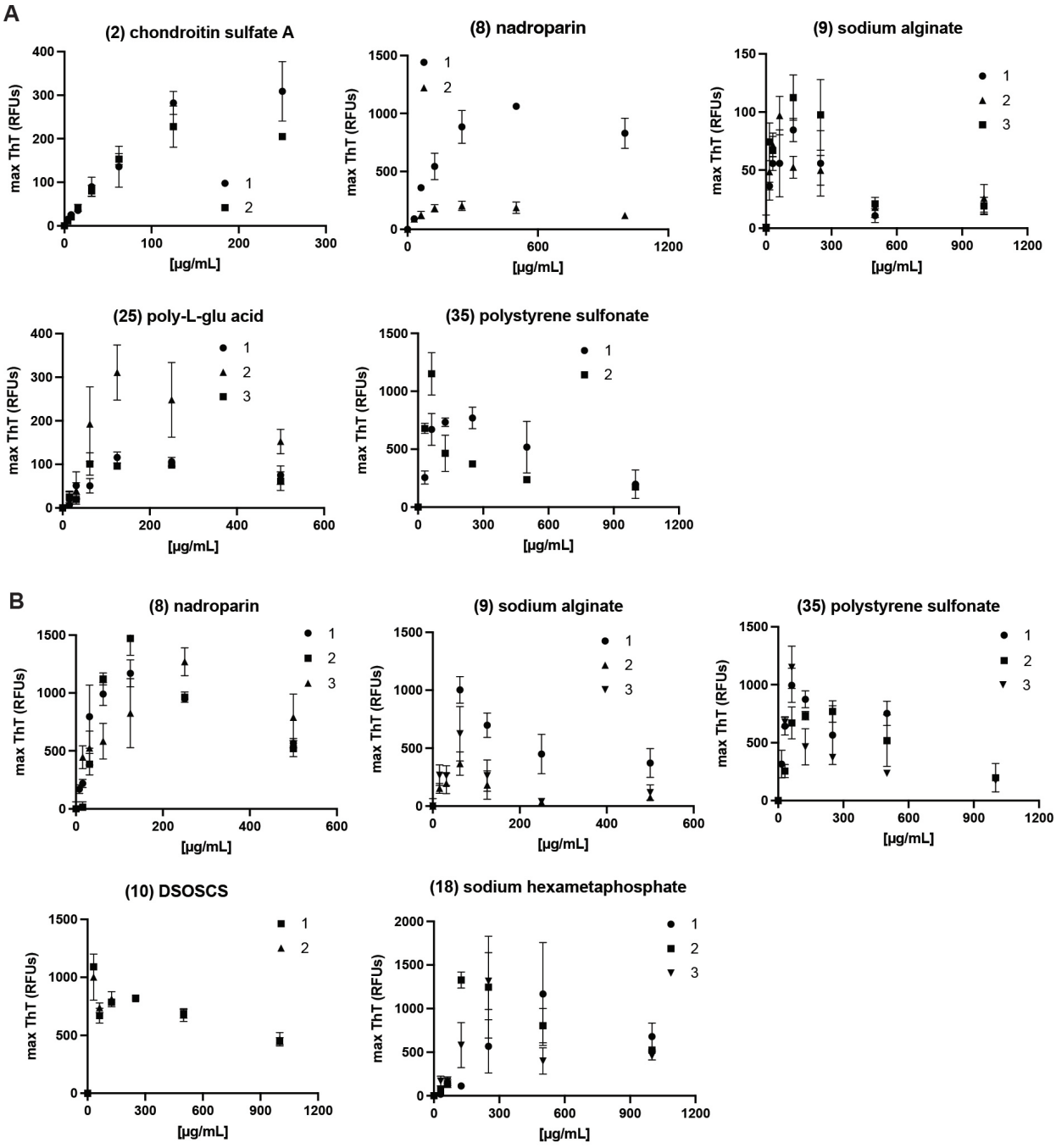

Figure 2.S6. Several anions accelerate aggregation at low concentrations, but then inhibit it at higher concentrations (producing a "hook effect"). Raw ThT results are shown for (A) WT Tau and (B) P301S tau. Each curve represents are the average of three experiments performed in technical triplicate and the error bars represent SEM (n=3). The two independent, biological replicates are shown (1, 2, etc.). As stated in the text, these inducers were used at EC50 values that were selected after excluding the higher concentrations.

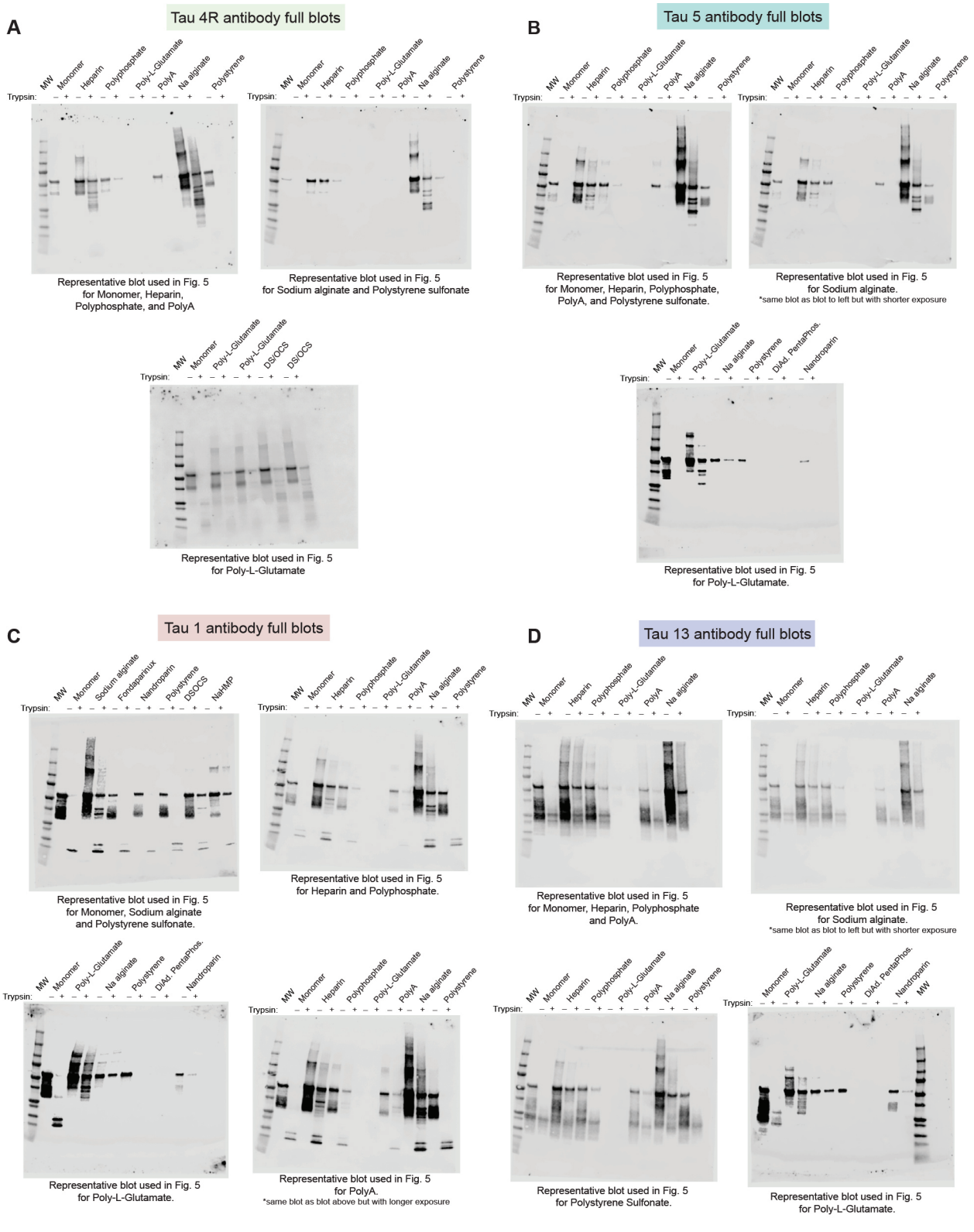

Figure 2.S7. Full Western blots for the images shown in the partial proteolysis studies (see Figure 4). The full, uncropped Western blots for the partial proteolysis studies, using antibodies (a) Tau 4R (b) Tau 5 (c) Tau 1 and (d) Tau 13. See text for details.

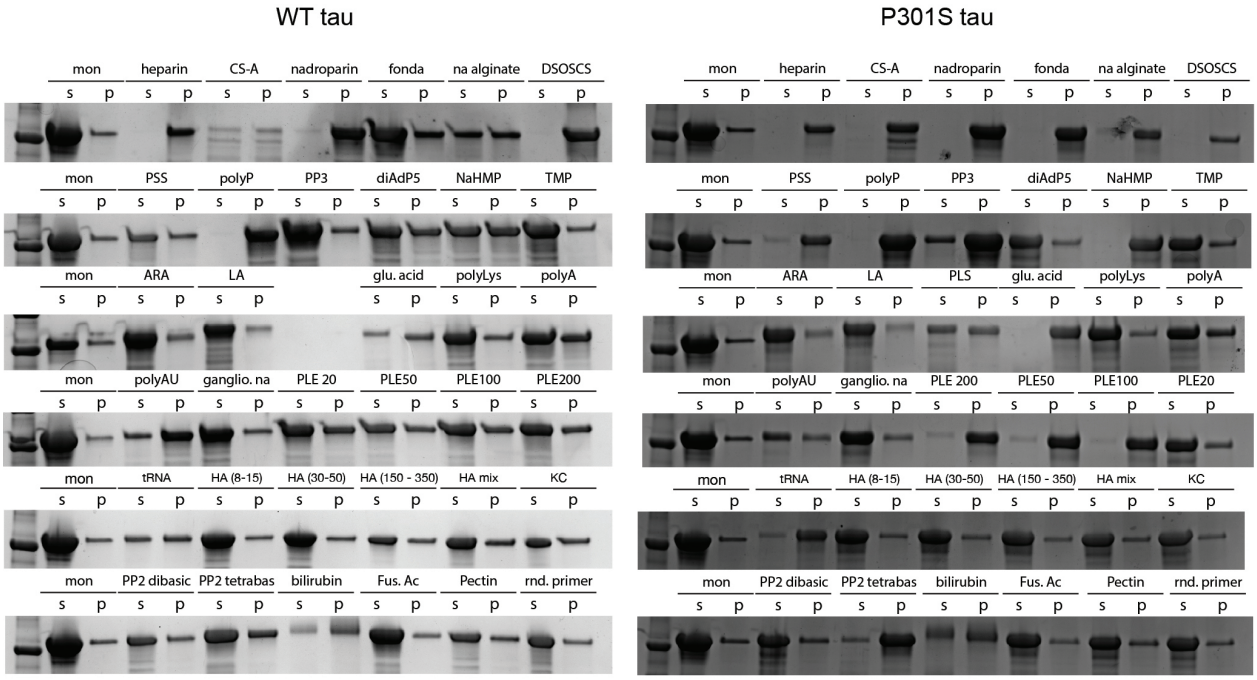

Figure 2.S8. Sedimentation assays reveal the extent of tau fibrilization. After incubation of tau with anions, centrifugation was used to separate the insoluble pellet (P) and soluble (S) components, followed by analysis by SDS-PAGE. The concentration of anion used in these studies is the “analysis concentration”, as denoted in SI Tables 1-2.

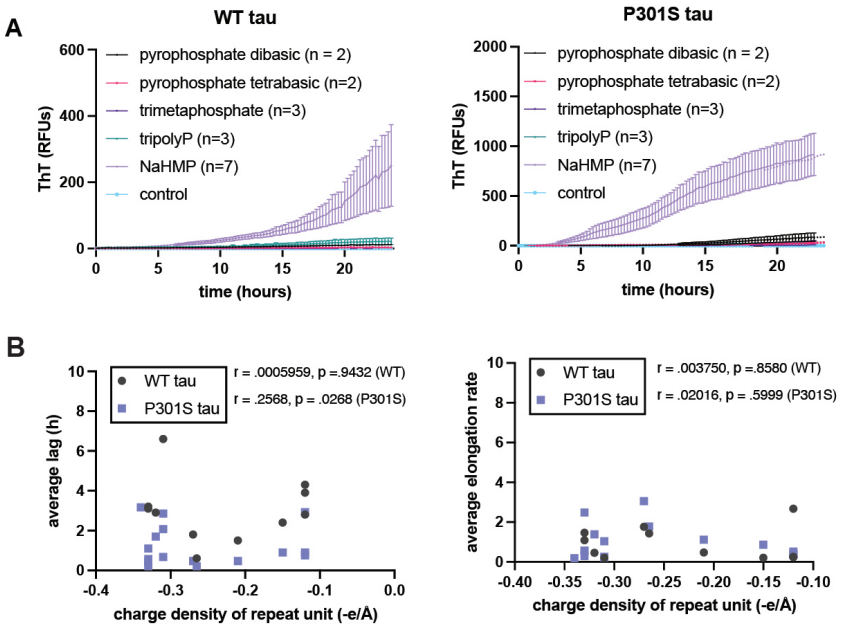

Figure 2.S9. Polyanion valency is an important parameter in dictating tau fibril formation. (A) 2N solutions of polyphosphates including pyrophosphate (13-14), tripolyphosphate (16), sodium hexametaphosphate (18) or sodium trimetaphosphate (19) were used to induce aggregation of WT (left) or P301S tau (right) . The relative valency is indicted (n=x). These results further support the conclusions in Figure 3. (B) Correlation analysis of the effect of charge density (as determined by approximate Angstrom distance of the repeat unit (-e/Å) on lag time (left) and elongation rate (right) using a Pearson t-test, demonstrating that these parameters do not correlate for either WT or P301S tau. These results support the conclusions in Figure 3.

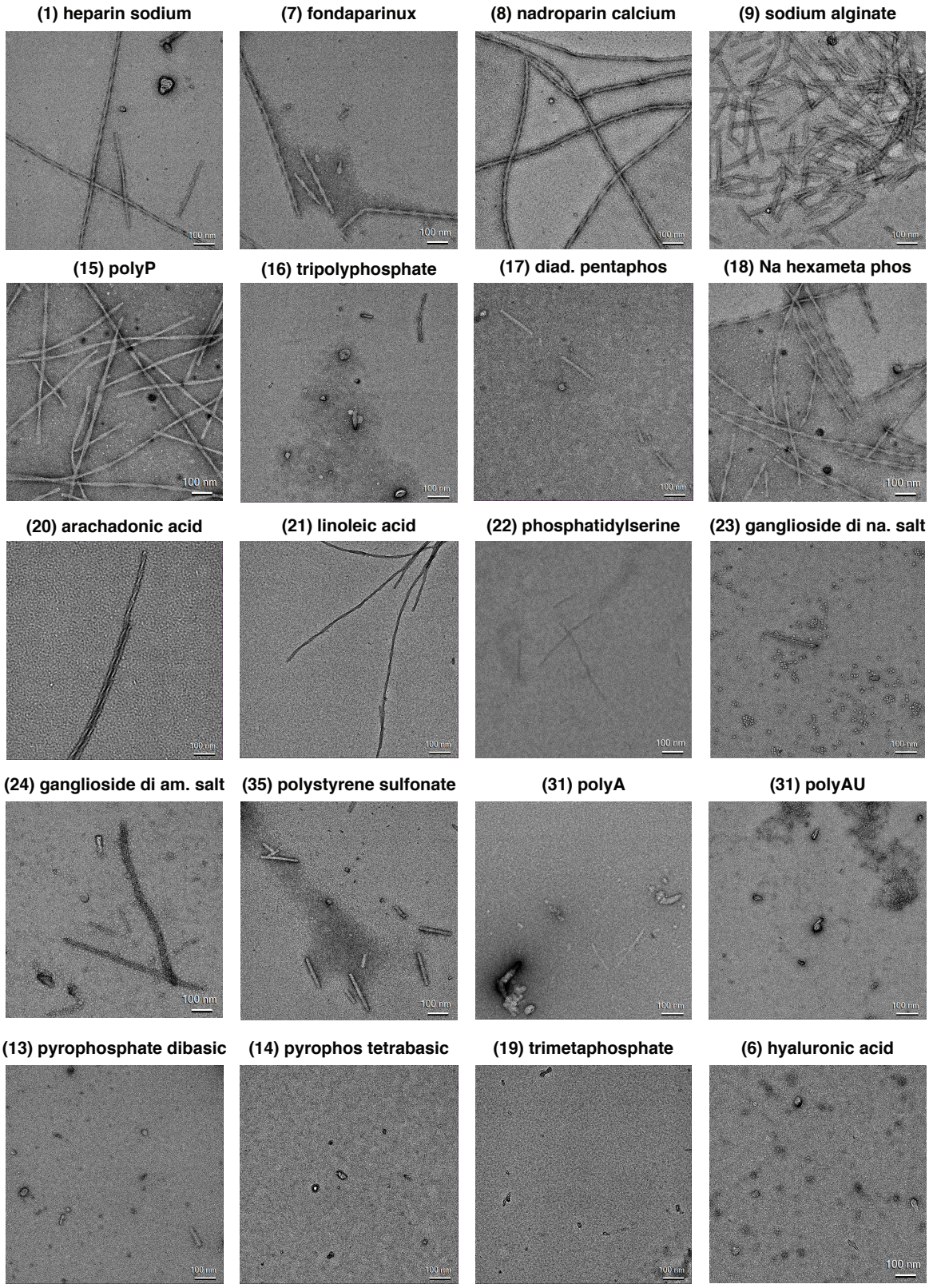

Figure 2.S10. Raw TEM images, supporting and extending the results from the ThT and sediminatation assays. Results are representative of collected images. Results are shown for WT tau. Inactives and weakly actives are grouped at the bottom. Scale bar is 100 nm.

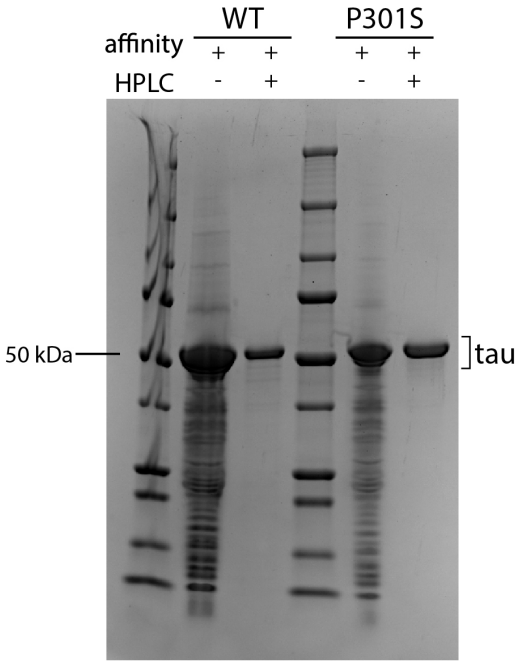

Figure 2.S11. Purity of expressed tau proteins, as judged by Coomassie gels. The samples are shown after the His-tag affinity step and after the final HPLC purification, for both the WT 0N4R tau and P301S 0N4R tau. The samples were 95% pure, as measured by ImageJ.

2.8 Supplemental Tables

Table 2.S1 Characteristics and results from the anion library screening against WT tau.

Nbr.	compound	CAS number	MW of repeat unit (Da)	MW range (Da)	charge per repeat unit	charge density (-e/kD)	charge density (-e/Å)	polymer classification	charged groups	dosing (ug/mL)	[EC50] (ug/mL)	[analysis] (ug/mL)	avg lag (hours)	avg elongation rate constant	endogenous in human systems?
1	heparin sodium salt	9041-08-1	573.40	17000 - 19000	-4	-6.98	-0.27	sugar	3 sulfates / 1 carboxyl	352 - 5.5	45.3	88	1.8	1.76	yes
2	chondroitin sulfate A ≠ψ	39455-18-0	475.38	6000 - 33000	-2	-4.21	-0.15	sugar	1 carboxyl / 1 sulfate	250 - 31.25	57.0	125	2.4	0.20	yes
3	hyaluronic acid (8-15 kD)	9067-32-7	402.31	8000 - 15000	-1	-2.49	-0.07	sugar	1 carboxyl	500 - 62.5	—	500	—	—	yes
4	hyaluronic acid (30-50 kD)	9067-32-7	402.31	30000 - 50000	-1	-2.49	-0.07	sugar	1 carboxyl	500 - 62.5	—	500	—	—	yes
5	hyaluronic acid (120-350 kD)	9067-32-7	402.31	120000 - 350000	-1	-2.49	-0.07	sugar	1 carboxyl	500 - 62.5	—	500	—	—	yes
6	hyaluronic acid (mixed mw)	9067-32-7	402.31	NA	-1	-2.49	-0.07	sugar	1 carboxyl	500 - 62.5	—	500	—	—	yes
7	fondaparinux sodium ┼	114870-03-0	1728.04	1728.04	-10	-5.79	-0.34	sugar	8 sulfates / 2 carboxyl	1000 - 31.25	—	500	—	—	no
8	nadroparin calcium ψ	37270-89-6	591.45	—	-6	-5.07	-0.21	sugar	4 sulfates/ 2 carboxyl	1000 - 31.25	54.8	125	1.5	0.47	no
9	sodium alginate ┼ ψ	9005-38-3	749.0	120000-190000	-2	-2.67	-0.12	sugar	2 carboxyls	1000 - 31.25	—	125	2.8	0.24	no
10	dermatan sulfate and oversulfated chondroitin sulfate	EPY0001321	475.38 696.52	NA	-2 -5	-4.21 -7.18	-0.15 -0.38	sugar	1 carboxyl / 1 sulfate 1 carboxyl / 4 sulfates	1000 - 61.25	88.4	125	0.6	1.43	yes
11	kappa carrageenan	11114-20-8	401.32	200000 - 800000	-1	-2.49	-0.08	sugar	1 sulfate	200 - 12.5	—	500	—	—	no
12	pectin	9000-69-5	353.3	50000 - 180000	-1	-2.83	-0.07	sugar	1 carboxyl	500 - 62.5	—	500	—	—	no
13	sodium pyrophosphate dibasic	7758-16-9	101.96	221.94	-1	-9.81	-0.31	phosphate	2 phosphates	4000 - 62.5	—	2000	—	—	yes
14	sodium pyrophosphate tetrabasic	7722-88-5	101.96	265.90	-1	-9.81	-0.31	phosphate	2 phosphates	4000 - 62.5	—	2000	—	—	yes
15	polyphosphate	10361-03-2	101.96	NA	-1	-9.81	-0.31	phosphate	1 phosphate	1000 - 125	167.0	250	6.6	0.20	yes
16	tripolyphosphate ┼	7758-29-4	101.96	367.85	-1	-9.81	-0.31	phosphate	3 phosphates	4000 - 500	—	2000	—	—	yes
17	Diadenosine pentaphosphate ┼	75522-97-3	101.96	916.37	-1	-9.81	-0.31	phosphate	5 phosphates	500 - 31.25	—	500	—	—	yes
18	sodium hexametaphosphate ┼	68915-31-1	101.96	611.77	-1	-9.81	-0.31	phosphate	6 phosphates	1000 - 15.6	—	500	9.2	0.22	no
19	sodium trimetaphosphate	7785-84-4	101.96	305.89	-1	-9.81	-0.31	phosphate	3 phosphates	4000 - 62.5	—	4000.0	—	—	no
20	Arachadonic acid	506-32-1	304.47	—	-1	-3.28	-0.12	lipid	1 carboxyl	30.5 - 1.9	—	31	3.9	0.25	yes
21	linoleic acid	60-33-3	280.45	—	-1	-3.57	-0.12	lipid	1 carboxyl	28.04 - 1.75	—	28	4.3	2.67	yes
22	phosphatidyl-l-serine	51446-62-9	792.07	—	-2	-2.53	-0.33	lipid	1 phospate / 1 carboxyl	18.5 - 1.16	—	79	3.2	1.09	yes
23	Ganglioside disodium salt ≠	37758-47-7	1470.80	—	-2	-1.36	-0.20	lipid	2 carboxyls	1000 - 31.25	—	100	—	—	yes
24	Ganglioside diammonium salt ≠	62010-37-1	1602.90	—	-2	-1.25	-0.20	lipid	2 carboxyls	1000 - 31.25	—	100	—	—	yes
25	poly-L-glutamic acid ψ	26247-79-0	151.10	50000-100000	-1	-6.62	-0.33	amino acid	1 carboxyl	500 - 15.6	37.0	62.5	3.1	1.46	yes
26	poly-L-glutamic acid (n = 20)	26247-79-0	151.10	3000.0	-1	-6.62	-0.33	amino acid	1 carboxyl	300 - 4.6	—	—	—	—	yes
27	poly-L-glutamic acid (n = 50)	26247-79-0	151.10	7500.0	-1	-6.62	-0.33	amino acid	1carboxyl	301 - 4.6	—	—	—	—	yes
28	poly-L-glutamic acid (n = 100)	26247-79-0	151.10	15000.0	-1	-6.62	-0.33	amino acid	1 carboxyl	302 - 4.6	—	—	—	—	yes
29	poly-L-glutamic acid (n = 200)	26247-79-0	151.10	30000.0	-1	-6.62	-0.33	amino acid	1 carboxyl	303 - 4.6	—	—	—	—	yes
30	poly-L-lysine	25104-18-1	151.10	150000-30000	1	6.62	0.33	amino acid	1 amine	500 - 31.25	—	—	—	—	yes
31	polyA (mRNA) ≠	26763-19-9	267.24	NA	-1	-3.74	-0.11	nucleic acid	1 phosphate	500 - 62.5	—	500	—	—	yes
32	Polyadenylic-polyuridylic acid (polyAU) ≠	24936-38-7	671.40	NA	-2	-2.98	-0.06	nucleic acid	2 phosphates	500 - 62.5	—	500.0	—	—	yes
33	tRNA (yeast) ≠	9014-25-9	—	25000.0	—	—	—	nucleic acid	—	500 - 15.6	—	500.0	—	—	yes
34	random nuc sequence	N8080127	—	—	—	—	—	nucleic acid	—	100 - 3.125	—	500.0	—	—	yes
35	polystyrene sulfonate ψ	PSS4K	184.2	4800.0	-1	-5.43	-0.32	synthetic	1 sulfate	500 - 31.25	—	62.5	2.9	0.45	no
36	Fusidic acid sodium salt ≠	751-94-0	538.7	—	-1	-1.86	-0.13	misc	1 carboxyl	1000 - 31.25	—	500	—	—	no
37	bilirubin	635-65-4	584.7	—	-2	-3.42	-0.10	misc	2 carboxyls	500 - 62.5	—	500	—	—	yes

Key

	active
┼	weak activator
	Inert
ψ	hook effect
≠	ThT reactivity

Table 2.S2 Characteristics and results from the anion library screening against P301S tau.

Nbr.	compound	CAS number	MW of repeat unit (Da)	MW range (Da)	charge per repeat unit	charge density (-e/kD)	charge density (-e/A)	polymer classification	charged groups	dosing (ug/mL)	[EC50] (ug/mL)	[analysis] (ug/mL)	lag (hours)	elongation rate constant	endogenous in human systems?
1	heparin sodium salt	9041-08-1	573.40	17000 - 19000	-4	-6.98	-0.27	sugar	3 sulfates / 1 carboxyl	352 - 11	13.5	88	0.47	3.05	yes
2	chondroitin sulfate A ≠	39455-18-0	475.38	6000 - 33000	-2	-4.21	-0.15	sugar	1 carboxyl / 1 sulfate	250 - 31.25	48.7	125	0.9	0.86	yes
3	hyaluronic acid (8-15 kD)	9067-32-7	402.31	8000 - 15000	-1	-2.49	-0.07	sugar	1 carboxyl	250 - 31.25	—	500.0	—	—	yes
4	hyaluronic acid (30-50 kD)	9067-32-7	402.31	30000 - 50000	-1	-2.49	-0.07	sugar	1 carboxyl	250 - 32.5	—	500.0	—	—	yes
5	hyaluronic acid (120-350 kD)	9067-32-7	402.31	120000 - 350000	-1	-2.49	-0.07	sugar	1 carboxyl	250 - 31.25	—	500.0	—	—	yes
6	hyaluronic acid (mixed mw)	9067-32-7	402.31	NA	-1	-2.49	-0.07	sugar	1 carboxyl	250 - 31.25	—	500.0	—	—	yes
7	fondaparinux	114870-03-0	1728.04	1728.04	-10	-5.79	-0.34	sugar	8 sulfates / 2 carboxyls	1000 - 31.25	72.5	500	3.17	0.18	no
8	nadroparin calcium Ψ	37270-89-6	591.45	—	-6	-5.07	-0.21	sugar	4 sulfates/ 2 carboxyl	1000 - 31.25	116.0	125	0.47	1.11	no
9	sodium alginate Ψ	9005-38-3	749.0	120000-190000	-2	-2.67	-0.12	sugar	2 carboxyls	1000 - 31.25	13.5	62.5	2.93	0.51	no
10	dermatan sulfate and oversulfated chondroitin sulfate Ψ	EPY0001321	475.38 696.52	NA	-2 -5	-4.21 -7.18	-0.15 -0.38	sugar	1 carboxyl / 1 sulfate 1 carboxyl / 4 sulfates	1000 - 61.25	49.3	250	0.2	1.77	yes
11	kappa carrageenan	11114-20-8	401.32	200000 - 800000	-1	-2.49	-0.08	sugar	1 sulfate	200 - 12.5	—	500.0	—	—	no
12	pectin	9000-69-5	353.35	50000 - 180000	-1	-2.83	-0.07	sugar	1 carboxyl	500 - 62.5	—	500.0	—	—	no
13	sodium pyrophosphate dibasic	7758-16-9	101.96	221.94	-1	-9.81	-0.31	phosphate	2 phosphates	4000 - 62.5	—	2000	—	—	yes
14	sodium pyrophosphate tetrabasic	7722-88-5	101.96	265.90	-1	-9.81	-0.31	phosphate	2 phosphates	4000 - 62.5	531.8	2000	2.85	0.25	yes
15	polyphosphate	10361-03-2	101.96	NA	-1	-9.81	-0.31	phosphate	1 phosphate	1000 - 125	146.3	250	0.67	1.04	yes
16	tripolyphosphate ⊥	7758-29-4	101.96	367.85	-1	-9.81	-0.31	phosphate	3 phosphates	4000 - 62.5	—	2000	—	—	yes
17	Diadenosine pentaphosphate ⊥	75522-97-3	101.96	916.37	-1	-9.81	-0.31	phosphate	5 phosphates	500 - 31.25	—	1000	—	—	yes
18	sodium hexametaphosphate Ψ	68915-31-1	101.96	611.77	-1	-9.81	-0.31	phosphate	6 phosphates	1000 - 15.6	65.1	125	2.07	0.22	no
19	sodium trimetaphosphate	7785-84-4	101.96	305.89	-1	-9.81	-0.31	phosphate	3 phosphates	4000 - 31.25	—	2000	—	—	no
20	Arachadonic acid	506-32-1	304.47	—	-1	-3.28	-0.12	lipid	1 carboxyl	30.5 - 1.9	—	31	0.75	0.37	yes
21	linoleic acid	60-33-3	280.45	—	-1	-3.57	-0.12	lipid	1 carboxyl	28.04 - 1.75	—	28	0.9	0.35	yes
22	phosphatidyl-l-serine	51446-62-9	792.07	—	-2	-2.53	-0.33	lipid	1 phospate / 1 carboxyl	18.5 - 1.16	—	79	1.1	0.29	yes
23	Gangloside disodium salt ≠	37758-47-7	1470.80	—	-2	-1.36	-0.20	lipid	2 carboxyls	1000 - 31.25	—	100	—	—	yes
24	Gangloside diammonium salt ≠	62010-37-1	1602.90	—	-2	-1.25	-0.20	lipid	2 carboxyls	1000 - 31.25	—	100	—	—	yes
25	poly-L-glutamic acid Ψ	26247-79-0	151.10	50000- 100000	-1	-6.62	-0.33	amino acid	1 carboxyl	500 - 15.6	26.0	62.5	0.57	2.48	yes
26	poly-L-glutamic acid (n = 20)	26247-79-0	151.10	3000.0	-1	-6.62	-0.33	amino acid	1 carboxyl	300 - 9.375	—	—	—	—	yes
27	poly-L-glutamic acid (n = 50)	26247-79-0	151.10	7500.0	-1	-6.62	-0.33	amino acid	1 carboxyl	300 - 9.375		75.0	0.4	0.55	yes
28	poly-L-glutamic acid (n = 100)	26247-79-0	151.10	15000.0	-1	-6.62	-0.33	amino acid	1 carboxyl	301 - 9.375		75.0	0.4	0.55	yes
29	poly-L-glutamic acid (n = 200)	26247-79-0	151.10	30000.0	-1	-6.62	-0.33	amino acid	1 carboxyl	302 - 9.375		75.0	0.2	0.52	yes
30	poly-L-lysine ⊥	25104-18-1	151.10	150000 - 300000	1	6.62	0.33	amino acid	1 amine	500 - 31.25	—	250	—	—	yes
31	polyA (mRNA) ≠	26763-19-9	267.24	NA	-1	-3.74	-0.11	nucleic acid	1 phosphate	1000 - 31.25	—	500	—	—	yes
32	Polyadenylic-polyuridylic acid (polyAU) ≠	24936-38-7	671.40	NA	-2	-2.98	-0.06	nucleic acid	2 phosphates	500 - 62.5	—	500	—	—	yes
33	tRNA (yeast) ≠	9014-25-9	—	25000.0	—	—	—	nucleic acid	—	500 - 62.5	—	500	2.1	0.49	yes
34	random nuc sequence	N8080127	—	—	—	—	—	nucleic acid	—	100 - 3.125	—	—	—	—	yes
35	polystyrene sulfonate Ψ	PSS4K	184.2	4800.0	-1	-5.43	-0.32	synthetic	1 sulfate	500 - 31.25	—	62.5	1.7	1.38	no
36	Fusidic acid sodium salt ≠	751-94-0	538.7	—	-1	-1.86	-0.13	misc	1 carboxyl	1000 - 31.25	—	—	500	—	no
37	bilirubin	635-65-4	584.7	—	-2	-3.42	-0.10	misc	2 carboxyls	500 - 62.5	—	—	500	—	yes

Key

	active
⊥	weak activator
	Inert
Ψ	hook effect
≠	ThT reactivity

2.9 References

(1) Orr, M. E.; Sullivan, A. C.; Frost, B. A Brief Overview of Tauopathy: Causes, Consequences, and Therapeutic Strategies. *Trends Pharmacol. Sci.* **2017**, *38* (7), 637–648. https://doi.org/10.1016/j.tips.2017.03.011.

(2) Holtzman, D. M.; Carrillo, M. C.; Hendrix, J. A.; Bain, L. J.; Catafau, A. M.; Gault, L. M.; Goedert, M.; Mandelkow, E.; Mandelkow, E.-M.; Miller, D. S.; Ostrowitzki, S.; Polydoro, M.; Smith, S.; Wittmann, M.; Hutton, M. Tau: From Research to Clinical Development. *Alzheimers. Dement.* **2016**, *12* (10), 1033–1039. https://doi.org/10.1016/j.jalz.2016.03.018.

(3) Wang, Y.; Mandelkow, E. Tau in Physiology and Pathology. *Nat. Rev. Neurosci.* **2016**, *17* (1), 5–21. https://doi.org/10.1038/nrn.2015.1.

(4) Goedert, M.; Eisenberg, D. S.; Crowther, R. A. Propagation of Tau Aggregates and Neurodegeneration. *Annu. Rev. Neurosci.* **2017**, *40*, 189–210. https://doi.org/10.1146/annurev-neuro-072116-031153.

(5) Jeganathan, S.; Von Bergen, M.; Mandelkow, E. M.; Mandelkow, E. The Natively Unfolded Character of Tau and Its Aggregation to Alzheimer-like Paired Helical Filaments. *Biochemistry* **2008**, *47* (40), 10526–10539. https://doi.org/10.1021/bi800783d.

(6) Friedhoff, P.; Schneider, A.; Mandelkow, E.-M.; Mandelkow, E. Rapid Assembly of Alzheimer-like Paired Helical Filaments from Microtubule-Associated Protein Tau Monitored by Fluorescence in Solution. *Biochemistry* **1998**, *37* (28), 10223–10230. https://doi.org/10.1021/bi980537d.

(7) Townsend, D.; Fullwood, N. J.; Yates, E. A.; Middleton, D. A. Aggregation Kinetics and Filament Structure of a Tau Fragment Are Influenced by the Sulfation Pattern of the Cofactor Heparin. *Biochemistry* **2020**, *59* (41), 4003–4014. https://doi.org/10.1021/acs.biochem.0c00443.

(8) Giamblanco, N.; Fichou, Y.; Janot, J.-M.; Balanzat, E.; Han, S.; Balme, S. Mechanisms of

Heparin-Induced Tau Aggregation Revealed by Single Nanopore. *ACS Sensors* **2020**, *5* (4), 1158–1167. https://doi.org/10.1021/acssensors.0c00193.

(9) Snow, A. D.; Mar, H.; Nochlin, D.; Kimata, K.; Kato, M.; Suzuki, S.; Hassell, J.; Wight, T. N. The Presence of Heparan Sulfate Proteoglycans in the Neuritic Plaques and Congophilic Angiopathy in Alzheimer's Disease. *Am. J. Pathol.* **1988**, *133* (3), 456–463.

(10) Li, D.; Liu, C. Hierarchical Chemical Determination of Amyloid Polymorphs in Neurodegenerative Disease. *Nat. Chem. Biol.* **2021**, *17* (3), 237–245. https://doi.org/10.1038/s41589-020-00708-z.

(11) Lövestam, S.; Koh, F. A.; van Knippenberg, B.; Kotecha, A.; Murzin, A. G.; Goedert, M.; Scheres, S. H. W. Assembly of Recombinant Tau into Filaments Identical to Those of Alzheimer's Disease and Chronic Traumatic Encephalopathy. *Elife* **2022**, *11*, 1–27. https://doi.org/10.7554/eLife.76494.

(12) Falcon, B.; Zhang, W.; Murzin, A. G.; Murshudov, G.; Garringer, H. J.; Vidal, R.; Crowther, R. A.; Ghetti, B.; Scheres, S. H. W.; Goedert, M. Structures of Filaments from Pick's Disease Reveal a Novel Tau Protein Fold. *Nature* **2018**, *561* (7721), 137–140. https://doi.org/10.1038/s41586-018-0454-y.

(13) Fitzpatrick, A. W. P.; Falcon, B.; He, S.; Murzin, A. G.; Murshudov, G.; Garringer, H. J.; Crowther, R. A.; Ghetti, B.; Goedert, M.; Scheres, S. H. W. Cryo-EM Structures of Tau Filaments from Alzheimer's Disease. *Nature* **2017**, *547*, 185.

(14) Dregni, A. J.; Mandala, V. S.; Wu, H.; Elkins, M. R.; Wang, H. K.; Hung, I.; DeGrado, W. F.; Hong, M. In Vitro 0N4R Tau Fibrils Contain a Monomorphic β-Sheet Core Enclosed by Dynamically Heterogeneous Fuzzy Coat Segments. *Proc. Natl. Acad. Sci. U. S. A.* **2019**, *116* (33), 16357–16366. https://doi.org/10.1073/pnas.1906839116.

(15) Frost, B.; Ollesch, J.; Wille, H.; Diamond, M. I. Conformational Diversity of Wild-Type Tau Fibrils Specified by Templated Conformation Change. *J. Biol. Chem.* **2009**, *284* (6), 3546–3551. https://doi.org/10.1074/jbc.M805627200.

(16) Kjaergaard, M.; Dear, A. J.; Kundel, F.; Qamar, S.; Meisl, G.; Knowles, T. P. J.; Klenerman, D. Oligomer Diversity during the Aggregation of the Repeat Region of Tau. *ACS Chem. Neurosci.* **2018**, *9* (12), 3060–3071. https://doi.org/10.1021/acschemneuro.8b00250.

(17) Patterson, K. R.; Remmers, C.; Fu, Y.; Brooker, S.; Kanaan, N. M.; Vana, L.; Ward, S.; Reyes, J. F.; Philibert, K.; Glucksman, M. J.; Binder, L. I. Characterization of Prefibrillar Tau Oligomers in Vitro and in Alzheimer Disease. *J. Biol. Chem.* **2011**, *286* (26), 23063–23076. https://doi.org/10.1074/jbc.M111.237974.

(18) Strang, K. H.; Croft, C. L.; Sorrentino, Z. A.; Chakrabarty, P.; Golde, T. E.; Giasson, B. I. Distinct Differences in Prion-like Seeding and Aggregation between Tau Protein Variants Provide Mechanistic Insights into Tauopathies. *J. Biol. Chem.* **2018**, *293* (7), 2408–2421. https://doi.org/10.1074/jbc.M117.815357.

(19) Xia, Y.; Xia, Y.; Prokop, S.; Prokop, S.; Prokop, S.; Prokop, S.; Gorion, K. M. M.; Gorion, K. M. M.; Kim, J. D.; Kim, J. D.; Sorrentino, Z. A.; Sorrentino, Z. A.; Bell, B. M.; Bell, B. M.; Manaois, A. N.; Manaois, A. N.; Chakrabarty, P.; Chakrabarty, P.; Chakrabarty, P.; Davies, P.; Giasson, B. I.; Giasson, B. I.; Giasson, B. I. Tau Ser208 Phosphorylation Promotes Aggregation and Reveals Neuropathologic Diversity in Alzheimer's Disease and Other Tauopathies. *Acta Neuropathol. Commun.* **2020**, *8* (1), 1–17. https://doi.org/10.1186/s40478-020-00967-w.

(20) Fischer, D.; Mukrasch, M. D.; Von Bergen, M.; Klos-Witkowska, A.; Biemat, J.; Griesinger, C.; Mandelkow, E.; Zweckstetter, M. Structural and Microtubule Binding Properties of Tau Mutants of Frontotemporal Dementias. *Biochemistry* **2007**, *46* (10), 2574–2582. https://doi.org/10.1021/bi061318s.

(21) Fichou, Y.; Lin, Y.; Rauch, J. N.; Vigers, M.; Zeng, Z.; Srivastava, M.; Keller, T. J.; Freed, J. H.; Kosik, K. S.; Han, S. Cofactors Are Essential Constituents of Stable and Seeding-Active Tau Fibrils. *Proc. Natl. Acad. Sci. U. S. A.* **2018**, *115* (52), 13234–13239.

https://doi.org/10.1073/pnas.1810058115.

(22) Fichou, Y.; Oberholtzer, Z. R.; Ngo, H.; Cheng, C. Y.; Keller, T. J.; Eschmann, N. A.; Han, S. Tau-Cofactor Complexes as Building Blocks of Tau Fibrils. *Front. Neurosci.* **2019**, *13* (December), 1–15. https://doi.org/10.3389/fnins.2019.01339.

(23) Ramachandran, G.; Udgaonkar, J. B. Understanding the Kinetic Roles of the Inducer Heparin and of Rod-like Protofibrils during Amyloid Fibril Formation by Tau Protein. *J. Biol. Chem.* **2011**, *286* (45), 38948–38959. https://doi.org/10.1074/jbc.M111.271874.

(24) Mok, S. A.; Condello, C.; Freilich, R.; Gillies, A.; Arhar, T.; Oroz, J.; Kadavath, H.; Julien, O.; Assimon, V. A.; Rauch, J. N.; Dunyak, B. M.; Lee, J.; Tsai, F. T. F.; Wilson, M. R.; Zweckstetter, M.; Dickey, C. A.; Gestwicki, J. E. Mapping Interactions with the Chaperone Network Reveals Factors That Protect against Tau Aggregation. *Nat. Struct. Mol. Biol.* **2018**, *25* (5), 384–393. https://doi.org/10.1038/s41594-018-0057-1.

(25) Dinkel, P. D.; Holden, M. R.; Matin, N.; Margittai, M. RNA Binds to Tau Fibrils and Sustains Template-Assisted Growth. *Biochemistry* **2015**, *54* (30), 4731–4740. https://doi.org/10.1021/acs.biochem.5b00453.

(26) Wickramasinghe, S. P.; Lempart, J.; Merens, H. E.; Murphy, J.; Huettemann, P.; Jakob, U.; Rhoades, E. Polyphosphate Initiates Tau Aggregation through Intra- and Intermolecular Scaffolding. *Biophys. J.* **2019**, *117* (4), 717–728. https://doi.org/10.1016/j.bpj.2019.07.028.

(27) Cremers, C. M.; Knoefler, D.; Gates, S.; Martin, N.; Dahl, J. U.; Lempart, J.; Xie, L.; Chapman, M. R.; Galvan, V.; Southworth, D. R.; Jakob, U. Polyphosphate: A Conserved Modifier of Amyloidogenic Processes. *Mol. Cell* **2016**, *63* (5), 768–780. https://doi.org/10.1016/j.molcel.2016.07.016.

(28) Huseby, C. J.; Bundschuh, R.; Kuret, J. The Role of Annealing and Fragmentation in Human Tau Aggregation Dynamics. *J. Biol. Chem.* **2019**, *294* (13), 4728–4737. https://doi.org/10.1074/jbc.RA118.006943.

(29) Abskharon, R.; Sawaya, M. R.; Cao, Q.; Nguyen, B. A.; Boyer, D. R.; Cascio, D.; Eisenberg, D. S. Cryo-EM Structure of RNA-Induced Tau Fibrils Reveals a Small C-Terminal Core That May Nucleate Fibril Formation. *Proc. Natl. Acad. Sci. U. S. A.* **2022**, *119* (15), 1–26. https://doi.org/10.1073/pnas.2119952119.

(30) Trzeciakiewicz, H.; Esteves-Villanueva, J. O.; Carlin, N.; Martić, S. Electrochemistry of Heparin Binding to Tau Protein on Au Surfaces. *Electrochim. Acta* **2015**, *162*, 24–30. https://doi.org/https://doi.org/10.1016/j.electacta.2014.08.101.

(31) Zhu, H. L.; Fernández, C.; Fan, J. B.; Shewmaker, F.; Chen, J.; Minton, A. P.; Liang, Y. Quantitative Characterization of Heparin Binding to Tau Protein: Implication for Inducer-Mediated Tau Filament Formation. *J. Biol. Chem.* **2010**, *285* (6), 3592–3599. https://doi.org/10.1074/jbc.M109.035691.

(32) Sibille, N.; Sillen, A.; Leroy, A.; Wieruszeski, J. M.; Mulloy, B.; Landrieu, I.; Lippens, G. Structural Impact of Heparin Binding to Full-Length Tau as Studied by NMR Spectroscopy. *Biochemistry* **2006**, *45* (41), 12560–12572. https://doi.org/10.1021/bi060964o.

(33) Wilson, D. M.; Binder, L. I. Free Fatty Acids Stimulate the Polymerization of Tau and Amyloid Beta Peptides. In Vitro Evidence for a Common Effector of Pathogenesis in Alzheimer's Disease. *Am. J. Pathol.* **1997**, *150* (6), 2181–2195.

(34) Chirita, C. N.; Necula, M.; Kuret, J. Anionic Micelles and Vesicles Induce Tau Fibrillization in Vitro. *J. Biol. Chem.* **2003**, *278* (28), 25644–25650. https://doi.org/10.1074/jbc.M301663200.

(35) Barracchia, C. G.; Tira, R.; Parolini, F.; Munari, F.; Bubacco, L.; Spyroulias, G. A.; D'Onofrio, M.; Assfalg, M. Unsaturated Fatty Acid-Induced Conformational Transitions and Aggregation of the Repeat Domain of Tau. *Molecules* **2020**, *25* (11), 1–21. https://doi.org/10.3390/molecules25112716.

(36) Lossos, A.; Reches, A.; Gal, A.; Newman, J. P.; Soffer, D.; Gomori, J. M.; Boher, M.;

Ekstein, D.; Biran, I.; Meiner, Z.; Abramsky, O.; Rosenmann, H. Frontotemporal Dementia and Parkinsonism with the P301S Tau Gene Mutation in a Jewish Family. *J. Neurol.* **2003**, *250* (6), 733–740. https://doi.org/10.1007/s00415-003-1074-4.

(37) Allen, B.; Ingram, E.; Takao, M.; Smith, M. J.; Jakes, R.; Virdee, K.; Yoshida, H.; Holzer, M.; Craxton, M.; Emson, P. C.; Atzori, C.; Migheli, A.; Crowther, R. A.; Ghetti, B.; Spillantini, M. G.; Goedert, M. Abundant Tau Filaments and Nonapoptotic Neurodegeneration in Transgenic Mice Expressing Human P301S Tau Protein. *J. Neurosci.* **2002**, *22* (21), 9340–9351. https://doi.org/10.1523/JNEUROSCI.22-21-09340.2002.

(38) Berriman, J.; Serpell, L. C.; Oberg, K. A.; Fink, A. L.; Goedert, M.; Crowther, R. A. Tau Filaments from Human Brain and from in Vitro Assembly of Recombinant Protein Show Cross-Beta Structure. *Proc. Natl. Acad. Sci. U. S. A.* **2003**, *100* (15), 9034–9038. https://doi.org/10.1073/pnas.1530287100.

(39) Rauch, J. N.; Olson, S. H.; Gestwicki, J. E. Interactions between Microtubule-Associated Protein Tau (MAPT) and Small Molecules. *Cold Spring Harb Perspect Med* **2017**, *7*, 1–14.

(40) Knowles, T. P. J.; Shu, W.; Devlin, G. L.; Meehan, S.; Auer, S.; Dobson, C. M.; Welland, M. E. Kinetics and Thermodynamics of Amyloid Formation from Direct Measurements of Fluctuations in Fibril Mass. *Proc. Natl. Acad. Sci. U. S. A.* **2007**, *104* (24), 10016–10021. https://doi.org/10.1073/pnas.0610659104.

(41) Wegmann, S.; Eftekharzadeh, B.; Tepper, K.; Zoltowska, K. M.; Bennett, R. E.; Dujardin, S.; Laskowski, P. R.; MacKenzie, D.; Kamath, T.; Commins, C.; Vanderburg, C.; Roe, A. D.; Fan, Z.; Molliex, A. M.; Hernandez-Vega, A.; Muller, D.; Hyman, A. A.; Mandelkow, E.; Taylor, J. P.; Hyman, B. T. Tau Protein Liquid–Liquid Phase Separation Can Initiate Tau Aggregation. *EMBO J.* **2018**, *37* (7), 1–21. https://doi.org/10.15252/embj.201798049.

(42) Wegmann, S.; Medalsy, I. D.; Mandelkow, E.; Müller, D. J. The Fuzzy Coat of

Pathological Human Tau Fibrils Is a Two-Layered Polyelectrolyte Brush. *Proc. Natl. Acad. Sci. U. S. A.* **2012**, *110* (4), E313–E321. https://doi.org/10.1073/pnas.1212100110.

(43) Mukrasch, M. D.; Bibow, S.; Korukottu, J.; Jeganathan, S.; Biernat, J.; Griesinger, C.; Mandelkow, E.; Zweckstetter, M. Structural Polymorphism of 441-Residue Tau at Single Residue Resolution. *PLoS Biol.* **2009**, *7* (2), 0399–0414. https://doi.org/10.1371/journal.pbio.1000034.

(44) Bibow, S.; Mukrasch, M. D.; Chinnathambi, S.; Biernat, J.; Griesinger, C.; Mandelkow, E.; Zweckstetter, M. The Dynamic Structure of Filamentous Tau. *Angew. Chemie - Int. Ed.* **2011**, *50* (48), 11520–11524. https://doi.org/10.1002/anie.201105493.

(45) Schwalbe, M.; Ozenne, V.; Bibow, S.; Jaremko, M.; Jaremko, L.; Gajda, M.; Jensen, M. R.; Biernat, J.; Becker, S.; Mandelkow, E.; Zweckstetter, M.; Blackledge, M. Predictive Atomic Resolution Descriptions of Intrinsically Disordered HTau40 and α-Synuclein in Solution from NMR and Small Angle Scattering. *Structure* **2014**, *22* (2), 238–249. https://doi.org/10.1016/j.str.2013.10.020.

(46) Zhang, W.; Falcon, B.; Murzin, A. G.; Fan, J.; Crowther, R. A.; Goedert, M.; Scheres, S. H. W. Heparin-Induced Tau Filaments Are Polymorphic and Differ from Those in Alzheimer's and Pick's Diseases. *Elife* **2019**, *8*, 1–24. https://doi.org/10.7554/eLife.43584.

(47) Dinkel, P. D.; Holden, M. R.; Matin, N.; Margittai, M. RNA Binds to Tau Fibrils and Sustains Template-Assisted Growth. *Biochemistry* **2015**, *54* (30), 4731–4740. https://doi.org/10.1021/acs.biochem.5b00453.

(48) Ingham, D. J.; Hillyer, K. M.; McGuire, M. J.; Gamblin, T. C. In Vitro Tau Aggregation Inducer Molecules Influence the Effects of MAPT Mutations on Aggregation Dynamics. *Biochemistry* **2022**, *61* (13), 1243–1259. https://doi.org/10.1021/acs.biochem.2c00111.

(49) Alquezar, C.; Arya, S.; Kao, A. W. Tau Post-Translational Modifications: Dynamic Transformers of Tau Function, Degradation, and Aggregation. *Front. Neurol.* **2020**, *11*, 595532. https://doi.org/10.3389/fneur.2020.595532.

(50) Wesseling, H.; Mair, W.; Kumar, M.; Schlaffner, C. N.; Tang, S.; Beerepoot, P.; Fatou, B.; Guise, A. J.; Cheng, L.; Takeda, S.; Muntel, J.; Rotunno, M. S.; Dujardin, S.; Davies, P.; Kosik, K. S.; Miller, B. L.; Berretta, S.; Hedreen, J. C.; Grinberg, L. T.; Seeley, W. W.; Hyman, B. T.; Steen, H.; Steen, J. A. Tau PTM Profiles Identify Patient Heterogeneity and Stages of Alzheimer's Disease. *Cell* **2020**, *183* (6), 1699-1713.e13. https://doi.org/10.1016/j.cell.2020.10.029.

(51) Limorenko, G.; Lashuel, H. A. Revisiting the Grammar of Tau Aggregation and Pathology Formation: How New Insights from Brain Pathology Are Shaping How We Study and Target Tauopathies. *Chem. Soc. Rev.* **2022**, *51* (2), 513–565. https://doi.org/10.1039/d1cs00127b.

(52) Despres, C.; Di, J.; Cantrelle, F. X.; Li, Z.; Huvent, I.; Chambraud, B.; Zhao, J.; Chen, J.; Chen, S.; Lippens, G.; Zhang, F.; Linhardt, R.; Wang, C.; Klärner, F. G.; Schrader, T.; Landrieu, I.; Bitan, G.; Smet-Nocca, C. Major Differences between the Self-Assembly and Seeding Behavior of Heparin-Induced and in Vitro Phosphorylated Tau and Their Modulation by Potential Inhibitors. *ACS Chem. Biol.* **2019**, *14* (6), 1363–1379. https://doi.org/10.1021/acschembio.9b00325.

(53) Wolfe, M. S. Tau Mutations in Neurodegenerative Diseases. *J. Biol. Chem.* **2009**, *284* (10), 6021–6025. https://doi.org/10.1074/jbc.R800013200.

(54) Jones, L. T. S.; Yazzie, B.; Middaugh, C. R. Polyanions and the Proteome. *Mol. Cell. Proteomics* **2004**, *3* (8), 746–769. https://doi.org/10.1074/mcp.R400008-MCP200.

(55) Speer, S. L.; Zheng, W.; Jiang, X.; Chu, I. Te; Guseman, A. J.; Liu, M.; Pielak, G. J.; Li, C. The Intracellular Environment Affects Protein-Protein Interactions. *Proc. Natl. Acad. Sci. U. S. A.* **2021**, *118* (11), 1–7. https://doi.org/10.1073/pnas.2019918118.

(56) Stadmiller, S. S.; Pielak, G. J. Protein-Complex Stability in Cells and in Vitro under Crowded Conditions. *Curr. Opin. Struct. Biol.* **2021**, *66*, 183–192. https://doi.org/10.1016/j.sbi.2020.10.024.

Publishing Agreement

It is the policy of the University to encourage open access and broad distribution of all theses, dissertations, and manuscripts. The Graduate Division will facilitate the distribution of UCSF theses, dissertations, and manuscripts to the UCSF Library for open access and distribution. UCSF will make such theses, dissertations, and manuscripts accessible to the public and will take reasonable steps to preserve these works in perpetuity.

I hereby grant the non-exclusive, perpetual right to The Regents of the University of California to reproduce, publicly display, distribute, preserve, and publish copies of my thesis, dissertation, or manuscript in any form or media, now existing or later derived, including access online for teaching, research, and public service purposes.

DocuSigned by:
Kelly Montgomery
C8B46D541052406...
Author Signature

2/22/2023
Date